A CHEMICAL AND SYSTEMS APPROACH TO STUDY THE WNT/β-CATENIN PATHWAY

By

Curtis Andrew Thorne

Dissertation

Submitted to the Faculty of the

Graduate School of Vanderbilt University

in fulfillment of the requirements

for the degree of

DOCTOR OF PHILOSOPHY

in

Cell and Developmental Biology

August, 2010

Nashville, Tennessee

Approved:

Ethan Lee

Kathleen Gould

Albert Reynolds

Michael Cooper

Guoqiang Gu

For Travis and Mitchell, my brothers

ACKNOWLEDGEMENTS

This work would not have been possible without the support and guidance of my mentor, Dr. Ethan Lee. I marvel at his energy and passion for what he does. He is a bottomless treasure trove of creative ideas and helps his students gain the courage to tackle the big, tough questions. He truly has an infectious excitement for conducting research and it rubs off on his students. I hope I take some of that enthusiasm with me as I move to the next stage of my career.

I would also like to thank Dr. Laurie Lee. Her clarity of thought is like a rushing wind through the fog-engulfed hills of Tennessee. She was also instrumental in keeping the line of communication open between Ethan and me. Ethan and Laurie together formed a lab for which I am very grateful. I am *sure* there is no work environment like this anywhere. A transcript of our daily interactions would be an award winning sitcom, I'm sure. I would like to make special mention of my long-time bench mate Michael Anderson or, Silent Thunder, as I like to call him. His steady temperament (except when he's driving) and perseverance are an inspiration. He was also very generous with his p10 pipettor that functioned as my emergency backup and got used often.

I am very grateful for my committee members, Kathy Gould, Al Reynolds, Michael Cooper and Guoqiang Gu. You genuinely supported my work, provided critical insight and motivated me. A Ph.D. student only gets one committee and I'm thrilled that scientists I admire guided my graduate studies.

The Gould lab was a home away from home for me. Kathy has built a great lab with a strong training environment. As a result, I benefitted from the friendships formed with her students, particularly Rachel Roberts-Galbraith, a classmate and scientific peer. I wish her the best in her future studies.

I must thank Reviewer #2 for holding me to the highest standards. Like tempered steel, my weaknesses have been purged by fire. My skin is now thick.

There have been numerous professors and scientists who have helped me get to this point in my development. I thank Dr. Anne Rushing and Darrel Vodopich at Baylor University. They were my first mentors, allowing me to spend a summer wading in the Brazos River asking questions about phenotypic plasticity. I thank Dr. Adrian Lee and Dr. Steffi Oesterreich at Baylor College of Medicine, who gave me my first exposure to modern biomedical research; it blew my mind. And I thank Dr. Adrian Salic, who welcomed me into his lab for what turned out to be the most productive week of my graduate career.

I would especially like to thank my parents who made me the person I am today. They instilled in me a work ethic and a moral conscience. They have always given me the freedom to explore my own passions and supported me along the way.

And most thanks and appreciation to my wife, Jamie, the love of my life. We have been married for nine and a half years and each year is better than the last! Your unwavering belief in me has carried me through many tough times. Your skills as an educator are unmatched and a daily inspiration to me. Now with little Peter and a Ph.D., we set sail for a new horizon.

TABLE OF CONTENTS

LIST OF FIGURES

CHAPTER I

INTRODUCTION TO WNT SIGNALING

Introduction

Wnt/β-catenin signaling plays a critical role in metazoan development, tissue homeostasis, and human disease (Nusse 2005; Clevers 2006). Core to the pathway is the existence of a multi-component destruction complex that targets the transcriptional co-activator β-catenin for degradation. Upon binding of a Wnt ligand to the cell surface receptors, Frizzled (Fz) and low-density lipoprotein receptor-related protein 5 or 6 (LRP5/6), the β-catenin destruction complex is inhibited, allowing β-catenin levels to rise, interact with DNA-bound nuclear factors, and activate a vast transcriptional program (MacDonald, Tamai et al. 2009). In this work, Chapter I sets the historical and mechanistic background for a chemical screen and systems-level analysis of the Wnt/β-catenin pathway described in Chapters III and IV. I conclude, in Chapter V and VI, with discussion and further studies that come from the findings presented here.

Cellular communication

What constitutes a cell? How do they communicate with each other? How do they respond to their environment? These questions have fascinated the scientific community since the inception of the field of Cell Biology in the mid 17th century, initiated by the discoveries of Robert Hooke, Anton van Leeuwenhoek, and others

(Porter 1976; Inwood 2002). By definition, all metazoan organisms consist of numerous cells coexisting to form a single reproducing animal (Schmidt-Nielsen 1990). The coexisting of cells within a highly organized animal requires the generation and passing of information among different cell types. This passing and processing of information is referred to as signal transduction (Gomperts, Tatham et al. 2009).

The components, structure, and control of signal transduction are major focuses of modern biological research. Cells contain receptors that bind signals and transmit a response inside the cell. Polypeptides and small molecules are the chemical entities that act as signals and are termed ligands. Additionally, forces on cells and temperature fluctuations can be thought of as non-canonical types of signals. Receptors can exist on the plasma membrane (e.g. insulin receptor) or as intracellular receptors (e.g. steroid receptor). Once a ligand binds its receptor, a series of intracellular biochemical reactions process these signals into a physiological response. This response can manifest as a variety of events including changes in metabolism, regulation of gene transcription, control of motility, or even initiation of cell death (Gomperts, Tatham et al. 2009).

Despite the vast diversity in shape and form of the animal kingdom, the last 25 years of molecular and genomic research have uncovered a surprisingly small set of core signal transduction pathways. Based on conserved molecular components, it is estimated as few as 17 pathways exist (Gerhart 1999). For this small metazoan "tool kit" to account for such wide phenotypic diversity, it must be used in complex patterns in time and space, as well as evolve novel linkages of cross-regulation

between pathways. An analogy I am fond of is that of the carpenter's toolbox. For a carpenter to build, he may need something to pound (hammer), something to cut (saw), something to measure (tape measure), something to smooth surfaces (sander) etc. With this small set of tools he can build something as simple as a chair or as complex as a house. Just as all carpenter's saws are not the same (circular, reciprocating, etc.), a result of evolution over time is that these signaling pathways have acquired (or lost) additional levels of regulation. Herein lies the challenge for current biologists; what is the exact "design" of each of these tools, when and where are they used, how has the functionality of the tools been expanded through evolution, and what are the consequences when misused through mutation or environmental perturbation?

Both sides of the coin: Wnt signaling in development and disease

The Wnt pathway is a highly conserved signal transduction pathways found throughout the animal kingdom. It has been under investigation for more than 30 years. Its name comes from a family of ligands identified to activate the pathway, Wnts. The historical events that lead to the discovery and naming of Wnt ligands highlight a fascinating convergence of disparate animal model systems of development and disease.

In 1976, Sharma and Chopra described a *Drosophila melanogaster* mutant that exhibited reduced or missing wings and halteres (Sharma and Chopra 1976). Based on the mutant phenotype, they named this locus *wingless* (*wg*) and suggested it played a developmental role. A few years later, Nusse and Varmus conducted a

forward genetic screen to identify genes in mice that could lead to tumorigenesis (Nusse, van Ooyen et al. 1984). Using mouse mammary tumor virus (MMTV) insertion sites, they identified a locus termed *int-1*, short for integration 1, that induced mouse mammary tumors. Comparative genomic studies revealed *wg* and *int-1* were orthologs. To clarify nomenclature, the names were merged into the mnemonic Wnt (Nusse, Brown et al. 1991). Overexpression of *int-1* in *Xenopus* embryos induced an ectopic axis, demonstrating it was not only an oncogene but also played an early role in developmental axis specification (McMahon and Moon 1989; McMahon and Moon 1989). These studies collectively drew a connection between the physiological role for Wnts in development and a pathophysiological role in carcinogenesis.

Beyond the identification of *wingless,* forward genetic studies in *Drosophila* have been crucial in identifying Wnt pathway components. In 1980, Eric Wieschaus and Christiane Nusslein-Volhard published a series of *Drosophila* mutants that controlled patterning of the embryo (Nusslein-Volhard and Wieschaus 1980). This work was nothing less than a watershed moment for the field of developmental biology and culminated in their receiving the Nobel Prize. The 15 years after their initial publication produced a number of genetic epistasis studies. These studies placed these mutants within signaling pathways and resulted in the discovery of a number of additional members of the Wnt pathway including *armadillo* (Riggleman, Wieschaus et al. 1989; Riggleman, Schedl et al. 1990), *disheveled* (Klingensmith, Nusse et al. 1994), *shaggy* (Siegfried, Chou et al. 1992) and *frizzled* (Bhanot, Brink et al. 1996). These will be discussed in further detail below.

Xenopus laevis also played a prominent role early on in the characterization of Wnt signaling in development. The activation of this pathway on the future dorsal side of the early *Xenopus* embryo is a critical event in the formation of the Spemann organizer, a tissue-organizing center found in vertebrates (Spemann and Mangold, 1924). This role for Wnt in organizer formation was uncovered when multiple groups injected mRNA of *Wnt-1* and *Xwnt8* in *Xenopus* blastomeres. Ectopic activation of Wnt signaling in the future ventral side of the embryo induces a second organizer that can coordinate the formation of a complete secondary body axis (Smith and Harland 1991; Sokol, Christian et al. 1991). This work helped uncover many of the molecular mysteries around specification and formation of the Spemann organizer. To date, almost all major members of the Wnt pathway have been validated through *Xenopus* axis specification studies.

As these early Wnt studies allude to, Wnts are profoundly involved in almost all aspects of development, from very early axis specification of a radial symmetric embryo, to maintenance of epithelial homeostasis in the adult organism. Years of continued examination of the pathway in fly, worm, frog, fish, and mouse have solidified involvement of Wnt signaling in cell differentiation, proliferation, migration, patterning and adult stem cell homeostasis. So it comes as no surprise, like the detrimental effects of experimental perturbation to the pathway, there exist a whole host of genetic and environmental perturbations that lead to many types of human diseases ranging from birth defects to cancers (table 1). One of the most established examples of the connection between the Wnt pathway and disease is a genetic lesion that occurs early in the onset of colon cancer. In 1991, a germline

mutation in the Wnt pathway component Adenomotous Polyposis Coli (APC, discussed below) was identified in patients with a form of hereditary cancer termed Familiar Adenomotous Polyposis (FAP) (Kinzler, Nilbert et al. 1991; Nishisho, Nakamura et al. 1991). These patients inherit one defective allele of APC and upon loss of the second allele, developed colon adenomas (Polyps) at an early age. These benign polyps frequently acquire other mutations and develop into invasive colon carcinomas. Later studies showed loss of both APC alleles occur in the large majority (>80%) of sporadic colorectal cancers as well (Kinzler and Vogelstein 1996). Following this work, oncogenic misregulation in Wnt signaling was found in many other cancers including liver cancer, skin cancer, lung cancer, Wilms' tumor, prostate cancer and possibly breast cancer (reviewed in (Klaus and Birchmeier 2008)). A variety of developmental genetic defects are known to occur as a result of Wnt misregulation, including defects in limb formation (tetra-amelia), bone density defects, eye vascularization defects, and tooth agenesis (Gong, Slee et al. 2001; Boyden, Mao et al. 2002; Lammi, Arte et al. 2004; Niemann, Zhao et al. 2004; Toomes, Bottomley et al. 2004; Xu, Wang et al. 2004). Understanding this vast array of human diseases and designing therapies to treat and prevent them requires a detailed molecular understanding of the Wnt pathway.

Introduction to the current model of the Wnt pathway

Wnt signals can direct a number of cellular responses and involve distinct and/or overlapping effectors often divided into so-called "canonical" and "noncanonical" pathways. Recent studies have questioned the simplicity of a clear

two-pathway response and so these terms have fallen into disfavor (van Amerongen 2008). For clarity, I will use the term Wnt/β-catenin signaling to identify what was commonly called "canonical" signaling. This nomenclature specifies the ligand (Wnt) and the essential downstream effector (β-catenin). Since my work almost exclusively focuses on Wnt/β-catenin signaling, the various forms of noncanonical signaling will not be discussed.

Wnt/β-catenin signal transduction can be coarsely divided into three central molecular events; 1) surface receptor activation, 2) inhibition of the β-catenin destruction complex, and 3) activation of a nuclear transcriptional complex. The so-called β-catenin destruction complex is a macromolecular machine that efficiently acts to phosphorylate β-catenin targeting it for degradation. I will first describe the players involved in formation of the β-catenin destruction complex (Figure 1) and follow with our current understanding of the behavior of the pathway upon receptor activation.

Axin

A central component of the β-catenin destruction complex is the protein Axin. It was first identified as the gene product of the locus *fused* in mouse (Zeng, Fagotto et al. 1997). It is described as a scaffold protein because of its role in directly binding to many of the other components of the destruction complex and bringing them within close proximity of each other. Two important features of Axin are its low cellular concentration (approximately 20 picomolar, > 2000 fold less

than all other components) and its regulation by the ubiquitin and proteosomal degradation system (Lee, Salic et al. 2003) (Yamamoto, Kishida et al. 1999).

β-catenin

β-Catenin is the substrate of the β-catenin destruction complex, hence the name. Although other substrates of the destruction complex have been identified, the physiological significance of these remain to be substantiated. β-Catenin was first identified in *Drosophila* as the segment polarity gene *armadillo* and also as a component of the adherens junction in *Xenopus* (Nusslein-Volhard and Wieschaus 1980; McCrea, Turck et al. 1991). Through its interaction with nuclear transcription factors, it is the key transcriptional co-activator that dictates the Wnt signaling response. The connection between β-catenin's gene transcriptional role and its more structural role in maintaining integrity of the adherens junction remains elusive.

GSK3

Glycogen synthesis kinase 3 (GSK3) is a ubiquitous serine/threonine protein kinase involved in numerous cellular processes (Forde and Dale 2007). In mammals, there are two distinct genes, alpha and beta, likely to have redundant activities. It was first identified for its role in the regulation of glucose metabolism, targeting muscle glycogen synthase (Embi, Rylatt et al. 1980). The homolog of GSK3 in Drosophila is *Shaggy* or *Zeste White 3* (Siegfried, Chou et al. 1992). The phosphorylation of substrates requires a priming phosphorylation event and thus

GSK3 is often found acting in concert with other kinases. In the Wnt pathway, GSK3 phosphorylates β-catenin, producing a motif that is recognized by the ubiquitin ligase/proteosome protein degradation system.

CK1 alpha

The casein kinase 1 family of kinases are serine/threonine kinases encoded by seven distinct genes in mammals (α, β, γ1, γ2, γ3, δ, and ε; although, β was identified in bovine and may not be found in humans). Like GSK3, casein kinase 1 (CK1) is a widely expressed kinase family with a large number of substrates (Knippschild, Gocht et al. 2005). All CK1 members are highly similar within their catalytic domains but differ significantly in length and sequence of their C-terminal non-catalytic domains. Of note, CK1α appears to be an outlier with a short (~24 amino acids) C-terminal domain compared with the other family members with much longer C-terminal tails (~200 amino acids). CK1α, γ, δ, ε have all been implicated in the Wnt pathway. CK1α has a clear role as a negative regulator through the phosphorylation of β-catenin, where as the others are best characterized as pathways activators. Much works remain to clearly decipher when and where these kinases act and what controls their specificity.

APC

Adenomatous polyposis coli (APC) is a complex and somewhat enigmatic protein. Vogelstein and colleagues first identified the gene in 1991 as the site of mutation of a familial form of colon cancer, familial adenomatous polyposis (FAP)

(Kinzler, Nilbert et al. 1991; Nishisho, Nakamura et al. 1991). APC plays a diverse role in cellular functions that include Wnt signaling, migration, mitotic spindle alignment and apoptosis. Its connection with Wnt signaling was identified in a series of studies that showed APC bound to β-catenin and mutation of APC caused elevated levels of β-catenin in cancer cells (Klaus and Birchmeier 2008).

Others destruction complex factors

Our understanding of all molecular players involved in β-catenin destruction is far from complete. Many other components have been implicated in preliminary molecular studies but have not received a thorough structural or biochemical analysis. Protein phosphatase 2a (PP2a) binds both APC and Axin and likely plays a significant role in β-catenin complex activity (Zhang, Yang et al. 2009). Overexpression studies in cultured cells and Xenopus embryos have shown both a positive and negative role for PP2a. The molecular complexity involving this phosphatase likely comes from the existence of multiple targets in the Wnt pathway that are differentially regulated upon signaling. WTX (Wilms tumor gene on the X chromosome) may have a role in β-catenin destruction. It can bind β-catenin, Axin, APC and β-Trcp and stimulate β-catenin ubiquitination, yet its precise biochemical role, and if it is required in all contexts, is unclear (Major, Camp et al. 2007). Diversin can interact with CK1 and Axin and is required in zebrafish axis specification (Schwarz-Romond, Asbrand et al. 2002). Recent studies though, suggest it may be primarily involved in destruction of β-catenin at certain subcellular localizations such as the centrosome (Itoh, Jenny et al. 2009).

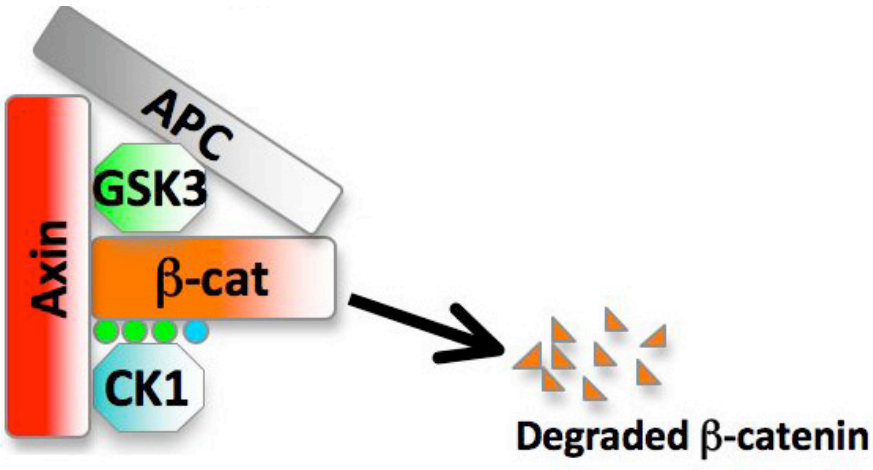

Figure 1.1. Schematic of β-catenin destruction complex. See text for details.

The β-catenin futile cycle

Due to ubiquitous expression of β-catenin and other pathway members, it is likely that all metazoan cells express a macromolecular machine termed the β-catenin destruction complex. Although commonly described as being located in the cytoplasm, the core components can be found in the nucleus as well and it is likely to exist and function there (MacDonald, Tamai et al. 2009). This machine is in a constitutively active state and contains a number of enzymes that target β-catenin for degradation. Thus, in the absence of a Wnt signal, β-catenin is caught in what, on a superficial level, appears to be a futile cycle of synthesis followed by rapid destruction.

Axin is the scaffold protein that nucleates the formation of this complex. It binds with high affinity the two kinases, GSK3 and CK1α. A well-defined α-helix in the middle of Axin anchors GSK3 whereas the site of CK1 has only been mapped to a

region more C-terminal (Dajani, Fraser et al. 2003; Sobrado, Jedlicki et al. 2005). Axin is an unstable protein that is ubiquitinated by an unknown mechanism and is degraded via the proteosome. Binding to GSK3 and CK1 initiates Axin phosphorylation, dramatically slowing its degradation kinetics (Yamamoto, Kishida et al. 1999; Lee, Salic et al. 2003; Cselenyi, Jernigan et al. 2008). APC binds an N-terminal region of Axin termed the RGS domain that has structural homology to domains found in regulators of G-protein signaling (Spink, Polakis et al. 2000).

β-Catenin enters the complex by binding both 15 aa repeats of APC and a single α-helix on Axin just C-terminal to the GSK3 binding site. The exact order and kinetics of the binding event are unclear. In fact, whether it is ordered at all or just stochastic is not known (Lee, Salic et al. 2003; MacDonald, Tamai et al. 2009). The N-terminal region of β-catenin is now positioned for rapid phosphorylation by CK1 at serine 45. This creates a priming site for subsequent and possessive phosphorylation by GSK3 at threonine 41, serine 37 and serine 33 (Amit, Hatzubai et al. 2002; Liu, Li et al. 2002). 20 aa repeats on APC are also phosphorylated by CK1 and GSK3 (Ha, Tonozuka et al. 2004). This increases the affinity of the 20 aa repeats of APC for β-catenin 140 fold and competes β-catenin off the α-helix binding site on Axin. Based on these observations, it as been proposed that APC phosphorylation triggers β-catenin removal from Axin allowing a new β-catenin species to enter the destruction complex (Kimelman and Xu 2006). Once β-catenin is phosphorylated at serine 33 and 37, a destruction consensus sequence is present that is recognized by β-TRCP, a specificity subunit of the Skp1-Cullin-F-box (SCF) ubiquitin ligase (Latres, Chiaur et al. 1999). β-TRCP/β-Catenin binding catalyzes the

polyubiquitination and consequential degradation through the proteosome. These events in totality ensure that newly synthesized, free cytosolic levels of β-catenin are kept below the necessary threshold for gene regulation.

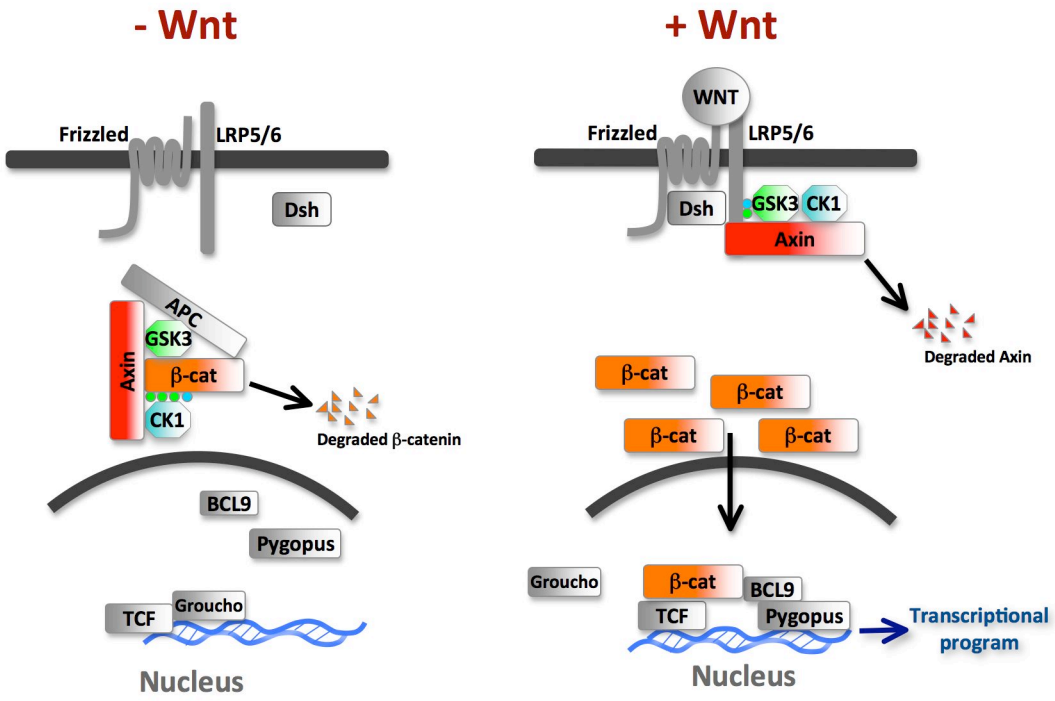

Figure 1.2. Schematic of the Wnt/β-catenin pathway.

Receptor activation

Wnt proteins are morphogens that can act in short and long range signaling. They contain an N-terminal signal peptide for secretion, are N-linked glycosylated and cysteine and serine palmitoleoyated (Willert, Brown et al. 2003; Komekado, Yamamoto et al. 2007) (Takada, Satomi et al. 2006). In mammals, a family of 19

different Wnt exist. All are cysteine rich proteins of ~350-400 amino acids in length.

The Wnt ligand binds two co-receptors Frizzled (Fz) and LRP5/6. Fz is a serpentine seven transmembrane domain protein with structural similarities to G-protein coupled receptors (GPCRs), whereas LRP5/6 is a single pass transmembrane receptor. Wnt physically interacts with the extracellular domains of both receptors. Although the existence of a trimeric complex has not been convincingly demonstrated, both receptors are required to transmit a Wnt signal. There is cell culture-based evidence that upon Wnt signaling Fz and LRP6 form clusters of so-called "signalosomes", but *in vivo*, physiological observation of such events has not been demonstrated (Bilic, Huang et al. 2007). Receptors tyrosine kinases (RYK) such as *Drosophila Derailed* and mouse Ror2 can bind Wnt but are not required. The downstream effectors involved with these receptors are not clear, and in some cases they may act to inhibit Wnt/β-catenin signaling (van Amerongen, Mikels et al. 2008).

There are several secreted proteins that agonize or antagonize Wnt/β-catenin signaling. One class of antagonists are Secreted Frizzled related proteins (sFRPs) and Wnt inhibitory protein (WIF) that bind Wnt ligands directly and block receptor activation (Bovolenta, Esteve et al. 2008). Another class of Wnt signaling antagonists, Dkk1 and Wise/SOST families bind LRP 5/6 and perturb interaction with Wnts (Semenov, Tamai et al. 2001; Mao, Wu et al. 2002). Shisa proteins trap Fz in the ER and prevent it from reaching the cell surface, though these proteins are not specific to Wnt signaling and can regulate FGF receptors as well (Yamamoto, Nagano

et al. 2005). Wnt/β-catenin pathway agonists, besides Wnts themselves, include Norrin and R-spondin (Xu 2004, Kazanskaya 2004, Kim 2005, Nam 2006, Wei 2007). Norrin is specific for Fz4 and is involved in retinal vascularization (Xu, Wang et al. 2004). The mechanism of R-spondin action is controversial because they have been shown to bind both Fz and LRP6, or just LRP6, or neither by three different labs.

Binding of Wnt to Fz and LRP6 initiates a chain of events that leads to the phosphorylation of the intracellular domain of LRP5/6. This receptor contains five PPPSPxS motifs on its intracellular domain that are required for transmission of the signal. In fact, these motifs are sufficient for β-catenin destruction complex inhibition as they can be transferred to heterologous receptors and activate β-catenin signaling (Tamai, Zeng et al. 2004; Zeng, Tamai et al. 2005; MacDonald, Tamai et al. 2009). Interestingly, the kinases involved in PPPSPxS phosphorylation have been identified as GSK3 and CK1 (Davidson, Wu et al. 2005; Zeng, Tamai et al. 2005). Although initial reports were somewhat contradictory as to the order of GSK3 and CK1 activity on LRP6, most recent studies have demonstrated Wnt induces PPPSP phosphorylation by GSK3 and this primes for xS phosphorylation by CK1. There are also CK1 sites outside the PPPSPxS motif in conserved S/T clusters that, when phosphorylated, mediate an interaction between LRP6 and GSK3. Phosphorylated PPPSP sites also act as a docking site for Axin, effectively recruiting cytoplasmic Axin/GSK3 complexes to the cell surface within 5 minutes of addition of Wnt ligand (Mao, Wang et al. 2001; Zeng, Huang et al. 2008). This is thought to further amplify the phosphorylation of additional PPPSP motifs.

Disheveled (Dvl) has long been known to be required genetically in the Wnt/β-catenin pathway (Klingensmith, Nusse et al. 1994). Concurrent with Wnt/receptor interaction, Dvl becomes phosphorylated and recruited to the receptor complex. Dvl and Axin share DIX domains that can polymerize and are required for receptor clustering to occur (Schwarz-Romond, Metcalfe et al. 2007). Loss-of-function studies show Dvl acts upstream of LRP6 (Tolwinski, Wehrli et al. 2003). Yet, in overexpression studies, Drosophila Disheveled and recombinant Dvl in *Xenopus* egg extracts can activate β-catenin signaling independent of Arrow/LRP6 (Salic, Lee et al. 2000; Wehrli, Dougan et al. 2000). Nematodes have no LRP6 homolog suggesting that Dvl could play a more central role in pathway activation in divergent phyla (Phillips and Kimble 2009). The precise involvement of Dvl in receptor activation and Axin recruitment is an area of current research in need of much clarification.

Inhibition of the β-catenin destruction complex

Elevation of β-catenin in response to the presence of Wnt is a hallmark of the Wnt/β-catenin pathway. The precise mechanism of destruction complex inhibition is under intense investigation and a number of proposed mechanisms exist. At the core of all the current models is the inhibition of GSK3's activity toward β-catenin (Kimelman and Xu 2006; MacDonald, Tamai et al. 2009). This has been proposed to arise through several distinct mechanisms: 1) dissociation of components of the β-catenin destruction complex, 2) phosphorylation of GSK3 at serine 9, inhibiting its

activity, 3) LRP6 binding and direct inhibition of GSK3 activity toward β-catenin, 4) Axin degradation upon signaling preventing destruction complex formation.

Several studies have described Axin-GSK3 dissociation upon signaling and suggest this might be the primary mode of destruction complex inhibition (Gao, Seeling et al. 2002; Liu, Li et al. 2002; Logan and Nusse 2004; Luo, Peterson et al. 2007). Early studies seem to suggest Dvl recruits GSK3 binding protein (GBP) to Axin where GSK3 is directly inhibited and dissociates from Axin (Yost, Farr et al. 1998; Farr, Ferkey et al. 2000). One caveat to these studies is the apparent lack of requirement of GBP. *Drosophila* does not have an ortholog of GBP and genetic knockout studies in mouse show no requirement in development or Wnt signaling (van Amerongen, Nawijn et al. 2005). G-protein signaling through Fz has also been proposed to lead to dissociation of the Axin-GSK3 complex (Liu, Rubin et al. 2005). Although intriguing, this work did not demonstrate this event to be required for gene transcription and has yet to be confirmed by other groups. In fact, recent studies appear to observe the opposite; the complex remains intact and localizes to the Fz/LRP6 co-receptors rapidly after Wnt stimulation (Mao, Wang et al. 2001; Yamamoto, Komekado et al. 2006; Bilic, Huang et al. 2007; Hendriksen, Jansen et al. 2008).

GSK3α/β is present in forms phosphorylated at serine 9/21 respectively, and when phosphorylated at this site, kinase activity is greatly reduced (Sutherland, Leighton et al. 1993; Cross, Alessi et al. 1995). Wnt induced stimulation of serine 9/21 phosphorylation has been speculated by a few groups (Ding, Chen et al. 2000; Yokoyama, Yin et al. 2007). However, elegant studies in mouse where non-

phosphorylatable forms of GSK3α/β were both knocked-in produced mice with no developmental defects and no observable perturbation in Wnt pathway activation (McManus, Sakamoto et al. 2005). These mice did not have insulin signaling defects either, raising the intriguing question, what is the physiological role of serine 9/21 phosphorylation?

A set of mammalian cell culture and biochemical studies suggest that the destruction complex moves to the cell surface upon Wnt stimulation, followed by the direct inhibition of GSK3 by LRP6 (Yamamoto, Komekado et al. 2006; Bilic, Huang et al. 2007; Cselenyi, Jernigan et al. 2008; Hendriksen, Jansen et al. 2008; Piao, Lee et al. 2008; Wu, Huang et al. 2009). The collective model from these studies suggests ligand-stimulated LRP6 phosporylation by GSK3 and CK1 creates a docking site for Axin and this in turn recruits the whole complex to the receptor where GSK3 is now the vicinity of multiple PPPSPxS motifs that directly inhibit GSK3s phosphorylation of β-catenin. High-resolution structural data are essential to clarify this model and explain how PPPSPxS motifs are sufficient for both Axin docking and GSK3 inhibition.

A compendium of studies from cell culture, *Xenopus* embryos and egg extract, and *Drosophila* suggest that a conserved and critical event is the degradation of Axin upon Wnt signaling (Yamamoto, Kishida et al. 1999; Tolwinski, Wehrli et al. 2003; Kofron, Birsoy et al. 2007; Cselenyi, Jernigan et al. 2008). In light of the fact that the concentration of Axin is the limiting factor, any regulation of Axin stability is likely to have a dramatic effect on signaling (Lee, Salic et al. 2003). In a set of genetics studies performed in Drosophla designed to get at the requirement of Axin

regulation, flies genetically null for *Zeste white 3* (GSK3 ortholog) had elevated armadillo (β-catenin ortholog) levels yet still had near wild-type embryonic patterning (Tolwinski, Wehrli et al. 2003). The conclusion being, control of Axin stability was sufficient to pattern the embryo. One caveat is these studies were performed in a genetic background of a hypomorphic allele of armadillo, otherwise the *Zeste white 3* patterning phenotype would have masked the effects of Axin regulation. Alternative to these *Drosophila* studies, other work has shown that Axin degradation appears to lag behind β-catenin stabilization and is not even necessary for β-catenin stabilization (Willert, Shibamoto et al. 1999; Hino, Tanji et al. 2005; Liu, Rubin et al. 2005; Cselenyi, Jernigan et al. 2008). These studies promote the model that GSK3 is first inhibited by LRP6 completely blocking β-catenin destruction and Axin is a secondary event of unknown relevance. Chapter IV presents experiments that attempt to solve this dilemma by demonstrating GSK3 inhibition and Axin degradation are both required for a sharp and decisive Wnt response.

β-Catenin-mediated gene transcription

Due to constitutive transcription and translation as well as signal-induced block in proteolysis, β-catenin protein levels rapidly rise after receptor activation (Bryja, Schulte et al. 2007). This occurs simultaneously with nuclear localization, which likely takes into account a number of factors. Early work demonstrated β-catenin could autonomously import by direct interaction with the nuclear pore complex (Henderson and Fagotto 2002). Additionally, Pygopus and BCL9

(described below) have been shown to anchor β-catenin in the nucleus (Bienz and Clevers 2003; Krieghoff, Behrens et al. 2006). Antagonistic to nuclear localization, Axin, APC and RanBP3 (Ran binding protein 3) all function to enrich β-catenin in the cytoplasm (Henderson and Fagotto 2002; Cong and Varmus 2004; Hendriksen, Fagotto et al. 2005). Another study found Rac1 GTPas and Jun N-terminal kinase 2 (JNK2) are activated upon Wnt signaling and are not involved in accumulation but instead promote β-catenin nuclear localization (Wu, Tu et al. 2008). Thus, nuclear and cytoplasmic shuttling of β-catenin involves numerous components for whose contributions we lack a quantitative understanding.

Wnt-induced nuclear β-catenin accumulation leads to an interaction with the TCF/LEF family of DNA-bound transcription factors critical for Wnt-mediated gene regulations (Hoppler and Kavanagh 2007). Invertebrates appear to have only one TCF gene, where as mammals have four, TCF1, LEF1, TCF3 and TCF4. In the absence of β-catenin, TCF interacts with Groucho (TLE1 in vertebrates), represses gene transcription and promotes chromatin compaction. TCF binds at a DNA consensus sequence termed the Wnt responsive element (WRE) of the sequence, CCTTTGXX (X can be either T or A). It has been predicted that there are greater than 6,000 high confidence WRE's in at least one studied colorectal cancer cell line and these collectively regulate 300-400 genes (Hatzis, van der Flier et al. 2008). Upon signaling, β-catenin displaces Groucho and recruits a number of cofactors to TCF and WREs.

Two notable cofactors, Pygopus (Pygo) and BCL9, are found in *Drosophila* and vertebrates (Belenkaya, Han et al. 2002; Parker, Jemison et al. 2002; Thompson,

Townsley et al. 2002). BCL9 binds β-catenin directly and links it to Pygo. Pygo can bind the multiprotein transcriptional coactivator, Mediator complex, and contains a plant homology domain (PHD) that binds dimethylated Histone 3 lysine 4 (H3K4) (Fiedler, Sanchez-Barrena et al. 2008). Thus TCF, β-catenin, BCL9 and Pygo represent a core transcriptional complex that is central to Wnt-mediated gene transcription (Figure 1.3). In *Drosophila* they are all strictly required, yet in mammals, there appears to be additional functional redundancy and cell type specific roles for BCL9 and Pygo (Schwab, Patterson et al. 2007; Sustmann, Flach et al. 2008).

Outside of Pygo and BCL9, β-catenin interacts with an extensive set of chromatin remodeling complexes that include p300/CBP and TRRAP/TIP60 histone acetyltransferase (HATS), the SWI/SNF family of ATPases for chromatin remodeling, PAF1 complex for transcription elongation and histone modification, and MLL1/2 histone methyltransferases (HMTs) (Willert and Jones 2006; Mosimann, Hausmann et al. 2009). Although it is known that most of these complexes interact with the C-terminal end of β-catenin, the order and timing of these interactions remains unclear. A role in extensive chromatin remodeling at TCF/β-catenin bound promoter regions appears to be an important aspect of Wnt signaling.

It is important to note an often-underappreciated role for TCF/β-catenin signaling in transcription repression. Studies have shown a number of potential mechanisms of repression including TCF/β-catenin competing with transcriptional activators, recruitment of co-repressors to WREs, or TCF binding to a novel consensus sequence that specifically mediates repression (Piepenburg, Vorbruggen

et al. 2000; Jamora, DasGupta et al. 2003; Kahler and Westendorf 2003; Theisen, Syed et al. 2007; Blauwkamp, Chang et al. 2008). In addition, there are a plethora of accounts of DNA-binding transcription factors (e.g. smad3, AP-1, RXR Kaiso, just to name a few) binding to β-catenin to activate or repress Wnt/β-catenin target genes. In light of the large number of TCF binding sites and numerous transcriptional co-regulators, it is clear the Wnt/β-catenin gene expression program is vast and induces dramatic changes in the physiological state of the cell, much of which remains to be understood.

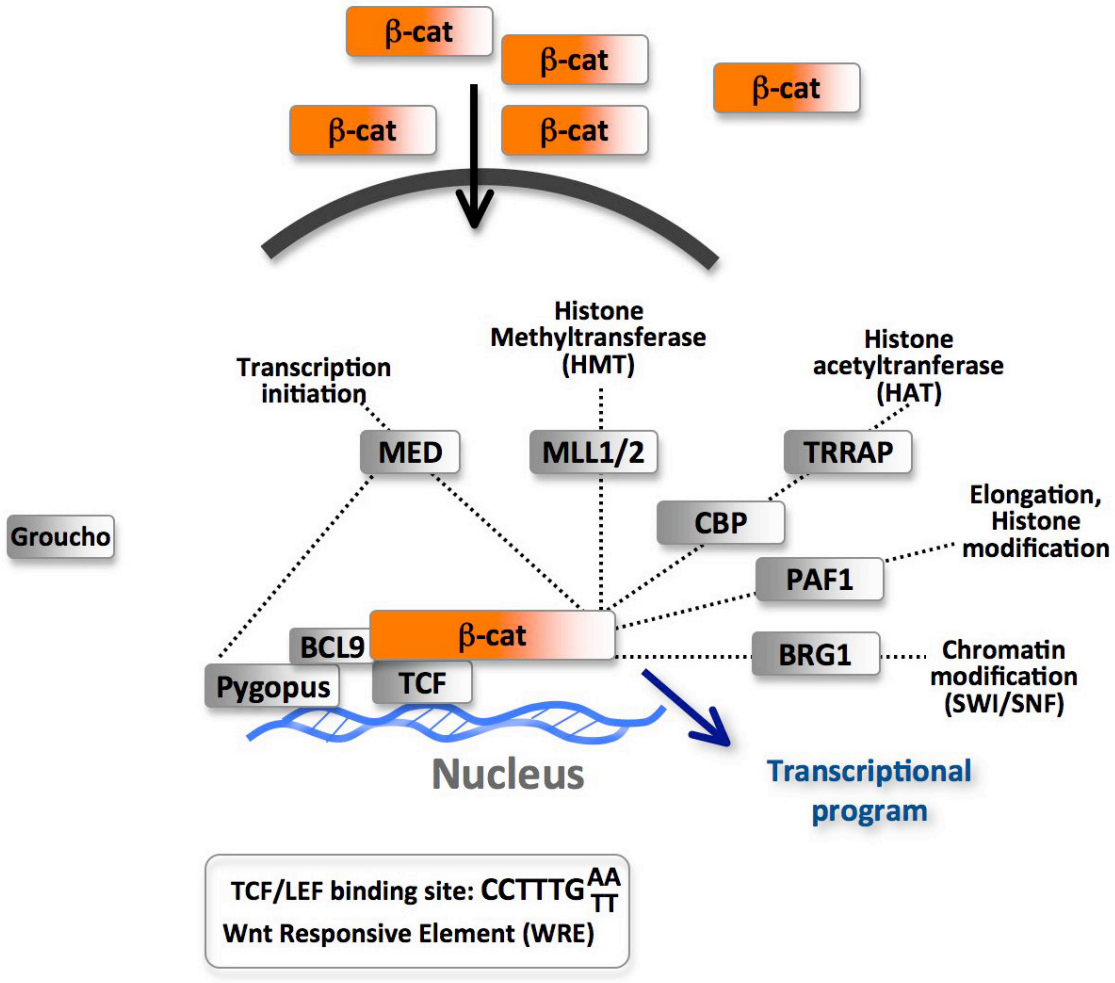

Figure 1.3. Schematic of the nuclear transcriptional machiner

Small molecule inhibition of the Wnt pathway

To date, the scientific community has made major advances in our understanding of molecules involved in misregulation of the Wnt pathway in various human disorders. I have already mentioned mutant APC is found in the large majority of sporadic colorectal cancers, but also less frequently, mutations in β-catenin and Axin are found. It is estimated that over 90% of colorectal cancers contain genetic lesions that disrupt β-catenin or the function of the β-catenin destruction complex. Currently there are no late-stage therapeutics that directly target the Wnt pathway.

Ideal drugs would restore activity of the β-catenin destruction complex or target the pathway downstream of it. Intuitively, disruption of the TCF-β-catenin interaction could be a promising drug target. Although drugs targeting protein-protein interactions have not been substantiated as valid therapies, dedicated efforts have been successful identifying small molecules that block TCF-β-catenin interaction (Clevers 2004; Lepourcelet, Chen et al. 2004). These compounds have been valuable as proof of principle tools yet there is one major caveat to the potential usefulness of these compounds; TCF, APC and E-caderin all bind β-catenin on significantly overlapping domains. Thus, an effective drug that targets this site would likely have pleiotropic effects on β-catenin's functions at adherens junctions and in the destruction complex. In addition, even though the TCF-β-catenin complex has been a high priority target for pharmaceuticals and biotechnology, no successful reports have emerged.

An *in silico* drug screen based on the crystal structure of Dvl's PDZ domain has produced a compound that can block Fz-Dvl interaction (Shan, Shi et al. 2005; Grandy, Shan et al. 2009; Shan and Zheng 2009). Unfortunately the extremely low affinity (K_d 237 μM) and its action upstream to the destruction complex has limited it usefulness as a therapy.

β-catenin binds the co-activator cAMP response element-binding protein (CREB) binding protein (CBP). Researchers identified a compound that selectively binds CBP and prevents its interaction with β-catenin (Emami, Nguyen et al. 2004). This compound efficiently decreased TCF-β-catenin reporter gene activity, yet only selectively blocked a small number of Wnt target genes responsible for suppression of apoptosis. Nonetheless, drug treatment induced apoptosis in colon cancer cell lines but not in non-transformed cells. Additionally, *in vivo* studies showed it reduced tumor burden in APC mutant mice. Despite these intriguing findings, for unknown reasons this compound has not moved into the clinic.

Recently, compounds that prevent Axin degradation through the inhibition of tankyrase have been identified (Chen, Dodge et al. 2009; Huang, Mishina et al. 2009). These finding were important because they validated the hypothesis that stabilization of Axin could overcome mutant APC and uncovered more details to mechanisms controlling Axin stability. As to their specificity (tankyrases have many substrates outside of the Wnt pathway) and efficacy (no *in vivo* cancer models tested) many outstanding questions for tankyrase inhibitors remain.

A Chemical and Systems approach

Central to my personal approach to scientific research is the following question: How can I address and solve difficult biological questions in ways others cannot or do not? If someone else can do exactly what I am doing, what am I contributing? This way of thinking is both inspirational and haunting to me, constantly pushing me outside my comfort zone. The fields of Chemical and Systems Biology are emerging fields asking new questions and providing novel approaches. They rely heavily on the blending of various scientific disciplines through collaboration, a process I find alluring. The work presented in this thesis roughly breaks into two sections, a chemical approach (Chapter III) and a systems approach (Chapter IV) to understanding mechanisms of Wnt signaling. My chemical studies have required I work hand-in-hand with experts in chemistry and robotics. My systems studies have necessitated collaborations with mathematicians and computer scientists. These collaborations and approaches have helped me answer pressing questions in Wnt signal transduction and uncover a few new questions along the way.

CHAPTER II

MATERIALS AND METHODS

Screen for chemical modulators of Wnt signaling

Radiolabeled β-catenin and Axin were generated in rabbit reticulocyte lysates (Promega). *Xenopus* egg extract preparation and degradation assays were performed as previously described(Murray 1991). β-catenin-FLuc and Axin-RLuc were generated in TNT SP6 High-Yield Protein Expression System (Promega). *In vitro*-translated (IVT) β-catenin-FLuc, Axin-RLuc, and LRP6ICD (400 nM) were added to 100 ml of egg extract and rotated end-over-end at 4°C for 10 minutes. Samples were dispensed into 384-well plates (5 μl/well) at 4°C prior to pin transfer of compounds at 25°C. Final concentrations of compounds ranged from ~40-200 μm in 2% DMSO. Plates were sealed, vortexed, and incubated for 4 hours at 25°C. After incubation, firefly and *Renilla* luciferase activities were measured using the Dual-Glo Luciferase Assay (Promega) on an EnVision plate reader (Perkin Elmer).

Screen statistics

We normalized each plate using the method outlined in Malo et al. (Malo, Hanley et al. 2006). The normalization procedure uses Tukey's median polish[2] to remove systematic row and column biases (e.g. edge effects). Following normalization, a B-score value was obtained for each well that represents log intensities for each compound in a well. The differences of the log intensities

between the Axin and β-catenin wells for each plate were obtained (equivalent to the ratio on the non-log scale). Compounds identified as hits (based on empirical distribution) in both replicates were added to the candidate list.

Chemical compounds and recombinant proteins

Reagents used include pyrvinium pamoate (MP Biomedicals); interleukin-4 (Sigma I4269); EGFR-c (gift from Marc Kirschner); TGF-alpha (gift from Robert Coffey); BMP4 (Sigma B2680); cycloheximide (Sigma, C7698); CK1-7 (Sigma C0742); CK1 alpha, gamma1, delta, and epsilon (Invitrogen); GSK3 and CK1 delta (1-317) (New England Biolabs); CAMKII, PKA, AKT1, and STK3 (SignalChem). LRP6ICD was prepared as previously described with modifications[4]. Bacterial pellets were denatured with 6 M guanidine HCl, and histidine-tagged LRP6ICD was bound to nickel resin and eluted with imidazole. Eluate was dialyzed to remove guanidine HCl. Pyrvinium iodide, VU-WS211, VU-WS113, and IWR-1 were synthesized by the Vanderbilt Institute of Chemical Biology's medicinal chemistry core. Chemical structures were drawn using CS ChemDraw Ultra. DMSO was used as vehicle for pyrvinium in all experiments unless otherwise stated.

Reporter assays

For cell-based luciferase assays, HEK 293 STF, CMV-Luc and *Drosophila* S2 cells were seeded into 96-well plates at sub-confluent levels and luciferase activities measured by Steady-Glo Luciferase Assay (Promega). Luciferase activities were normalized to viable cell number using the CellTiter-Glo Assay (Promega). TOPflash

experiments in HCT116 WTKO and SW480 cells were normalized to co-transfected *Renilla* gene expression. All graphs were made in Prism 4 (GraphPad Software, inc.) with nonlinear regression fit to a sigmoidal dose-response curve (variable slope). BRE, SRE, and STAT6 reporter assays were performed as previously described(Mithani, Balch et al. 2004) (Gille, Kortenjann et al. 1995) (Goenka and Boothby 2006). For siRNA silencing, HEK 293 STF cells were transfected with ON-TARGETplus siRNA (Thermo Scientific Dharmacon) against Axin1 (J-009625-06), Axin2 (J-008809-05), or APC (J-003869-09) for 48 hours according to manufacturer's protocol. Cells were then treated with pyrvinium for 24 hours prior to performing luciferase and cell viability assays. Silencing of CK1α in Jurkat cells has been previously described(Bidere, Ngo et al. 2009). Briefly, CK1α^{sh} or control^{sh} cells were treated for 48 hours with doxycycline, then 24 hours with Wnt3a-conditioned media in the presence or absence of pyrvinium. For TOPflash in Jurkat cells, cell were transfected with TOPflash reporter and Renilla transfection control 24 hours after doxycycline treatement. Wnt3a and pyrvinium were added 24 hours after transfection for an additional 24 hours. For apoptosis assays, SW620 cells were seeded in 96-well plates at $5x10^3$ cells/100 ul/well, and pyrvinium and/or 5-FU were added after attachment. After 24 hours, phase contrast micrographs were obtained and caspase 3/7 activity measured by Apo-ONE Homogeneous Caspase-3/7 Assay (Promega) according to manufacturer's instructions.

Cell lines

The following cell lines were gifts: HEK 293 STF (Jeremy Nathans), HCT116 WTKO (Robert Coffey), S2 TOPflash (Roel Nusse), and Jurkat CK1α^{sh} and control^{sh} cells (Michael Lenardo). HEK 293, IEC-6, SW480, RKO, and L Wnt3a and L cells were purchased from ATCC. Wg-secreting cells were purchased from the *Drosophila* Genomics Resource Center. A HEK 293 cell line stably expressing firefly luciferase under the control of the CMV promoter (CMV-Luc) was generated using standard methods. Mammalian cell lines were maintained in DMEM (except SW480 cells, which were maintained in RPMI), 10% fetal bovine serum (FBS), and antibiotics. *Drosophila* S2 cells were maintained in Schneider's medium plus 10% FBS. Cells are treated with compounds and/or Wnt for 24 hours unless otherwise stated.

Dot blots

For ligand dot blot assay, purified protein (0.5 μg) was dotted on wet nitrocellulose membranes and blocked for 1 hour using 5% milk in TBS. Pyrvinium was then added to the blocking solution and incubated for 3 hours at 23°C or overnight at 4°C. After incubation with pyrvinium, the membrane was washed three times for 5 minutes in TBS plus 0.1 % Tween 20. The pyrvinium fluorescence image was acquired on a Xenogen IVIS 200 using excitation 500-550 and emission 575-650 spectrum fluorescence settings. Replicate dot blots were stained with Colloidal Gold (Bio-Rad) to visualize total protein bound to membrane.

Kinase assays

In vitro kinase assays were performed as previously described.[4] For CK1 isoforms and GSK3, casein (1 μM; Sigma C8032) was used as substrate. All other kinases were tested with previously characterized and commercially available peptide substrates (400 μM; Invitrogen, SignalChem, New England Biolabs) and diluted to a concentration at which activity was linear with respect to time and enzyme concentration.

Mass spectrometry

HEK 293 cells expressing HA-CK1α, HA-GSK3, or HA (control) were treated for 24 hours with pyrvinium (100 nM). HA-tagged proteins were immunoprecipitated from cell lysates and subjected to liquid chromatography-mass spectrometry (LC-MS). The amount of pyrvinium within immunoprecipitates (based on relative abundance) was quantified. Non-specific binding of pyrvinium to beads (HA control) was subtracted from measurements for HA-GSK3 and HA-CK1α samples. LC-MS was performed by Vanderbilt University's Mass Spectrometry Service Laboratory.

Antibodies

Immunoblotting was performed using the following antibodies: α-β-catenin (BD Transduction Labs); α-phospho-βcat (p33, 37, 41), α-MAPK 137F5, α-pSMAD1/5 41D10, α-SMAD1, α-pSTAT6 C11A12, α-STAT6 (Cell Signaling); mouse α-Axin1 (Zymed); goat α-Axin1 (R&D Antibodies); α-actin (ImmunO); α-ac-H3

(Upstate); α-Ki-67 (Abcam); α-ZO-1 (Invitrogen); α-HA 3F10 (Roche); rabbit α-hPygo2 H-216, rabbit α-CK1α (Santa Cruz); α-β-galactosidase, α-pMAPK (Promega); *Xenopus* β-catenin antibody (gift from Barry Gumbiner).

Plasmids

β-catenin-FLuc and Axin-RLuc fusions were generated using standard PCR-based cloning strategies and subcloned into the pCS2 vector. The bacterial expression construct of LRP6ICD has been described(Cselenyi, Jernigan et al. 2008). The following plasmids were gifts: HA-hPygo2 (Mariann Bienz), HA-TCF4 (Scott Hiebert), and HA-BCL9 (Konrad Basler).

Immunoblot analysis

Cells were lysed in non-denaturing buffer (50 mM Tris-Cl (pH 7.4), 300 mM NaCl, 5 mM EDTA, 1% (w/v) Triton X-100) and the soluble fraction used for immunoblotting. For HA-tagged protein expression, cells were seeded in a 60 mm dish and transfected overnight (Lipofectamine 2000, Invitrogen) with 8 μg HA-tagged construct and 2 μg β-galactosidase (internal control). Cells were then split into separate wells, allowed to adhere, and treated as indicated. For cycloheximide (CHX)-chase experiments, cells were treated with 50 ug/ml CHX for the indicated time. For Axin immunoblots, Axin was immunoprecipitated with mouse anti-Axin antibodies (Zymed) and immunoblotted with anti-Axin1 goat antibody (R&D Antibodies). Cytoplasmic/nuclear fractionation was performed as follows. Cells were incubated on ice for 15 minutes in lysis buffer (10 mM HEPES (pH 7.8), 10 mM

KCl, 2 mM $MgCl_2$, 0.1 mM EDTA), scraped, transferred to microfuge tubes, and NP-40 was added to 0.5%. Lysates were vortexed, sheared through a 23-gauge needle, and spun at 16,000Xg for 2 minutes. Supernatants (cytoplasmic fractions) were recovered. Pellets were resuspended in extraction buffer (50 mM HEPES (pH 7.8), 50 mM KCl, 300 mM NaCl, 0.1 mM EDTA, 10% glycerol), vortexed, incubated on ice for 30 minutes, centrifuged at 3,000Xg for 30 seconds, and supernatants discarded. Pellets were resuspended in extraction buffer, vortexed, spun at 3,000Xg and supernatants discarded. Pellets (nuclear fraction) were resuspended in RIPA buffer (50 mM Tris (pH 8.0), 150 mM NaCl, 1% NP40, 0.5% deoxycholic acid, 0.1% SDS, 0.5 mM EDTA).

Immunofluorescence

Cells were seeded on fibronectin-coated coverslips, fixed in 3.7% formaldehyde, stained, and mounted in VectaShield with DAPI (Vector Laboratories). Images were acquired using a CoolSNAP ES camera mounted on a Nikon Eclipse 80i fluorescence microscope with 60X or 100X objectives.

Real-time RT-PCR

Total RNA was isolated from HEK 293 cells 24 hours after pyrvinium treatment using RNAeasy RNA extraction kit (Qiagen) and cDNA generated using High Capacity cDNA Reverse Transcription kit (Applied Biosystems, ABI). Real-time PCR assays were performed in quadruplicate using TaqMan Gene Expression Master

Mix (ABI), gene-specific TaqMan TAMRA probes (ABI), and an ABI 7000 sequence detection system.

Xenopus laevis studies

Xenopus embryos were *in vitro* fertilized, dejellied, maintained, and injected as previously described(Peng 1991). Pyrvinium was dissolved in 100% DMSO for injections. Capped Xwnt8 mRNA was generated using mMessage mMachine (Ambion) according to manufacturer's instructions. Whole-mount *in situ* hybridization was performed as described for *chordin*(Harland 1991). Animal caps were cut from stage 9 embryos cultured until stage 11, and RT-PCR for *siamois, Xnr3, and ODC* was performed as described(Cselenyi, Jernigan et al. 2008).

Drosophila studies

Drosophila embryos (0-30 minutes) were dechorionated, desiccated, and microinjected within 45 minutes according to standard techniques. Embryos were injected with pyrvinium (300 μM in 20 mM HEPES (pH 7.5), 150 mM NaCl, 10% methyl-β-cyclodextrin, and 10% DMSO) in ~1-5% of total embryo volume, coated with halocarbon oil 27, and incubated for 24 hours at 25°C. Cuticle preparations were performed as described[7].

C. elegans studies

(performed by Judson Schneider in Dr. David Miller's lab)

C*. elegans* were grown on a lawn of *E. coli* on plates containing nematode

growth media (NGM). Pyrvinium was dissolved in either ethanol or DMSO. For vulval morphology experiments, worms were treated from L1 larval until adult stages (3 days) on plates containing pyrvinium (10 μM) or vehicle (0.1% ethanol). Worms were picked off plates and placed on glass slides for visual inspection of vulval morphology under Nomarski optics. Eggs retained in the uterus were counted for each treatment group and the two groups compared using a one-tailed t-test. Q neuroblast daughter cells, QL and QR, were marked by *mec-7*::GFP 8, and Q neuroblast migration was scored at the L4 larval stage using a fluorescent stereo dissecting scope. For all of these experiments, the observer was blinded to the specific treatment to avoid bias.

Trypsin Digest

Recombinant CK1α (0.5 ug) was preincubated for 5 min at RT in the presence or absence of 100 nM pyrvinium followed by incubation at RT with bovine pancreatic trypsin (50 ng). After 10 minutes, excess soybean trypsin inhibitor was added and samples analyzed by SDS-PAGE followed by silver staining.

Flow cytometry

MeOH, 16% formaldehyde, and Incubation buffer (1% BSA in PBS) were used for the following method. Volumes are for one well of a 6-well dish with ~0.5 – 1 million cells. All spins are at 200xg for 5 mins. First, cells were washed with PBS and trypsinized with 250 ul trypsin. 2 mls of culture medium was added to the wells and cells resuspended. Cells were fix by adding 250 ul of 16% formaldehyde to the cells

suspended in media, incubate at RT for 10 mins. Cells were spun down, media poured off. 1ml of ice cold MeOH was added and vortex vigorously for 5 sec. Incubated on ice for 30 min. Spun down, poured off MeOH, and washed twice with 3 ml of incubation buffer. Samples were Incubated in 2 ml incubation buffer for 10 mins to block nonspecific antibody binding, spun down and buffer poured off. Cells were resuspend in 100ul incubation buffer, 50 ng of primary antibody was added and incubate at RT for 30 min. Samples were washed twice in incubation buffer, resuspended in 100 ul incubation buffer, and fluorescent secondary antibody (1:500) was added. Samples incubated at RT for 30 mins and kept covered from light for all subsequent steps. Cells were washed twice in incubation buffer, resuspended in 500 ul of PBS. For staining of DNA, PBS contained 200 ug/ml RNase A and 10 ug/ml Propidium iodide. Samples were read at the Vanderbilt flow cytometry core.

Chemical synthesis

(Performed by the Vanderbilt Chemical Synthesis Core)

General: All NMR spectra were recorded on a Varian Inova 400 (400 MHz) spectrophotometer located in the Small Molecule NMR Facility at Vanderbilt University. 1H chemical shifts are reported in δ values in ppm downfield from TMS as the internal standard. Data are reported as follows: chemical shift, multiplicity, coupling constant (Hz), integration. Splitting patterns describe apparent multiplicities and are designated as s (singlet), d (doublet), t (triplet), q (quartet), m (multiplet), br (broad). 13C chemical shifts are reported in δ values in ppm. Low-

resolution mass spectra were obtained on an Agilent 1200 LCMS with electrospray ionization. High-resolution mass spectra were recorded on a Waters Qtof- API-US plus Acquity system. Analytical thin layer chromatography was performed on 250 mM silica gel 60 F254 plates. Analytical HPLC was performed on an Agilent 1200 analytical LCMS with UV detection at 214 nm and 254 nm along with ELSD detection. Flash column chromatography was performed on silica gel (230-400 mesh, Merck) or using automated silica gel chromatography (Isco, Inc. 100sg Combiflash).

Preparation of IWR-1

This molecule was prepared according to the published methods, with all characterization data in agreement: "Small molecule–mediated disruption of Wnt-dependent signaling in tissue regeneration and cancer" Chen, B.; Dodge, M. E.; Tang, W.; Lu, J.; Ma, Z.; Fan, C-W; Wei, S.; Hao, W.; Kilgore, J.; Williams, N. S.; Roth, M. G.; Amatruda, J. F.; Chen, C.; Lum, L. *Nature Chemical Biology* 2009, *5*, 100 – 107.

Preparation of VU-WS211

1-(2,5-Dimethyl-1-phenyl-1*H*-pyrrol-3-yl)-2-(quinolin-2-yl)ethanol: A solution of 2-methylquinoline (0.27 mL, 2.0 mmol) in THF (7 mL) was cooled to -78 ^{o}C. To this solution was added *n*-BuLi in hexanes (2.5 M, 0.88 mL, 2.21 mmol), and the mixture was allowed to warm 0 ^{o}C and stirred for 60 min followed by warming to room temperature with additional stirring for 30 min. The reaction was cooled (-78 ^{o}C) and 2,5-dimethyl-1-phenyl-1H-pyrrole-3-carbaldehyde (0.4 g, 2.0 mmol) in THF (2

mL) was added over 5 min. The reaction mixture was allowed to warm to room temperature over a 60 min period, stirred for 3 h, diluted in ethyl acetate, and then washed with saturated NH_4Cl (3 x 10 mL). The organic phase was dried over $MgSO_4$ and evaporated *in vacuo* affording crude product which was purified by flash column chromatography on silica gel (hexane/ethyl acetate = 4/1) to provide oil product 1 (0.59 g, 86%). ^1H NMR ($CDCl_3$, 400 MHz) ∂ (ppm) 8.09 (dd, *J* = 4.0, 8.4 Hz, 2H), 7.80 (d, *J* = 8.0 Hz, 1H), 7.71 (t, *J* = 7.2 Hz, 1H), 7.52 (t, *J* = 7.2 Hz, 1H), 7.46 (t, *J* = 7.2 Hz, 2H), 7.39 (t, *J* = 7.2 Hz, 1H), 7.30 (d, *J* = 8.4 Hz, 1H), 7.22 (d, *J* = 7.6 Hz, 2H), 6.13 (s, 1H), 5.34 (dd, *J* = 2.4, 10.0 Hz, 1H), 3.58 (dd, *J* = 10.0, 15.6 Hz, 1H), 3.31 (dd, *J* = 2.4, 15.6 Hz, 1H), 2.05 (s, 6H); ^{13}C NMR ($CDCl_3$, 100 MHz) ∂ (ppm) 161.34, 147.20, 138.83, 136.42, 129.53, 128.96, 128.78, 128.35, 128.27, 127.57, 127.48, 126.77, 125.95, 125.42, 122.20, 121.43, 104.19, 66.63, 45.44, 12.87, 10.85; LCMS showed dehydrated peak.

(*E*)-2-(2-(2,5-Dimethyl-1-phenyl-1*H*-pyrrol-3-yl)vinyl)quinoline (VU-WS211): To a solution of 1-(2,5-dimethyl-1-phenyl-1H-pyrrol-3-yl)-2-(quinolin-2-yl)ethanol (0.59 g, 1.82 mmol) in dichlromethane (9 mL) were added MsCl (0.28 mL, 3.64 mmol) and pyridine (0.44 mL, 5.46 mmol) at 0 ^oC. The reaction mixture was allowed to warm to room temperature, stirred overnight, and then washed with saturated NH_4Cl (3 x 10 mL). The resulting aqueous solution was extracted with CH_2Cl_2 (3 x 15 mL). The combined organic layer was dried over $MgSO_4$ and evaporated. The crude product was purified by flash column chromatography on silica gel (hexane/ethyl acetate = 4/1) to provide VUWS211 (0.24 g, 41%). ^1H NMR ($CDCl_3$, 400 MHz) d (ppm) 8.04 (t, *J* = 8.0 Hz, 2H), 7.74-7.61 (m, 4H), 7.48 (t, *J* = 7.6 Hz, 2H), 7.42 (t, *J* = 7.6 Hz, 2H), 7.22

(d, *J* = 7.6 Hz, 2H), 7.06 (d, *J* = 16.0 Hz, 1H), 6.38 (s, 1H), 2.19 (s, 3H), 2.05 (s, 3H); ^{13}C NMR ($CDCl_3$, 100 MHz) d (ppm) 157.47, 148.27, 138.23, 135.77, 130.34, 130.26, 129.35, 129.16, 128.70, 128.13, 128.01, 127.70, 127.33, 126.80, 125.17, 123.37, 118.84, 118.20, 103.53, 12.83, 10.96; LCMS, single peak, 1.36 min, *m/e*, 325.2 (M+1); m.p.: 58 - 60^{o}C; HRMS (ESI TOF) calcd for $C_{23}H_{21}N_2$ $(M + H)^+$ 325.1705, found 325.1703.

Preparation of pyrvinium iodide

(*E*)-2-(2-(2,5-Dimethyl-1-phenyl-1*H*-pyrrol-3-yl)vinyl)-*N*,*N*-dimethylquinolin-6-amine: This compound was synthesized by the same methods used above, except using N,N,2-trimethylquinolin-6-amine. ^{1}H NMR ($CDCl_3$, 400 MHz) ∂ (ppm) 7.91 (d, *J* = 9.6 Hz, 1H), 7.87 (d, *J* = 8.8 Hz, 1H), 7.57-7.38 (m, 5H), 7.32 (dd, *J* = 2.8, 9.2 Hz, 1H), 7.21 (d, *J* = 6.8 Hz, 2H), 7.02 (d, *J* = 16.0 Hz, 1H), 6.78 (d, *J* = 2.4 Hz, 1H), 6.35 (s, 1H), 3.06 (s, 6H), 2.16 (s, 3H), 2.04 (s, 3H); ^{13}C NMR ($CDCl_3$, 100 MHz) ∂ (ppm) 153.62, 148.02, 138.40, 134.23, 130.10, 129.65, 129.16, 128.22, 127.95, 125.66, 123.69, 119.27, 118.93, 118.40, 105.52, 103.51, 40.77, 12.88, 10.98; LCMS, single peak, 1.48 min, *m/e*, 368.2 (M+1); m.p.: 158 – 161^{o}C; HRMS (ESI TOF) calcd for $C_{25}H_{26}N_3$ $(M + H)^+$ 368.2127, found 368.2123.

Pyrvinium iodide ((*E*)-2-(2-(2,5-dimethyl-1-phenyl-1*H*-pyrrol-3-yl)vinyl)-6-(dimethylamino)-1-methylquinolin-1-ium iodide): A mixture of (E)-2-(2-(2,5-dimethyl-1-phenyl-1H-pyrrol-3-yl)vinyl)-N,N-dimethyl quinolin-6-amine (100 mg, 0.27 mmol), methyl iodide (20 mL, 0.33 mmol), and toluene (3 mL) was heated in a sealed tube at 80 ^{o}C for 24 h. The solvent was removed *in vacuo* and then triturated

with ethyl acetate (3 x 7 mL) to provide a red solid product (90 mg, 87 %). ^{1}H NMR (DMSO, 400 MHz) ∂ (ppm); 8.51 (d, *J* = 9.2 Hz, 1H), 8.44 (d, *J* = 9.2 Hz, 1H), 8.21 (d, *J* = 10.0 Hz, 1H), 8.08 (d, *J* = 15.2 Hz, 1H), 7.61 – 7.49 (m, 4H), 7.35 (d, *J* = 7.6 Hz, 2H), 7.23 (d, *J* = 8.0 Hz, 1H), 7.21 (d, *J* = 10.0 Hz, 1H), 6.72 (s, 1H), 4.35 (s, 3H), 3.10 (s, 6H), 2.23 (s, 3H), 2.00 (s, 3H); ^{13}C NMR ($CDCl_3$, 100 MHz) ∂ (ppm) 151.55, 148.81, 139.84, 138.92, 136.93, 135.96, 131.37, 131.29, 129.61, 128.74, 128.69, 127.93, 127.85, 121.39, 120.09, 119.51, 119.04, 111.64, 106.40, 104.65, 40.34, 38.45, 12.65, 10.82; LCMS, single peak, 1.55 min, *m/e*, 383.7 (M+1); m.p.; 255 – 258 ^{o}C; HRMS (ESI TOF) calcd for $C_{26}H_{28}N_3$ $(M + H)^+$ 382.2283, found 382.2282.

Preparation of VU-WS113

N-(6-bromoquinolin-2-yl)-2,5-dimethyl-1-phenyl-1H-pyrrole-3-carboxamide: In a conical shaped microwave vial was added 2-amino-6-bromoquinoline hydrochloride (100 mg, 0.385 mmol) and dichloroethane (DCE, 3.8 mL). To this suspension was added Hunig's base (0.30 mL, 1.73 mmol). The solution turned deep brown and the solids dissolved. 2,5-dimethyl-1-phenyl-1H-pyrrole-3-carboxylic acid (107 mg, 0.501 mmol) and 1-[chloro(pyrrolidin-1-yl)methylene]pyrrolidin-1-ium hexafluorophosphate(V) (PyClU, 256 mg, 0.771 mmol) were added. The microwave vial was capped and heated under microwave irradiation for 1.5 h at 110 °C. After cooling, the solution was concentrated and the residue was purified on silica gel using a Biotage SNAP cartridge (2% to 20% MeOH in dicholormethane) to yield 144 mg (0.34 mmol, 89%) of the desired compound as a beige powder. LCMS: R_T = 1.44 min, >90% @ 254 nm, >92% @ 220 nm; *m/z* $(M + 1)^+$ = 420. ^{1}H NMR (400

MHz, CD_3OD, δ (ppm)): 8.6 (d; *J* = 9.2 Hz; 1 H), 8.0 (d; *J* = 9.2 Hz; 1H), 7.9 (s; 1H), 7.8 (s; 1H), 7.5-7.4 (m; 4H), 7.2 (d; J = 6.8 Hz; 2H), 6.3 (s; 1H), 2.4 (s; 3H), 2.0 (s; 3H). ^{13}C NMR (100 MHz; CD_3OD, δ (ppm)): 164.4, 152.4, 145.5, 137.6, 137.3, 136.5, 133.2, 129.7, 129.6, 129.4, 129.0, 128.9, 128.2, 127.3, 118.1, 115.6, 133.8, 104.9, 12.9, 12.7. HRMS calculated for $C_{22}H_{19}N_3OBr$ $(M+H)^+$ *m/z*: 420.0711, measured 420.0707.

2,5-dimethyl-N-(6-(morpholinomethyl)quinolin-2-yl)-1-phenyl-1H-pyrrole-3-carboxamide (VU-WS113): In a conical shaped microwave vial was added N-(6-bromoquinolin-2-yl)-2,5-dimethyl-1-phenyl-1H-pyrrole-3-carboxamide (71 mg, 0.169 mmol), potassium trifluoro(morpholinomethyl)borate (70 mg, 0.338 mmol), 2-Dicyclohexylphosphino-2□,4□,6□-triisopropylbiphenyl (XPhos, 16.1 mg, 0.034 mmol), cesium carbonate (165 mg, 0.507 mmol), and palladium (II) acetate (3.8 mg, 0.017 mmol), THF (0.63 mL) and water (0.06 mL). The microwave vial was capped and the solids were stirred at RT for 5 min to aid in dissolution. Once a clear solution was observed, the vial was heated to 80 °C for 10 min followed by heating to 145 °C for 45 min. After cooling, the solution was diluted with dichloromethane and dried over $MgSO_4$. The solution was filtered, concentrated and purified on silica gel using a Biotage SNAP cartridge (2 % to 20% MeOH in dichloromethane) to yield 71 mg (0.16 mmol, 95%) of VU-WS113 as a yellow oil: LCMS: R_T = 1.11 min; *m/z* $(M + 1)^+$ = 441. ^1H NMR (400 MHz, $CDCl_3$, δ (ppm)): 8.4 (d; *J* = 8.8 Hz; 1H), 8.3 (d; *J* = 8.8 Hz; 1H), 7.8-7.7 (m; 5H), 7.3 (d; *J* = 7.2Hz; 2H), 6.5 (s; 1H), 3.8-3.7 (m; 10H), 2.5-2.4 (m; 8H), 2.3 (s; 3H), 2.0 (s; 3H). ^{13}C NMR (100 MHz; $CDCl_3$, δ (ppm)): 166.7, 152.0, 147.3, 139.5, 138.9, 135.6, 132.8, 130.7, 130.5, 130.0, 129.5, 129.4, 129.1,

128.0, 127.1, 116.2, 114.9, 106.3, 67.8, 64.0, 54.7, 12.8, 12.7. HRMS calculated for $C_{27}H_{29}N_4O_2$ $(M+H)^+$ *m/z*: 441.2291, measured 441.2291.

CHAPTER III

SMALL MOLECULE INHIBITION OF WNT SIGNALING THROUGH ACTIVATION OF CASIEN KINASE 1 ALPHA

Introduction

Control of β-catenin levels is a critical event of Wnt signaling. In the absence of Wnt ligand, cytoplasmic β-catenin is maintained at low levels by its constitutive degradation. β-catenin degradation occurs primarily via its association with a complex consisting of glycogen synthase kinase 3 (GSK3), Casein Kinase 1α (CK1α), Adenomatous Polyposis Coli (APC), and Axin. Within this destruction complex, β-catenin is phosphorylated by GSK3 and targeted for degradation by the ubiquitin-proteasome pathway. Upon binding of Wnt ligand to Frizzled and low-density lipoprotein-related receptor 5/6 (LRP5/6), β-catenin destruction is inhibited, and the scaffold protein Axin is degraded(Yamamoto, Kishida et al. 1999) (Tolwinski, Wehrli et al. 2003) (Kofron, Birsoy et al. 2007) (Cselenyi, Jernigan et al. 2008). Thus, Wnt signaling increases cytoplasmic levels of β-catenin, which enters the nucleus and interacts with other factors to activate a TCF/Lef1-mediated transcriptional program(Thompson, Townsley et al. 2002) (Parker, Jemison et al. 2002) (Kramps, Peter et al. 2002) (Clevers 2006).

Demonstration that loss of *APC* (the cause of familial adenomatous polyposis, a hereditary cancer syndrome) results in β-catenin accumulation was the first indication that constitutive activation of the Wnt pathway can lead to epithelial cell

transformation(Kinzler, Nilbert et al. 1991) (Nakamura, Nishisho et al. 1991). Over 80% of sporadic colon cancers are associated with mutation of APC and 10% with mutation of β-catenin, both of which lead to Wnt pathway activation(Barker and Clevers 2006) (Klaus and Birchmeier 2008).

Xenopus egg extracts have been shown to faithfully recapitulate many events of the Wnt pathway with *in vivo* reaction kinetics(Salic, Lee et al. 2000). In the current report, we describe a novel, high-throughput screen for chemical modulators of Wnt signaling using *Xenopus* egg extract. We identified pyrvinium, an FDA-approved drug, as a potent inhibitor of the Wnt pathway (Fig. 3.1). We provide evidence that pyrvinium may represent a new class of compounds that inhibit the Wnt pathway by allosteric activation of Casein Kinase 1α.

Results

Xenopus egg exract screen for small molecule regulators of the Wnt pathway

Recently, we reconstituted Wnt signaling in *Xenopus laevis* egg extract using a soluble form of LRP6 (LRP6ICD) (Cselenyi, Jernigan et al. 2008). We adapted this system for high-throughput approaches and performed a small molecule screen for modulators of Wnt signaling (Fig. 3.2A). We assessed the status of Wnt activation by monitoring levels of β-catenin-firefly luciferase and Axin-*Renilla* luciferase fusion proteins. We reasoned that the reciprocal stability of β-catenin and Axin in response

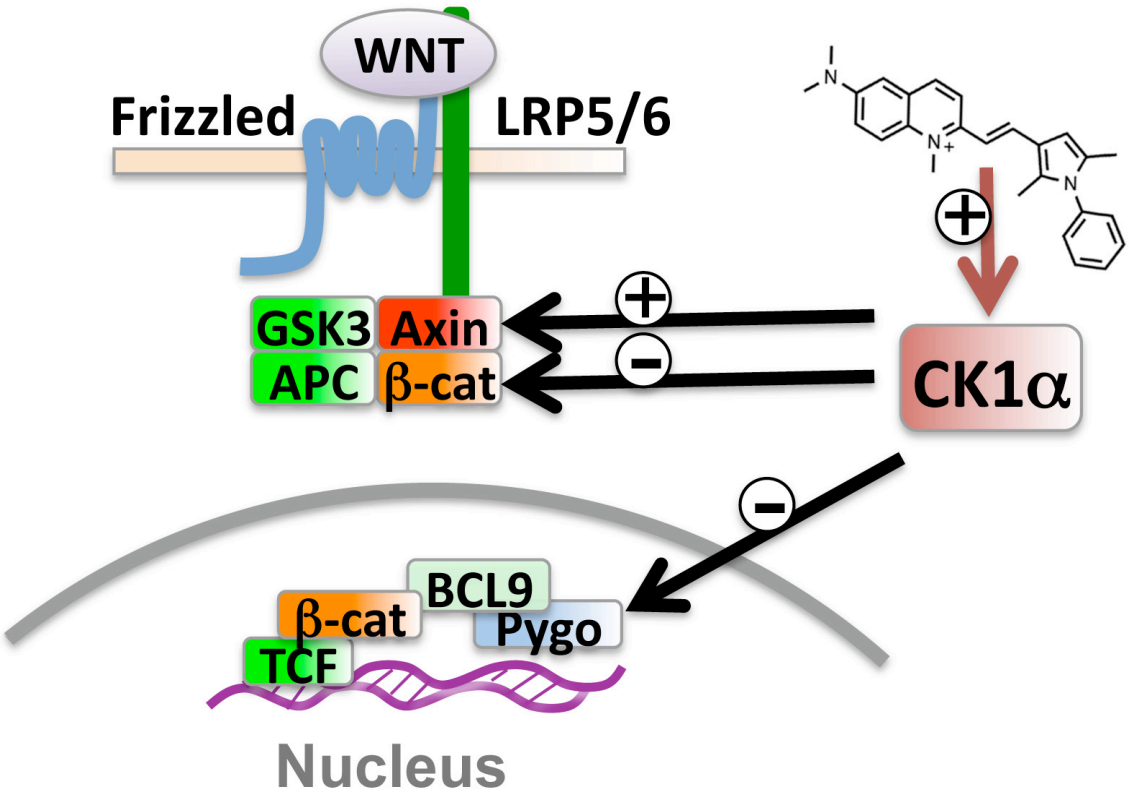

Figure 3.1. A model of the effects of pyrvinium on multiple levels of the Wnt pathway. Inhibition of Wnt signaling by pyrvinium is due to allosteric activation of CK1α to regulate the stability of β-catenin and Axin in the cytoplasm and Pygopus and TCF/Lef1 in the nucleus in the nucleus.

to LRP6-mediated signaling (increased and decreased, respectively) would be a powerful readout to identify specific modulators of the Wnt pathway. Compounds that interfere with energy metabolism should reduce both firefly and *Renilla* signals. Conversely, general inhibitors of protein degradation (e.g. proteasome inhibitors) should enhance both luciferase signals.

Xenopus egg extract used in our screen is transcriptionally and translationally inactive. Thus, observed effects on the Wnt/β-catenin pathway are due to post-translational events. We titrated LRP6ICD to half-maximal activity in the extract (Fig. 3.3A). We used FDA-approved drug libraries from the National Institute of Neurological Disorders and Stroke (NINDS) custom collection and the Prestwick Chemical Library at the Harvard Medical School Institute for Chemistry and Cell Biology (ICCB) in our screen. From our primary screen, we identified ~20 candidate Wnt pathway activators and inhibitors that altered the β-catenin/Axin luciferase ratio at least three deviations from the mean (Fig. 3.2B).

Pyrvinium pamoate, an antihelminthic drug, inhibited LRP6-mediated Axin-*Renilla* luciferase degradation and β-catenin-firefly luciferase stabilization with the greatest potency in our screen. Pyrvinium is a quinoline-derived cyanine dye previously used in the treatment of pinworms (*Enterobius vermicularis*) that is also efficacious towards animal-like protists, *Plasmodium falciparum* and *Cryptosporidium parvum* (Fig. 3.2C) (Hempelmann 2007) (Downey, Chong et al. 2008). Despite its past medicinal use for over 50 years, the mode of action of pyrvinium remains unknown(Sheth 1975). We performed kinetic experiments and found that pyrvinium reversed the effects of LRP6ICD on the turnover rates of β-

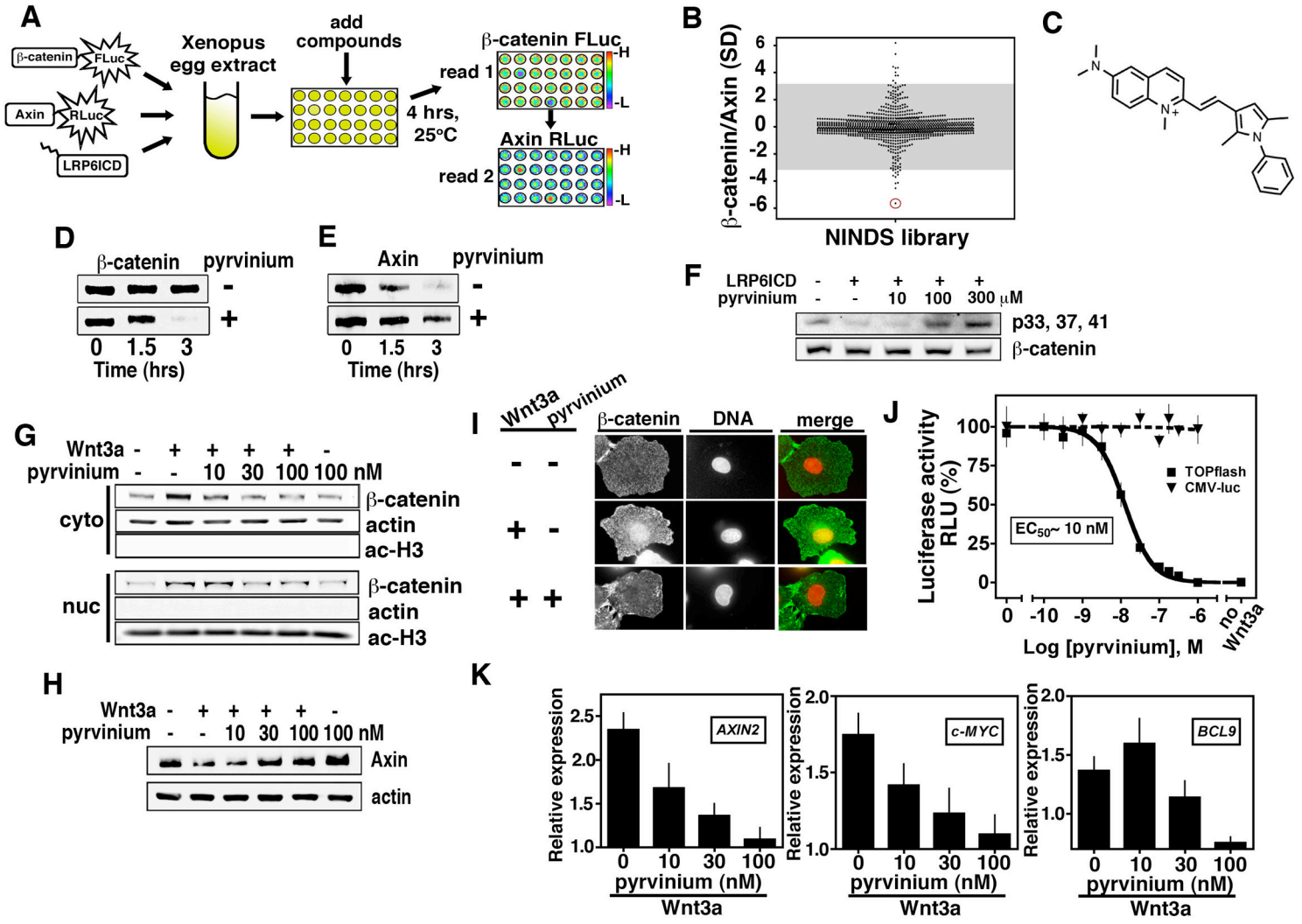
A
β-catenin
FLuc
Axin
RLuc
LRP6ICD
Xenopus egg extract
add compounds
4 hrs, 25°C
β-catenin FLuc
read 1
Axin RLuc
read 2
H
L
B
β-catenin/Axin (SD)
NINDS library
C
D
β-catenin
pyrvinium
Time (hrs)
E
Axin
F
LRP6ICD
p33, 37, 41
G
Wnt3a
cyto
nuc
actin
ac-H3
H
I
DNA
merge
J
Luciferase activity RLU (%)
TOPflash
CMV-luc
EC50~ 10 nM
Log [pyrvinium], M
no Wnt3a
K
Relative expression
AXIN2
c-MYC
BCL9
pyrvinium (nM)

Figure 3.2. *Xenopus* egg extract screen identifies pyrvinium as an inhibitor of Wnt signaling. (A) Schematic of high-throughput screen assay. β-catenin-firefly luciferase (β-catenin-FLuc), Axin-*Renilla* luciferase (Axin-RLuc), and LRP6ICD were added to *Xenopus* egg extract and aliquoted into 384-well plates at 4°C. Compounds from chemical libraries were added and plates incubated at 25°C for 4 hours. β-catenin-FLuc and Axin-RLuc activities were measured by dual luciferase assay. "H" and "L" represent high and low luciferase signals, respectively. **(B)** Scatter plot of change in standard deviation (ΔSD) of normalized β-catenin/Axin ratios for FDA-approved compounds from NINDS library. Unshaded regions represent compound with activities greater than 3 standard deviations (SD) from the mean. Pyrvinium is circled in red. **(C)** Chemical structure of pyrvinium. **(D, E)** Radiolabeled β-catenin or Axin was added to *Xenopus* extract containing LRP6ICD (200 nM) minus or plus pyrvinium (100 μM). Samples were removed at indicated times and processed for SDS-PAGE/autoradiography. **(F)** LRP6 inhibition of GSK3-mediated β-catenin phosphorylation is reversed by pyrvinium. *Xenopus* extracts treated as indicated were immunoblotted for total β-catenin or GSK3 phosphorylation sites on β-catenin required degradation. **(G)** Pyrvinium decreases cytoplasmic and nuclear β–catenin levels. HEK 293 cells were treated for 16 hours as indicated, and fractionated lysates were immunoblotted for β-catenin. Purity of nuclear and cytoplasmic preparations was assessed by immunoblotting for acetylated Histone H3 and actin, respectively. **(H)** Pyrvinium increases cellular Axin levels. Lysates from HEK 293 cells treated for 16 hours as indicated were immunoblotted for Axin and actin (loading control). **(I)** Pyrvinium blocks Wnt-mediated nuclear accumulation of β-catenin. IEC-6 cells treated as indicted were stained for β-catenin and DNA. Over 500 cells were scored. **(J)** Pyrvinium inhibits TOPflash activation with an EC_{50} of ~10 nM. HEK 293 STF (TOPflash) or constitutively expressing (CMV-Luc) luciferase reporter cells were treated was indicated. Graph represents mean ± s.e.m of TOPflash signal normalized to cell number (performed in quadruplicate). **(K)** Pyrvinium decreases levels of endogenous Wnt target transcripts. Data shown represent mean of four independent real-time PCR reactions, graphed as relative expression to unstimulated cells and normalized to β-actin. Error bars, RQ values >95% confidence. LRP6-mediated signaling (increased and decreased, respectively)

catenin (increased by pyrvinium) and Axin (decreased by pyrvinium) (Figs. 3.2D,E and 3.3B,C). We also found that pyrvinium modestly promoted the basal rate of β-catenin degradation in the absence of LRP6ICD (data not shown). We previously demonstrated using *Xenopus* egg extract that LRP6ICD inhibits the phosphorylation of β-catenin by GSK3, which promotes its ubiquitin-mediated degradation(Cselenyi, Jernigan et al. 2008). Consistent with these data, we found that pyrvinium reversed the effects of LRP6ICD on β-catenin phosphorylation (Fig. 3.2F).

To assess whether pyrvinium regulates β-catenin and Axin levels in other systems, we tested its effects on cultured mammalian cells. Stimulation of human embryonic kidney (HEK) 293 cells with Wnt3a resulted in elevation of cytoplasmic and nuclear β-catenin levels and reduction of Axin levels. Pyrvinium reversed the effects of Wnt3a in a concentration-dependent manner such that both cytoplasmic and nuclear pools of β-catenin were decreased and Axin levels were increased to levels similar to that observed in the absence of Wnt3a (Fig. 3.2G,H). Furthermore, pyrvinium caused an increase in Axin levels in cells not treated with Wnt3a (Fig 3.2H).

A cellular pool of β-catenin that binds E-cadherin at cell-cell junctions is essential for maintaining epithelial cell polarity and tissue architecture(Perez-Moreno and Fuchs 2006). We assessed whether pyrvinium affects this membrane-bound pool of β-catenin, using a nontransformed rat small intestine epithelial cell line, IEC-6. Addition of Wnt3a to IEC-6 cells resulted in accumulation of nuclear β-catenin in approximately 50% of the cells observed. Treatment of IEC-6 cells with

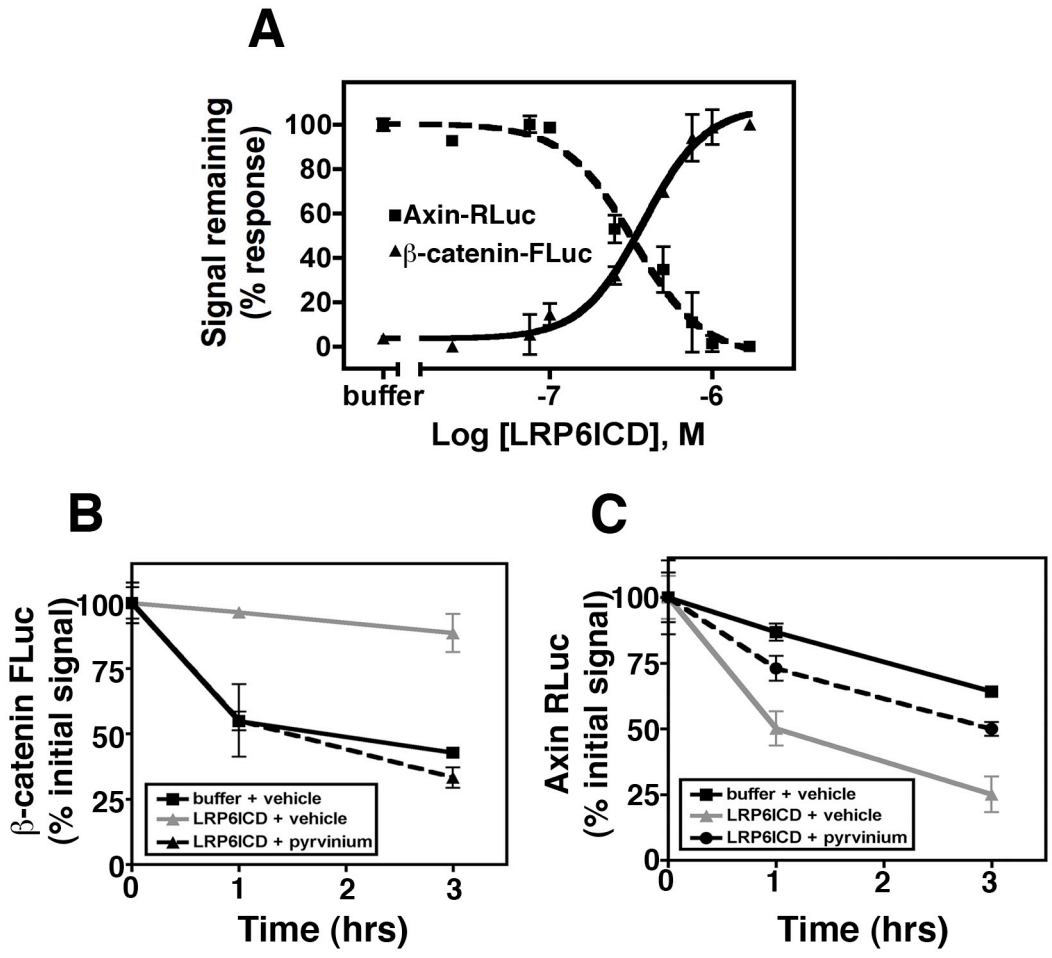

Figure 3.3. (A) β-catenin-FLuc and Axin-RLuc are regulated by LRP6ICD in a concentration-dependent manner in *Xenopus* egg extract. Extract was prepared as described in methods. The mean ± s. e. m. of the signal remaining after 4 hours is shown (performed in duplicate, graphed as percent total response). **(B, C)** Pyrvinium reverses the effects of LRP6ICD on β-catenin and Axin stability in *Xenopus* extracts. β–Catenin-FLuc **(B)** or Axin-RLuc **(C)** were added to extract in the presence of buffer, LRP6ICD, or LRP6ICD + 100 μM pyrvinium. Aliquots were removed at the indicated times and luciferase assays performed in triplicate in two independent experiments. Mean ± s.e.m. is shown.

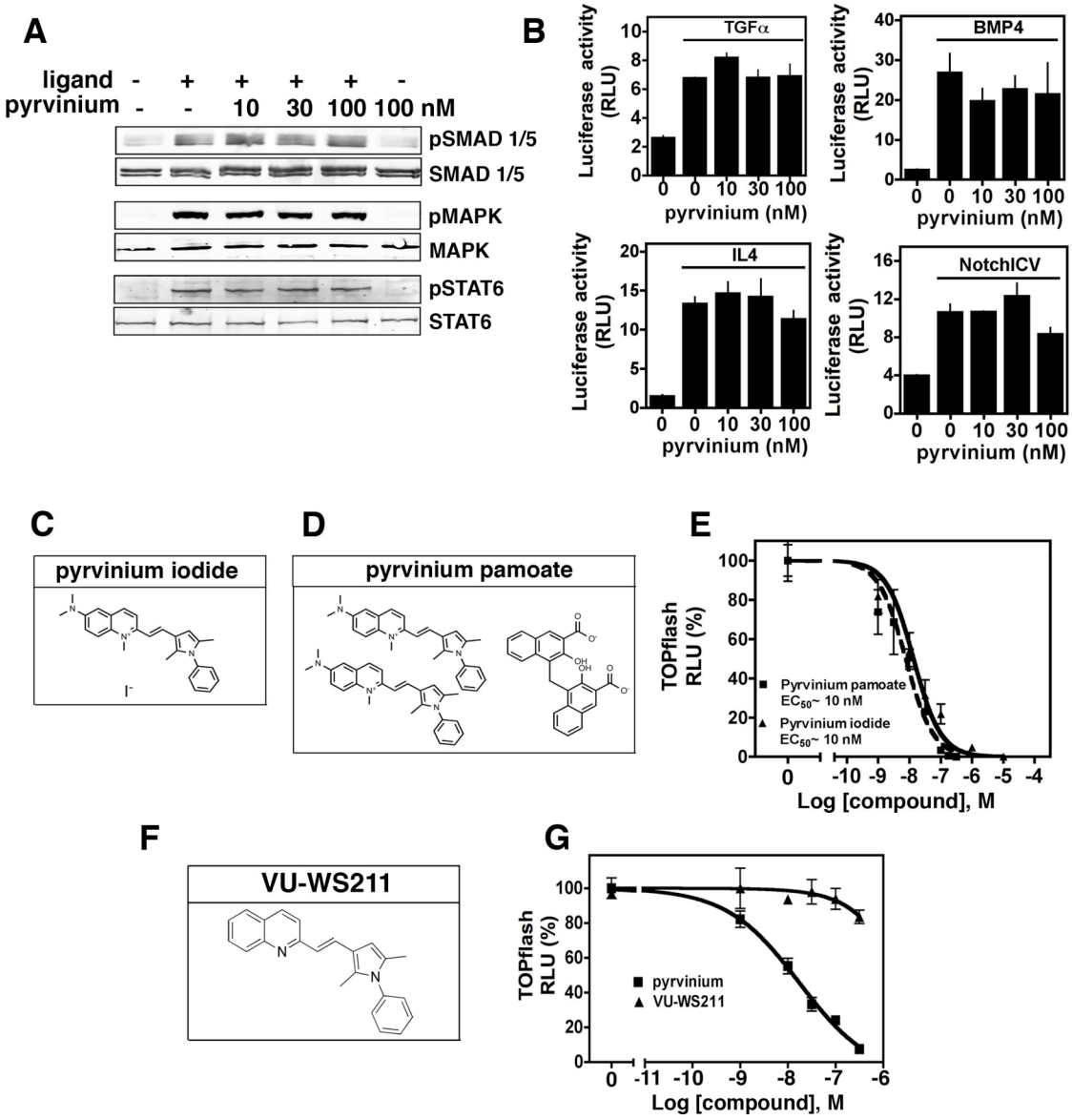
A
ligand - + + + + -
pyrvinium - - 10 30 100 100 nM
pSMAD 1/5
SMAD 1/5
pMAPK
MAPK
pSTAT6
STAT6
B
TGFα
BMP4
IL4
NotchICV
Luciferase activity (RLU)
pyrvinium (nM)
C
pyrvinium iodide
D
pyrvinium pamoate
E
TOPflash RLU (%)
Pyrvinium pamoate EC50~ 10 nM
Pyrvinium iodide EC50~ 10 nM
Log [compound], M
F
VU-WS211
G
TOPflash RLU (%)
pyrvinium
VU-WS211
Log [compound], M

Figure 3.4. (A, B) Pyrvinium does not affect BMP4, TGF-α, or IL-4 signaling pathways. **(A)** Pyrvinium has no observable biochemical effect on BMP4, TGF-α, or IL-4 signaling. HEK 293 cells were pretreated with pyrvinium (100 nM) for 2 hours prior to addition of ligands (BMP4, 50 ng/ml; TGF-α, 10 nM; or IL-4, 0.1 ng/ml) and lysed 30 minutes later for immunoblotting using antibodies against downstream effectors pSMAD1/5, pMAPK, or pSTAT6, respectively. **(B)** Pyrvinium does not block BMP4, TGF-α, IL-4, or Notch pathway reporter gene activation. BMP4, TGF-α, and IL-4 treated cells were transfected with luciferase-based reporter constructs as described in methods and treated as in (F) for 24 hours. For activation of the Notch pathway, NotchICV was cotransfected with luciferase-based reporter construct as previously described. Mean ± s.e.m. of luciferase signal normalized to a cotransfected Renilla luciferase control is shown (performed in quadruplicate). **(C-G)** Regulation of Wnt signaling by pyrvinium salts and the a pyrvinium analog. Structures of **(C)** pyrvinium iodide and **(D)** pyrvinium pamoate. **(E)** Both the iodide and pamoate salts of pyrvinium inhibited TOPflash activation with essentially identical EC_{50}s (~10 nM). **(F)** Structure of VU-WS211, a pyrvinium analog. **(G)** VU-WS211 fails to inhibit TOPflash. HEK 293 STF cells were treated with Wnt3a and compounds.

pyrvinium prevented nuclear accumulation of β-catenin but had no obvious effect on membrane-bound pools of β-catenin in all cells (Fig. 3.2I).

Wnt signaling leads to changes in transcription of a large set of genes that drive proliferation, growth, and cell fate determination(Clevers 2006). To evaluate whether pyrvinium inhibits Wnt-mediated transcription, we used a luciferase-based reporter containing TCF/LEF binding sites (TOPflash) stably transfected in HEK 293 cells (HEK 293 STF)(Xu, Wang et al. 2004). Pyrvinium inhibited Wnt3a-mediated luciferase activity in a dose-dependent with an EC_{50} of ~10 nM (Fig. 3.2J). Pyrvinium had no effect on expression of luciferase driven by a constitutive CMV promoter (CMV-Luc) or FOPflash, a scrambled TCF/LEF promoter element (Fig. 3.2J and data not shown). Consistent with the effect of pyrvinium on the TOPflash reporter, activation of endogenous target genes *AXIN2*, *c-MYC*, and *BCL9* by Wnt3a was inhibited by pyrvinium in a dose-dependent manner to nearly basal (i.e. minus Wnt3a) levels (Fig. 3.2K) (He, Sparks et al. 1998; Jho, Zhang et al. 2002; Lustig, Jerchow et al. 2002; de la Roche, Worm et al. 2008). In contrast, pyrvinium had no discernible effect on the biochemical and/or transcriptional responses of four other major signaling pathways (TGFα, BMP4, IL-4, and Notch), thereby demonstrating specificity of pyrvinium for Wnt signaling (Fig. 3.4A,B).

Chemical specificity was confirmed by experiments showing that the pamoate salt of another antihelminthic compound (pyrantel pamoate) did not inhibit Wnt signaling, whereas the iodide salt of pyrvinium inhibited Wnt signaling with an EC_{50} essentially identical to that of pyrvinium pamoate (Fig. 3.4C-E and data

not shown). As an additional control, a structurally related analog of pyrvinium had no effect on TOPflash activity (Fig. 3.4F,G).

The much lower concentration of pyrvinium needed to inhibit Wnt signaling in cultured mammalian cells compared to its effect on β-catenin and Axin turnover in *Xenopus* egg extracts was not unexpected (Figs. 3.2D,E and 3.3B,C). These extracts contain high concentrations of proteins and lipids, which can sequester exogenously added compounds; hence, many well-characterized compounds have been shown to be ~1000-fold less potent in *Xenopus* egg extract compared to cell-based assays(Li and Blow 2005) (Miyamoto, Perlman et al. 2004).

Pyrvinium inhibits Wnt signaling during development across phyla

To determine whether pyrvinium inhibits Wnt signaling in a developing organism, we investigated its effects in *Xenopus laevis*. Canonical/β-catenin Wnt signaling leads to accumulation of β-catenin on the dorsal side of the embryo that patterns dorsal-anterior structures(Larabell, Torres et al. 1997; De Robertis and Kuroda 2004). Experimental activation of the Wnt pathway in ventral blastomeres (e.g. via *Xwnt8* mRNA injection) induces secondary organizer and formation of an ectopic axis (Fig. 3.5A). Co-injection of pyrvinium inhibited *Xwnt8*-mediated secondary axis formation in a dose-dependent manner, whereas co-injection with vehicle control or an inactive analog had no effect (Figs. 3.5A and 3.6A). Injection of pyrvinium into dorsal blastomeres at the 4-cell stage resulted in ventralized embryos, indicating inhibition of endogenous Wnt signaling, whereas an inactive analog had no effect (Fig. 3.6B).

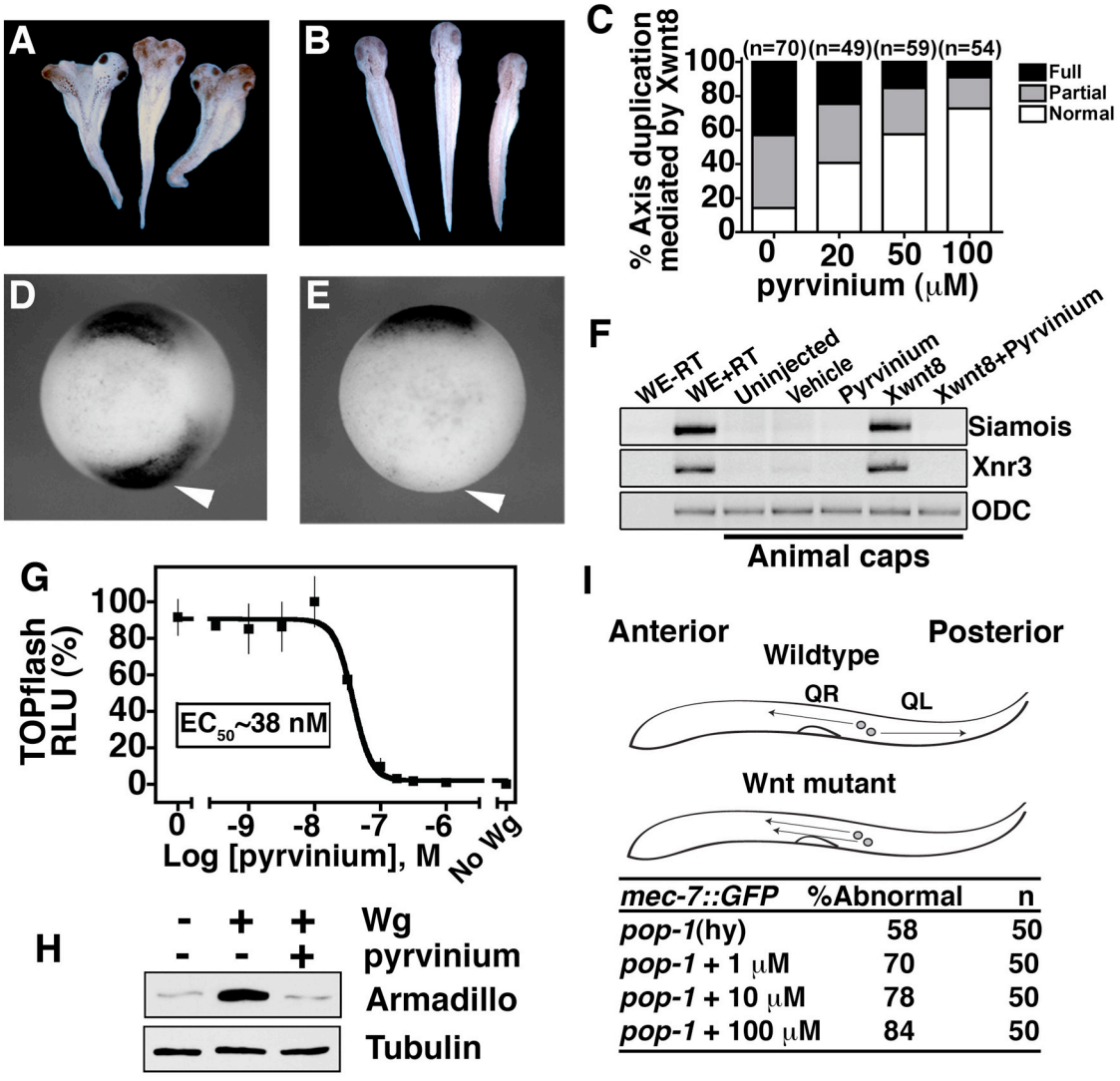

mec-7::GFP	%Abnormal	n
pop-1(hy)	58	50
pop-1 + 1 μM	70	50
pop-1 + 10 μM	78	50
pop-1 + 100 μM	84	50

Figure 3.5. Pyrvinium inhibits Wnt signaling *in vivo*. (A-C) Pyrvinium blocks secondary axis induction in *Xenopus* in a dose-dependent manner. 4-8 cell stage embryos were injected ventrally with *Xwnt8* mRNA (0.5 pg) plus vehicle or pyrvinium, allowed to develop, and scored for secondary axis formation. n=number of embryos. **(D,E)** Pyrvinium blocks expression of chordin. Embryos injected with *Xwnt8* plus vehicle or 200 μM pyrvinium were probed by *in situ* hybridization (stage 10.5) for chordin (arrowheads). Vegetal view, dorsal side up. **(F)** Pyrvinium inhibits Xwnt8 induction of Wnt target genes *Siamois* and *Xnr3* in *Xenopus* animal cap explants. RT-PCR of total RNA extracted from animal caps. WE, whole embryo. Ornithine decarboxylase (ODC), loading control. (**G**) Pyrvinium inhibits Wg signaling in *Drosophila* S2 cells. Cells stably transfected with a TOPflash reporter were treated with Wg and/or pyrvinium. Graph represents mean ± s.e.m. of luciferase signal normalized by cell number (performed in quadruplicate). **(H)** Pyrvinium decreases cellular Armadillo levels. Lysates from S2 cells treated with Wg were immunoblotted for Armadillo. Tubulin, loading control. **(I)** Pyrvinium enhances Q cell migration defect of hypomorphic TCF (*pop-1*) mutants. *pop-1*; *mec-7*::GFP worms were treated with pyrvinium and QL cell migration scored. n= number of embryos.

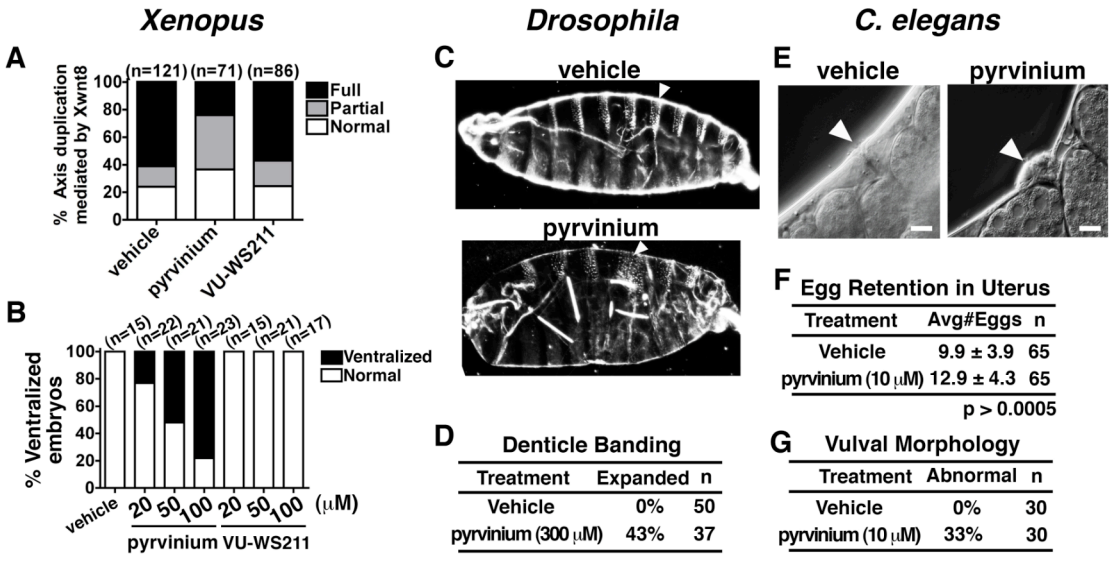

Figure 3.6. (A, B) Comparison of the effects of pyrvinium and VU-WS211, a structurally related analog, on axis formation in *Xenopus*. **(A)** VU-WS211 fails to inhibit Xwnt8-induced secondary axis formation in Xenopus. Embryos (4-8 cell stage) were injected ventrally with *Xwnt8* mRNA (0.5 pg) plus vehicle, pyrvinium (100 μM), or VU-WS211 (100 μM) and scored for axis duplication. **(B)** Dorsal injection of pyrvinium ventralizes *Xenopus* embryos in a dose-dependent manner. Embryos (2-4 cell stage) were injected dorsally with vehicle, pyrvinium, or VU-WS211 and scored for ventralization. Dorsal anterior index (DAI) of ventralized embryos ranged from 2-4. n=number of embryos injected. **(C, D)** Pyrvinium causes denticle band expansion in *Drosophila*. Embryos were injected with vehicle or pyrvinium prior to cellularization and cuticle prepared after 24 hours for dark field imaging. **(C)** Denticle belts (arrowheads) are expanded in pyrvinium-treated animals. Cuticles are shown at 20X magnification. **(D)** Quantification of the denticle banding pattern in *Drosophila* first instar larvae injected with pyrvinium during embryogenesis. **(E-G)** Pyrvinium induces defects in *C. elegans* vulval development that phenocopy Wnt inhibition. **(E)** Vulval morphology (arrowheads) is defective in pyrvinium-treated animals. Quantification of abnormal egg retention **(F)** or vulval morphology **(G)** in *C. elegans* treated with pyrvinium compared to vehicle-treated animals. Scale bar, 1 μm. n=number of animals. For *C. elegans* studies, vehicle is 0.1% ethanol.

Organizer formation is regulated by canonical Wnt signaling, which directly induces expression of *Xnr3*, *Siamois*, and other target genes(De Robertis and Kuroda 2004). Pyrvinium inhibited ectopic expression of chordin (marks the organizer) in early gastrulae co-injected with *Xwnt8* (Fig. 3.5B). Similarly, *Xwnt8*-induced expression of *Siamois* and *Xnr3* in ectodermal explants was inhibited by co-injection of pyrvinium (Fig. 3.5C).

We next investigated the effects of pyrvinium using two invertebrate model systems in which Wnt signaling has been extensively characterized. Pyrvinium inhibited Wingless (Wg)-mediated gene transcription in *Drosophila* S2 cells with an EC_{50} (~38 nM) comparable to that of HEK 293 cells (Fig. 3.5D) (Bhanot, Brink et al. 1996). Furthermore, pyrvinium blocked the increase in Armadillo (β-catenin homolog) levels induced by Wg ligand (Fig. 3.5E). Wg signaling establishes segment polarity during embryogenesis and controls larval cuticle patterning(Bejsovec and Martinez Arias 1991). Pyrvinium injection into wild-type embryos produced larvae with slightly expanded denticles, a phenotype consistent with loss of Wg signaling (Fig. 3.6C,D).

During *C. elegans* development, vulval differentiation and Q neuroblast migration depend on Wnt signaling(Whangbo and Kenyon 1999; Gleason, Korswagen et al. 2002). The QL cell expresses the hox gene *MAB-5* in response to a posterior Wnt signal, which is required for its posterior migration. In contrast, the QR cell, which does not respond to Wnt, migrates anteriorly(Whangbo and Kenyon 1999). Using a weak allele of *pop-1* (TCF homolog) as a sensitized background, pyrvinium treatment resulted in a dose-dependent disruption of posterior QL cell

migration (Fig. 3.5F) (Herman 2001; Korswagen, Coudreuse et al. 2002). Previous studies have shown that the cuticle and hypodermis of *C. elegans* is often impermeable to pharmacological agents(Lewis, Wu et al. 1980). Thus, the high doses of pyrvinium we used to observe an effect may reflect its poor absorption. Alternatively, it may reflect differences in the sequences of the vertebrate and *C. elegans* genes encoding the cellular target of pyrvinium. Pyrvinium treatment also produced vulval defects, a phenotype consistent with decreased Wnt signaling (Fig. 3.6E-G). The range of phenotypes observed included protruding vulva and vulvaless. The phenotypic effects of pyrvinium in *Xenopus*, *Drosophila*, and *C. elegans* are consistent with inhibition of Wnt-mediated developmental processes. Taken together, our studies suggest that pyrvinium acts as a Wnt pathway inhibitor *in vivo* and that its target is conserved across phyla.

Identification of Casein Kinase 1α as the target of pyrvinium

We have shown that pyrvinium promotes β-catenin and inhibits Axin turnover (Fig. 3.2G,H). The simplest model is that pyrvinium regulates the activity of a single target that acts on both proteins. We assembled a complex consisting of purified GSK3, CK1, Axin, and β-catenin and tested the effect of pyrvinium on β-catenin phosphorylation, a prerequisite for its degradation. Addition of pyrvinium at low nanomolar concentrations to this purified system resulted in a striking increase in β-catenin phosphorylation, including sites specific for GSK3 and CK1α (Figs. 3.7A).

We next tested the four proteins included in our *in vitro* β-catenin

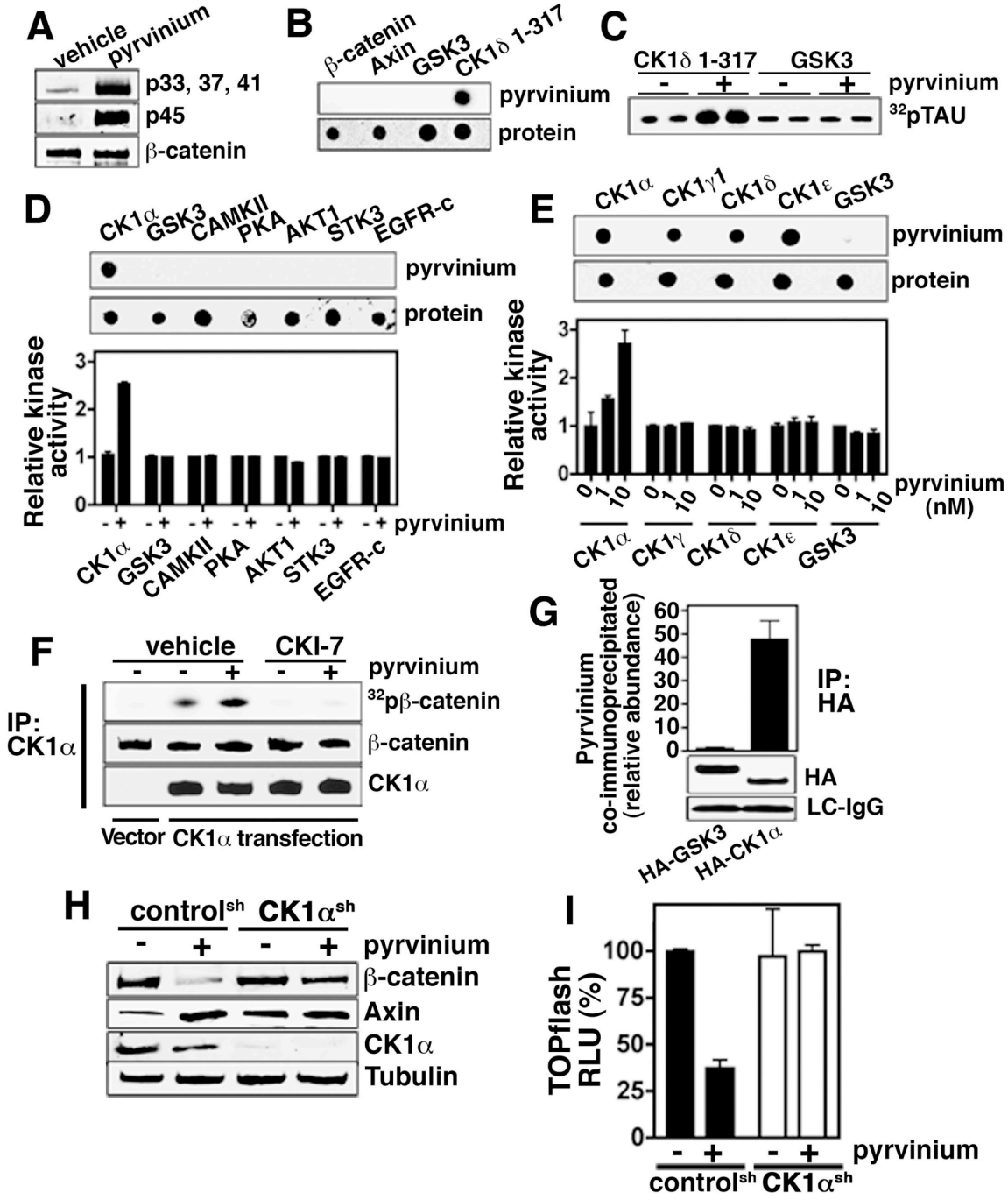
A
vehicle
pyrvinium
p33, 37, 41
p45
β-catenin
B
β-catenin
Axin
GSK3
CK1δ 1-317
pyrvinium
protein
C
CK1δ 1-317
GSK3
pyrvinium
32pTAU
D
CK1α
GSK3
CAMKII
PKA
AKT1
STK3
EGFR-c
pyrvinium
protein
Relative kinase activity
E
CK1α
CK1γ1
CK1δ
CK1ε
GSK3
pyrvinium
protein
Relative kinase activity
pyrvinium (nM)
F
vehicle
CKI-7
pyrvinium
IP: CK1α
32pβ-catenin
β-catenin
CK1α
Vector
CK1α transfection
G
Pyrvinium co-immunoprecipitated (relative abundance)
IP: HA
HA
LC-IgG
HA-GSK3
HA-CK1α
H
controlsh
CK1αsh
pyrvinium
β-catenin
Axin
CK1α
Tubulin
I
TOPflash RLU (%)
pyrvinium
controlsh
CK1αsh

Figure 3.7. Casein kinase 1α is the critical target of pyrvinium. (A) Pyrvinium stimulates β-catenin phosphorylation *in vitro*. A kinase reaction was assembled *in vitro* with purified β-catenin, Axin, GSK3, and a constitutively active, truncated form of CK1d (CK1d1-317) (100 nM each) plus or minus pyrvinium (10 nM). Phosphorylation of β-catenin on GSK3 sites (p33,37,41) and the priming CK1α site (p45) was detected by immunoblotting. **(B)** Pyrvinium binds CK1 *in vitro*. β-catenin, Axin, GSK3, and CK1d1-317 (0.5 μg each) were spotted on nitrocellulose, incubated with pyrvinium (10 nM), and bound pyrvinium detected using a Xenogen IVIS 200 **(**excitation/emission=550nm/600nm). Equivalent amounts of protein as detected by Colloidal Gold Total protein stain (Bio-Rad) were spotted. **(C)** Pyrvinium stimulates CK1 activity *in vitro*. CK1d1-317 (100 nM) was incubated with recombinant Tau (100 nM) plus or minus pyrvinium (10 nM) in a kinase reaction containing [γ^{32}P]ATP followed by SDS-PAGE/autoradiography. (**D,E**) Pyrvinium (10 nM) was incubated with purified recombinant kinases, and binding and kinase activities were assessed. For binding assays, 0.5 ug of protein was used. **(D)** Pyrvinium binds and activates CK1α but not kinases representative of other major branches of the kinome. (**E)** Pyrvinium binds all full-length CK1 isoforms tested, but only activates CK1α. **(F)** Pyrvinium activates CK1α in cultured cells. HEK 293 cells overexpressing CK1α were treated with pyrvinium (100 nM). CK1α immunoprecipitated from lysates was incubated with purified β-catenin (100 nM) in a kinase assay containing [γ^{32}P]ATP. Samples were processed for SDS-PAGE/autoradiography. As control, immunoprecipitates were treated with the CK1 inhibitor, CKI-7 (1 μM). Immunoblots of β-catenin and CK1α show equivalent amounts of protein were used in each sample. **(G)** Pyrvinium co-immunoprecipitates with CK1α. HEK 293 cells expressing HA-GSK3, HA-CK1α, or HA alone (vector control) were treated with pyrvinium (100 nM). Immunoprecipitates were analyzed by LC-MS. Graph represents mean ± s.e.m. of relative abundance of pyrvinium normalized to bead control (performed in triplicate). Immunoblots show that comparable amounts of HA-tagged proteins and light chain IgG (LC-IgG) were present in the immunoprecipitates. **(H,I)** Downregulating CK1α blocks the biochemical and transcriptional responses to pyrvinium. A Jurkat cell line expressing inducible shRNA for CK1α (CK1α^{sh}) was incubated with pyrvinium (30 nM) for 24 hours. Lysates were immunoblotted for **β-**catenin, Axin, and Tubulin (loading control) **(H)** or assayed for TOPflash to assess Wnt signaling **(I)**. For the TOPflash assays, cells were treated with Wnt3a. Graph shows mean ± s.e.m., normalized to cell number and performed in triplicate.

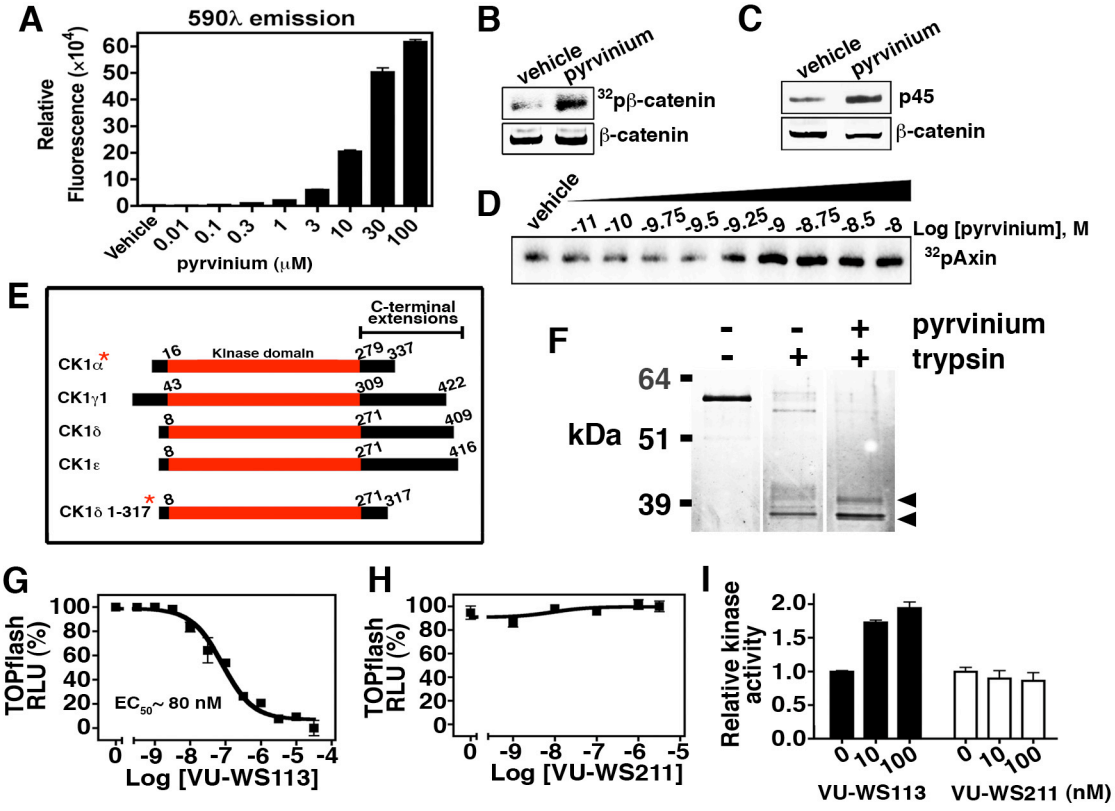
A
590λ emission
Relative Fluorescence (x10^4)
60
50
40
30
20
10
0
Vehicle
0.01
0.1
0.3
1
3
10
30
100
pyrvinium (μM)
B
vehicle
pyrvinium
32pβ-catenin
β-catenin
C
vehicle
pyrvinium
p45
β-catenin
D
vehicle
-11
-10
-9.75
-9.5
-9.25
-9
-8.75
-8.5
-8
Log [pyrvinium], M
32pAxin
E
C-terminal extensions
CK1α*
16
Kinase domain
279
337
CK1γ1
43
309
422
CK1δ
8
271
409
CK1ε
8
271
416
CK1δ 1-317
*
8
271
317
F
pyrvinium
trypsin
64
kDa
51
39
G
TOPflash RLU (%)
100
80
60
40
20
0
EC50~ 80 nM
0
-9
-8
-7
-6
-5
-4
Log [VU-WS113]
H
TOPflash RLU (%)
100
80
60
40
20
0
0
-9
-8
-7
-6
-5
Log [VU-WS211]
I
Relative kinase activity
2.0
1.5
1.0
0.5
0.0
0
10
100
0
10
100
VU-WS113
VU-WS211 (nM)

Figure 3.8. (A) Fluorescence signal of pyrvinium. The indicated concentrations of pyrvinium were excited at 540λ and emission signals determined at 590λ. **(B, C)** Pyrvinium stimulates phosphorylation of β-catenin by CK1 *in vitro*. **(B)** Purified β-catenin and CK1 (100 nM each) were incubated in a kinase reaction containing [γ^{32}P]ATP in the absence or presence of pyrvinium (1 nM). Samples were analyzed by SDS-PAGE/autoradiography. **(C)** CK1 and β-catenin (100 nM each) were incubated in a kinase reaction and phospho-Ser45 β-catenin (p45) detected by immunoblotting. **(D)** Pyrvinium stimulates *in vitro* phosphorylation of Axin by CK1 in a dose-dependent manner. Purified Axin and CK1 (100 nM each) were incubated in a kinase reaction containing [γ^{32}P]ATP in the absence or presence of varying concentrations of pyrvinium. Samples were analyzed by SDS-PAGE/autoradiography. Recombinant CK1d1-317 was used as the source of CK1. **(E)** Diagram of CK1 isoforms. Autophosphorylation of the C-terminal extensions of CK1 isoforms has been shown to inhibit kinase activity. Of particular note is that CK1α contains a shorter C-terminal extension compared to the other CK1 isoforms. CK1d1-317 is a truncated form that lacks a portion of the C-terminal extension of CK1d. Asterisks mark isoforms activated by pyrvinium (α and d1-317). **(F)** Pyrvinium affects the conformation of CK1α *in vitro* as assayed by limited trypsin proteolysis. Arrowheads indicate prominent CK1α fragments that only appear when CK1α is trypsinized in the presence of pyrvinium (100 nM). **(G-I)** Derivatives of pyrvinium that inhibit Wnt signaling also activate CK1α. HEK 293 STF cells were treated with Wnt3a and the indicated concentrations of VU-WS113 **(G)** or VU-WS211 **(H)** and assayed for luciferase activity. Mean ± s.e.m. of TOPflash activity normalized to cell number is shown (performed in quadruplicate and displayed as percent response). **(I)** CK1α (100 nM) was incubated with recombinant casein (100 nM) in the presence or absence of compounds in a kinase reaction containing [γ^{32}P]ATP. Samples were analyzed by SDS-PAGE/autoradiography and the extent of ^{32}P incorporation into casein assessed.

phosphorylation assay for binding to pyrvinium. Using a ligand-binding assay based on the innate fluorescent property of pyrvinium, we observed pyrvinium binding only for CK1 (Figs. 3.7B and 3.8A). We next tested whether pyrvinium binding affects CK1 activity towards its substrates (β-catenin, Axin, and Tau) (Liu, Li et al. 2002) (Gao, Seeling et al. 2002) (Pierre and Nunez 1983). Pyrvinium enhanced phosphorylation of all CK1 substrates tested but had no observable effect on GSK3 activity (Figs. 3.7C and 3.8B-D). Based on our estimated EC_{50} for Axin phosphorylation by CK1 (< 1nM), pyrvinium is ~ten-fold more potent in promoting the activity of purified CK1 compared to its inhibition of Wnt signaling (EC_{50} ~10 nM) in cultured cells (Figs. 3.2J and 3.8D). A difference in potency between the effects of small molecules in assays using purified components versus cell-based assays is characteristic of small molecule kinase inhibitors(Knight and Shokat 2005).

CK1 represents a branch of the family of serine/theronine protein kinases(Knippschild, Gocht et al. 2005). To demonstrate specificity for CK1, we tested the capacity of pyrvinium to bind and activate representative kinases from major branches of the kinase superfamily. We observed pyrvinium binding and activation of CK1α alone (Fig. 3.7D). Previous studies implicated all of the mammalian CK1 isoforms (α, γ1-3, δ and ε) in Wnt signal transduction(Price 2006). We found that pyrvinium binds all of the CK1 isoforms tested but only activates CK1α (Fig. 3.7E). This result was surprising because our *in vitro* kinase assays utilized a truncated form of CKIδ1-317, lacking the C-terminal regulatory domain (Fig. 3.8E). Compared to other isoforms, CK1α has a minimal C-terminal domain.

These findings suggest that the C-terminal regulatory domain of CK1 kinases may interfere with their activation by pyrvinium. If pyrvinium induces a conformational change to activate CK1α, we hypothesized that this may be reflected in a difference in its proteolytic digestion pattern upon trypsin treatment. Incubation of purified recombinant CK1α with pyrvinium yields a tryptic pattern distinct from CK1α alone, suggesting that pyrvinium alters the conformation of CK1α (Fig. 3.8F).

To provide evidence that pyrvinium activates CK1α *in vivo*, we immunoprecipitated CK1α from cells treated with or without pyrvinium and assessed kinase activity. CK1α isolated from cells treated with pyrvinium has enhanced kinase activity (Fig. 3.7F). To demonstrate interaction between pyrvinium and CK1α within cells, we treated HEK 293 cells expressing HA-tagged CK1α with pyrvinium, immunoprecipitated HA-CK1α, and performed mass spectrometry. Significant amounts of pyrvinium were co-immunoprecipitated with HA-CK1α relative to an HA-tagged GSK3 control (Fig. 3.7G).

If Wnt pathway inhibition by pyrvinium is mediated by CK1α activation, a structural analog of pyrvinium (VU-WS113) that has retained the capacity to inhibit Wnt signaling should also activate CK1α. Indeed, we found this to be the case (Fig. 3.7G,I). In contrast, a pyrvinium derivative (VU-WS211) that does not inhibit Wnt signaling failed to activate CK1α (Figs. 3.4F,G and 3.8H,I). If pyrvinium inhibits Wnt signaling via CK1α activation, we reasoned that loss of CK1α should abrogate the effects of pyrvinium on Wnt signaling. Using a cell line with significantly reduced CK1α levels due to inducible expression of shRNA against CK1α, we found that, in contrast to control cells, β-catenin and Axin levels were unaltered by pyrvinium

treatment (Fig. 3.7H)(Bidere, Ngo et al. 2009). Furthermore, pyrvinium failed to inhibit TOPflash activity in shRNA CK1α cells (Fig. 3.7I). These results indicate that the effects of pyrvinium on β-catenin and Axin levels and on Wnt signaling are mediated by its activation of CK1α.

Pyrvinium bypasses the destruction complex and β-catenin stabilization to inhibit Wnt signaling

Axin acts as a molecular scaffold to facilitate formation of the β-catenin destruction complex(Ikeda, Kishida et al. 1998; Itoh, Krupnik et al. 1998; Sakanaka, Weiss et al. 1998). Our biochemical studies suggest that pyrvinium-mediated inhibition of Wnt signaling could be due to increased levels of the β-catenin destruction complex secondary to Axin stabilization. This type of mechanism has been proposed as the basis for inhibition of Wnt signaling by recently reported compounds(Huang, Mishina et al. 2009) (Chen, Dodge et al. 2009). To determine whether pyrvinium acts at the level of the β-catenin destruction complex, we downregulated its components (Axin1/2 or APC) or treated cells with lithium (GSK3 inhibitor), all of which activate Wnt signaling. Surprisingly, these perturbations were all inhibited by pyrvinium (Fig. 3.9A). Overexpression of CK1α was similarly sufficient to inhibit lithium activation of Wnt signaling, consistent with CK1α mediating pyrvinium's inhibition of Wnt signaling downstream of the β-catenin destruction complex (Fig. 3.9B).

Because CK1α-pyrvinium bypasses the β-catenin destruction complex, we tested the activity of pyrvinium in SW480 cells, which have two mutant copies of the

APC gene. In addition to decreasing b-catenin levels and increasing Axin levels, pyrvinium also inhibited Wnt signaling (Figs. 3.9C and 3.10A,B). A common lesion in colon cancer is mutation in the GSK3 phosphorylation sites of β-catenin that inhibits its degradation(Sparks, Morin et al. 1998) (Polakis 2000). Pyrvinium had no effect on cytoplasmic β-catenin levels in the colon cancer line HCT-116 WTKO (expresses a non-degradable mutant allele of β-catenin and a knocked-out wild-type allele), yet it potently inhibited Wnt signaling (Figs. 3.9C and 3.10B). In contrast, treatment with the Axin stabilizer, IWR-1, failed to inhibit Wnt signaling in HEK 293 STF cells activated by lithium or in HCT-116 WTKO cells (Figs. 3.10C-F) (Chen, Dodge et al. 2009).

One possible explanation for inhibition of Wnt signaling by pyrvinium in the context of elevated β-catenin levels is that pyrvinium might block nuclear accumulation of β-catenin. This possibility is ruled out, however, by our finding that pyrvinium had no effect on nuclear entry of β-catenin in lithium-treated cells (Fig. 3.9D,E). Taken together, our results suggest that, in addition to its effects on Axin and β-catenin stability, CK1α-pyrvinium acts downstream and/or at the level of β-catenin.

Pyrvinium promotes Pygopus degradation

We assessed the effects of pyrvinium on levels of several nuclear factors required for β-catenin-mediated transcription: BCL9, Pygopus, and TCF4 (Kramps, Peter et al. 2002) (Thompson, Townsley et al. 2002) (Parker, Jemison et al. 2002) (Korinek, Barker et al. 1998). HEK 293 STF cells were treated with lithium (to

inhibit β-catenin degradation and activate Wnt signaling) and pyrvinium. A significant decrease in Pygopus levels was detected in response to pyrvinium that paralleled the decrease in luciferase expressed from the TOPflash reporter (Fig. 3.9F). No change in abundance or gel migration, however, was detected for TCF4 or BCL9 (Fig. 3.9G,H). Furthermore, pyrvinium treatment caused loss of nuclear GFP-Pygopus signal in HeLa cells and reduced levels of overexpressed and endogenous Pygopus in colon cancer cell lines (Figs. 3.9I and 3.10B,G). This correlation between Wnt signaling and Pygopus levels is supported by our finding that the EC_{50} values for Wnt inhibition and stimulation of Pygopus degradation by pyrvinium are nearly identical (Fig. 3.9J).

We found that Wnt signaling inhibits Pygopus degradation (half-life ~1.5 hour in the absence of Wnt and >5 hours in the presence of Wnt) and that pyrvinium reverses the effect of Wnt in a post-translational manner (half-life ~1 hour; Fig. 3.9K). In the absence of Wnt, pyrvinium had only a modest effect on the rate of Pygopus turnover (half-life ~1 hour). The effect of CK1α-pyrvinium on Pygopus degradation may be via a direct mechanism because CK1α co-immunoprecipitates with Pygopus (Fig. 3.9L). Finally, we show that shRNA against CK1α blocks the effect of pyrvinium on Pygopus levels, confirming that pyrvinium regulates Pygopus stability via CK1α (Fig. 3.9M).

To determine whether Pygopus is the most downstream target of CK1α-pyrvinium in the Wnt pathway, we tested whether pyrvinium could inhibit activation of Wnt signaling by LEFΔN-VP16. The fusion protein LEFΔN-VP16 has been shown to act independently of β-catenin to activate TCF/Lef1-responsive

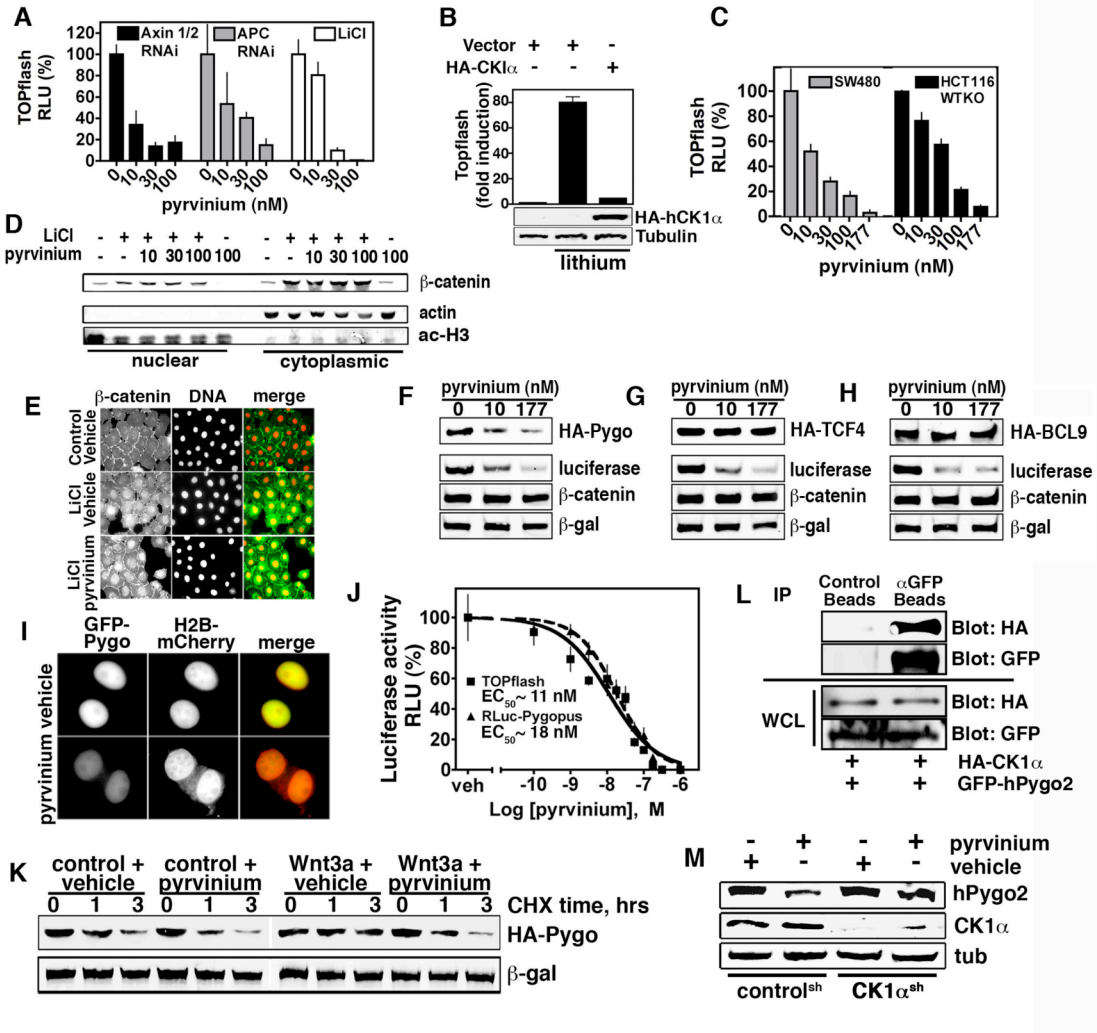
A
TOPflash RLU (%)
Axin 1/2 RNAi
APC RNAi
LiCl
pyrvinium (nM)
B
Vector
HA-CKIα
Topflash (fold induction)
HA-hCK1α
Tubulin
lithium
C
TOPflash RLU (%)
SW480
HCT116 WTKO
pyrvinium (nM)
D
LiCl
pyrvinium
β-catenin
actin
ac-H3
nuclear
cytoplasmic
E
β-catenin
DNA
merge
Control Vehicle
LiCl Vehicle
LiCl pyrvinium
F
pyrvinium (nM)
HA-Pygo
luciferase
β-catenin
β-gal
G
pyrvinium (nM)
HA-TCF4
luciferase
β-catenin
β-gal
H
pyrvinium (nM)
HA-BCL9
luciferase
β-catenin
β-gal
I
GFP-Pygo
H2B-mCherry
merge
pyrvinium vehicle
J
Luciferase activity RLU (%)
TOPflash EC50~ 11 nM
RLuc-Pygopus EC50~ 18 nM
veh
Log [pyrvinium], M
L
IP
Control Beads
αGFP Beads
Blot: HA
Blot: GFP
WCL
HA-CK1α
GFP-hPygo2
K
control + vehicle
control + pyrvinium
Wnt3a + vehicle
Wnt3a + pyrvinium
CHX time, hrs
HA-Pygo
β-gal
M
pyrvinium
vehicle
hPygo2
CK1α
tub
control^sh
CK1α^sh

Figure 3.9. Pyrvinium promotes Pygopus degradation. (A) Pyrvinium inhibits ligand-independent Wnt activation. HEK 293 STF cells were treated with Axin siRNA, APC siRNA, or LiCl (50 mM) followed by pyrvinium. Lysates were assayed for TOPflash activity. **(B)** Overexpression of human CK1α inhibits activation of the Wnt pathway by lithium. HEK 293 STF cells were transfected as indicated and treated with pyrvinium (100 nM). Lysates were analyzed by TOPflash assay and immunoblotting. Lithium (50 mM) was added at the same time as pyrvinium. Tubulin, control. **(C)** Pyrvinium inhibits Wnt signaling in colon cancer cells. Cells transfected with TOPflash reporter and *Renilla* luciferase control plasmid were treated with pyrvinium. Lysates were assayed for luciferase activity. For A-C, graphs show mean ± s.e.m. of luciferase signal normalized by cell number (performed in quadruplicate). **(D,E)** Pyrvinium has no effect on β-catenin nuclear accumulation in cells treated with lithium. **(D)** HEK 293 cells were treated with LiCl (50 mM) and/or pyrvinium. Cytoplasmic and nuclear fractions were immunoblotted for β-catenin. Purity of nuclear and cytoplasmic preparations was assessed by immunoblotting for acetylated Histone H3 and actin, respectively. NaCl and vehicle were used in LiCl and pyrvinium minus lanes, respectively. **(E)** IEC-6 cells were treated with LiCl (50 mM) and/or pyrvinium (100 nM), fixed, and stained for β-catenin and DNA. **(F-H)** Pyrvinium promotes turnover of Pygopus, but not TCF4 or BCL9. HEK 293 STF cells expressing indicated HA fusions were treated with pyrvinium. LiCl (50 mM) was included in the media to activate Wnt signaling and inhibit β-catenin degradation. Lysates were immunoblotted for HA, luciferase (to confirm inhibition of Wnt signaling by pyrvinium), and β-galactosidase (transfection control). **(I)** Pyrvinium reduces nuclear Pygopus levels. HeLa cells expression GFP-Pygopus and histone H2B-mCherry (marks DNA) were treated with pyrvinium (100 nM). **(J)** Pyrvinium inhibits Wnt signaling and promotes Pygopus turnover to a similar degree. HEK 293 STF cells expressing *Renilla*-luciferase-Pygopus (RLuc-Pygopus) fusion and β-galactosidase were treated with pyrvinium. Mean ± s.e.m. of *Renilla* luciferase signal normalized to β-galactosidase is shown (performed in quadruplicate, displayed as percent response). **(K)** Pyrvinium reverses Wnt-mediated inhibition of Pygopus degradation. HEK 293 STF cells expressing HA-Pygopus were treated with Wnt3a and/or pyrvinium (100 nM) for 30 minutes prior to cycloheximide (CHX; 50 μg/ml) addition (time=0). Lysates were prepared at indicated times for immunoblotting. β-galactosidase, loading control. **(L)** CK1α interacts with Pygopus. HEK293 cells were transfected with HA-CK1α and GFP-Pygopus. Cells were lysed and immunoprecipitated with either anti-GFP beads or control beads. HA-CK1α and GFP-Pygopus were detected by immunoblotting with HA and GFP antibodies. **(M)** Downregulating CK1α blocks pyrvinium-stimulated Pygopus turnover. A Jurkat cell line expressing $CK1\alpha^{sh}$ was incubated with pyrvinium (30 nM) for 24 hours. Lysates were immunoblotted for Pygopus and Tubulin (loading control).

genes(Aoki, Hecht et al. 1999). We found that activation of transcription by LEFΔN-VP16 was sensitive to pyrvinium and CK1α (~50% reduction), indicating that CK1α-pyrvinium also acts at the level TCF/Lef1, albeit weakly (Fig. 3.11).

Pyrvinium decreases viability and proliferation of colon cancer cells with activating mutations in the Wnt pathway

Given the potent effect of pyrvinium on Wnt signaling in a variety of contexts, we next tested its effects on Wnt-mediated cellular transformation and proliferation. Wnt3a induced rounding of HEK 293 cells and formation of colonies in which cells grew on top of each other as well as loss of ZO-1, a tight junction marker; these effects were reversed by pyrvinium treatment (Fig. 3.12A,B). Pyrvinium caused substantial reduction in Ki-67 staining (a cellular marker for proliferation) in HCT-116 cells (Fig. 3.12C). Pyrvinium had no obvious effect, however, on the cell-cycle phasing of SW480 cells as assessed by DNA content (Fig. 3.12D).

For concentrations of pyrvinium at which we observe significant inhibition of Wnt signaling, we did not observe significant cytotoxicity. Rather, cellular growth/proliferation was substantially inhibited (Fig. 3.13). Consistent with lack of cytotoxicity, we found that pyrvinium poorly induced Caspase 3/7 activity in SW620 cells, a highly metastatic colon cancer cell line with mutant APC that is resistant to apoptosis (Fig. 3.14). We found, however, that a combination of pyrvinium and 5-fluorouracil (5-FU), a chemotherapeutic agent, synergized to induce a high degree of apoptosis.

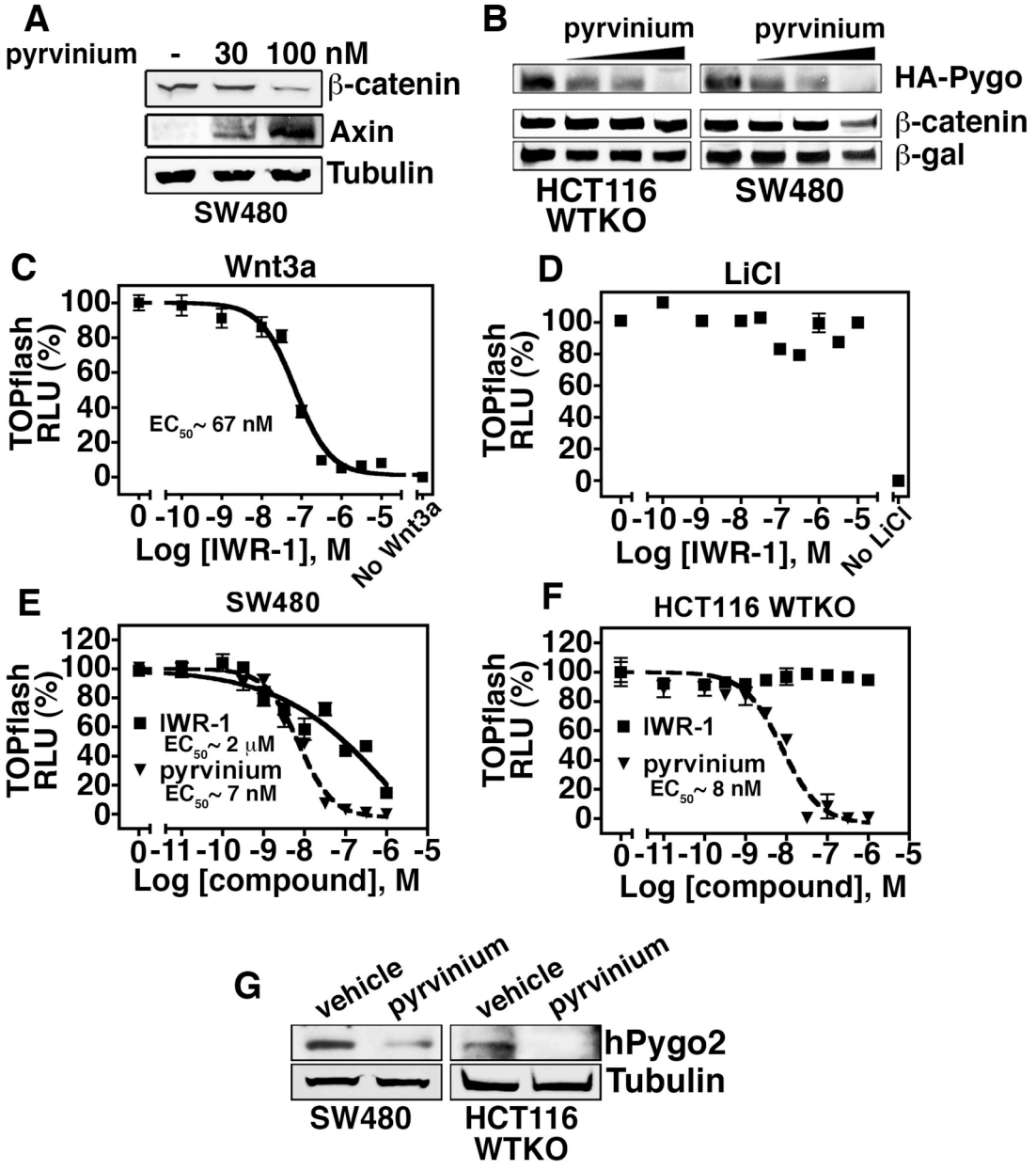
A
pyrvinium - 30 100 nM
β-catenin
Axin
Tubulin
SW480
B
pyrvinium
pyrvinium
HA-Pygo
β-catenin
β-gal
HCT116 WTKO
SW480
C
Wnt3a
TOPflash RLU (%)
EC50~ 67 nM
Log [IWR-1], M
No Wnt3a
D
LiCl
TOPflash RLU (%)
Log [IWR-1], M
No LiCl
E
SW480
TOPflash RLU (%)
IWR-1
EC50~ 2 μM
pyrvinium
EC50~ 7 nM
Log [compound], M
F
HCT116 WTKO
TOPflash RLU (%)
IWR-1
pyrvinium
EC50~ 8 nM
Log [compound], M
G
vehicle
pyrvinium
vehicle
pyrvinium
hPygo2
Tubulin
SW480
HCT116 WTKO

Figure 3.10. (A) Pyrvinium decreases β-catenin and increases Axin levels in a colon cancer line mutant for APC. SW480 cells were treated with pyrvinium (100 nM) and lysates immunoblotted for β-catenin and Axin. Tubulin, loading control. **(B)** Effects of pyrvinium on levels of overexpressed Pygopus and β-catenin in HCT116 WTKO and SW480 cell lines. Transfected cells expressing HA-tagged Pygopus were treated with pyrvinium (100 nM). Lysates were immunoblotted for HA and β-catenin. β-galactosidase (β-gal), loading control. **(C-F)** Inhibition of Wnt signaling by an Axin stabilizing compound, IWR-1, differs from that of pyrvinium. **(C, D)** HEK 293 STF reporter cells were treated with Wnt3a **(E)** or LiCl (50 mM) **(F)** with indicated doses of IWR-1. **(E,F)** Compared to the effects of pyrvinium on inhibition of TOPflash, IWR-1 is less potent in SW480 cells **(E)** or is ineffective in HCT116 WTKO cells **(F)**. Graphs show mean ± s.e.m. of luciferase signal normalized by cell number (performed in quadruplicate). **(G)** Pyrvinium stimulates turnover of Pygopus in colorectal cancer lines. HCT116 WTKO and SW480 cell lines were treated with pyrvinium (100 nM) and immunoblotted for endogenous Pygopus. Tubulin, loading control.

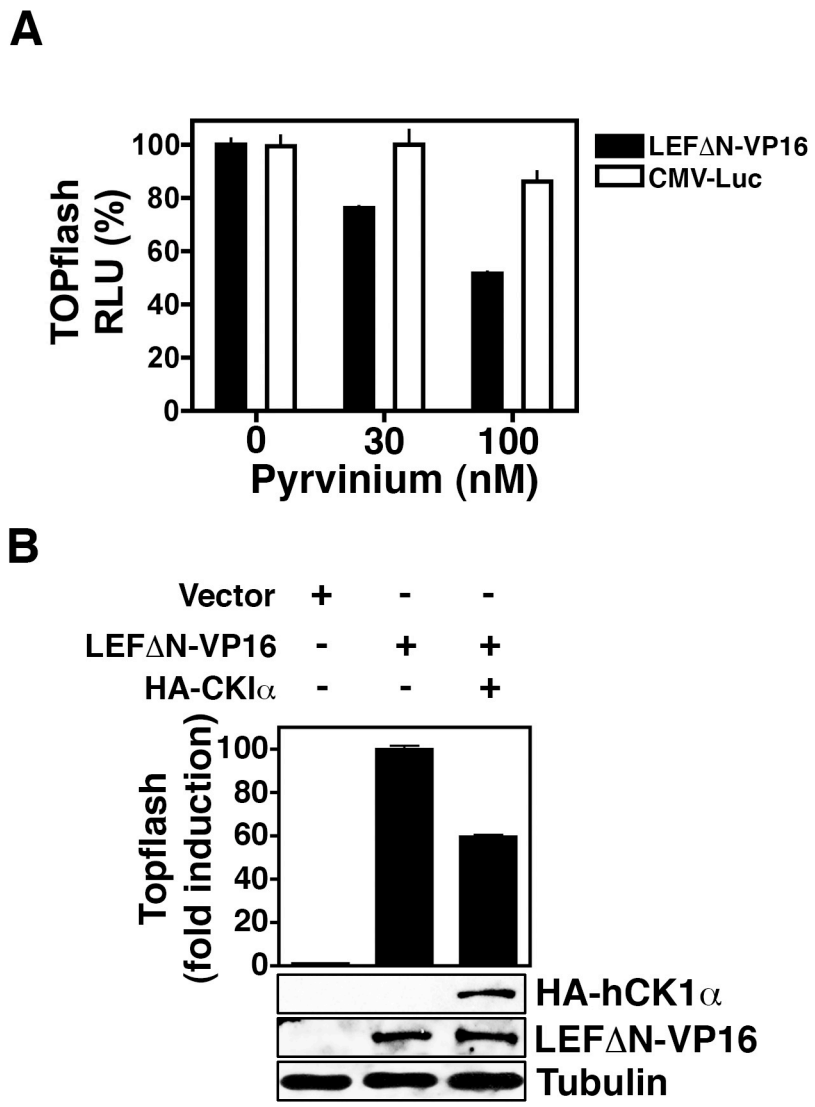

Figure 3.11. (A. B) Pyrvinium inhibits TCF/Lef1-mediated Wnt signaling. HEK 293 STF cells were **(A)** transfected with LEFDN-VP16 or CMV-Luc followed by pyrvinium treatment or **(B)** transfected with LEFDN-VP16 plus or minus CK1α. Lysates were assayed for TOPflash activity. Mean ± s.e.m. of TOPflash activity is graphed (performed in quadruplicate and displayed as percent response).

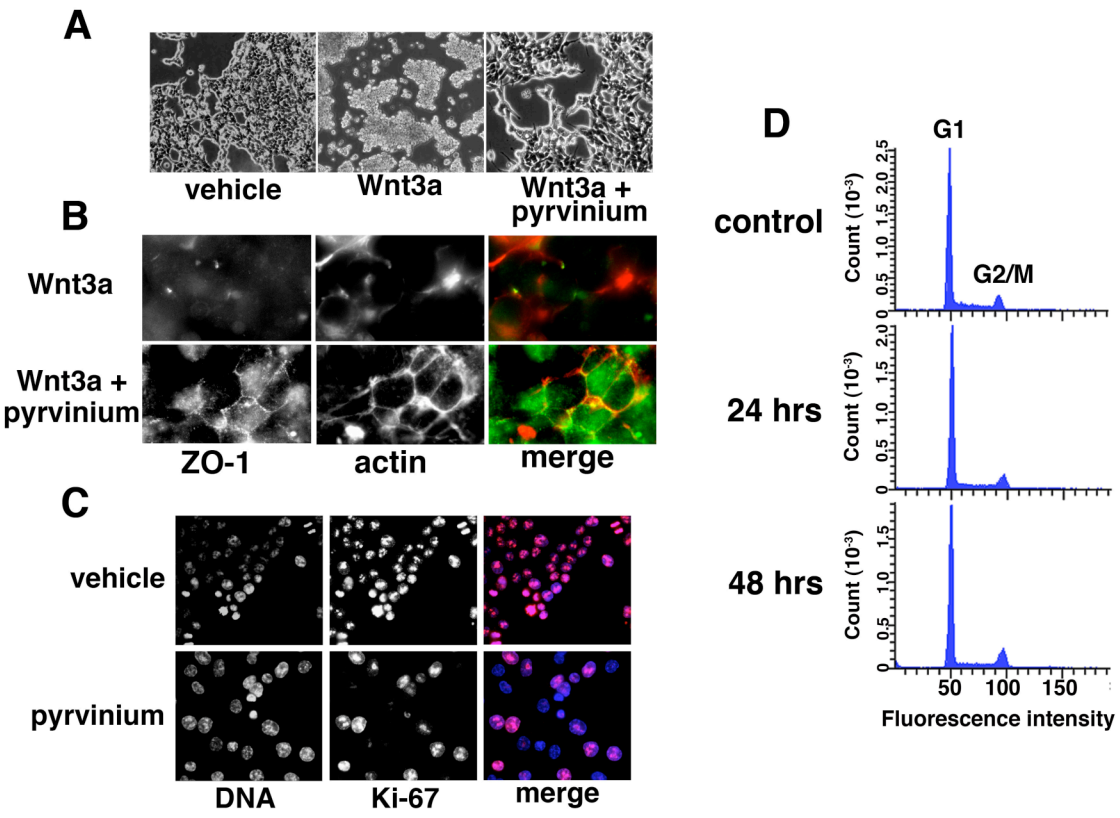

Figure 3.12. (A, B) Pyrvinium inhibits Wnt3a-induced changes in cell morphology and repression of the junction marker, ZO-1. HEK 293 cells were treated Wnt3a in the absence or presence of pyrvinium (10 nM) for 7 days. **(A)** Phase-contrast micrographs (20X magnification) show reversion of Wnt3a-induced changes in morphology by pyrvinium. **(B)** Immunofluorescent micrographs (40X magnification) show that pyrvinium enhances ZO-1 staining in Wnt3a-treated cells. Phalloidin staining of actin marks the cell cortex. **(C, D)** Pyrvinium decreases proliferation of HCT116 WTKO cells without affecting cell-cycle phasing. **(C)** Cells were treated with pyrvinium (100 nM) for 48 hours, fixed, and stained for Ki-67, a proliferation marker. Cells are shown at 100X magnification. **(D)** Cells were treated with pyrvinium (100 nM) for 24 or 48 hours, fixed, stained with DAPI, and analyzed by FACS.

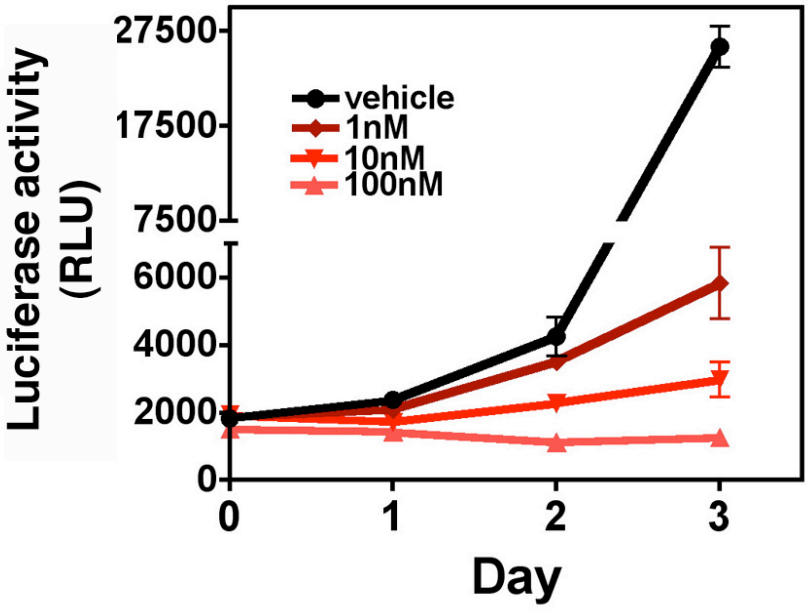

Figure 3.13. Pyrvinium inhibits the growth/proliferation of cultured cancer cells in a dose-dependent manner. HCT116 cells were incubated with varying concentrations of pyrvinum and viability assessed using CellTiter-Fluor (Promega) at the indicated times.

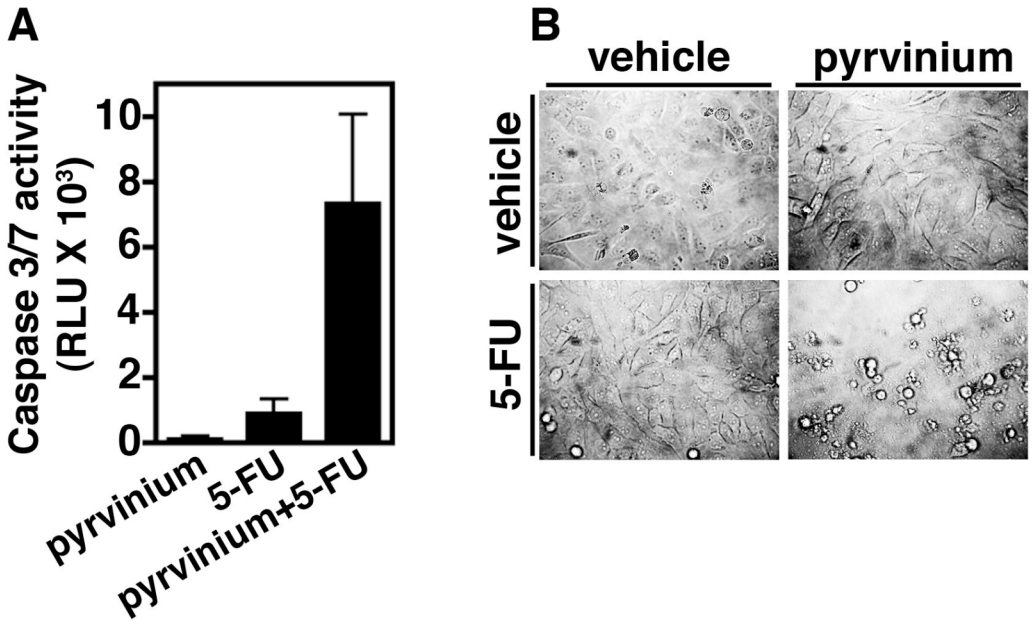

Figure 3.14. Pyrvinium potentiates the apoptotic effects of 5-FU on colon cancer cells. The highly metastatic colon cancer line, SW620, was treated with combinations of pyrvinium (100 nM) and 5-FU (5 μM). **(A)** Mean ± s.e.m. of caspase 3/7 activity normalized to vehicle-treated cells is graphed (performed in triplicate). **(B)** Phase contrast micrographs (20X magnification) show enhanced blebbing of cells treated with both compounds (indicative of apoptosis).

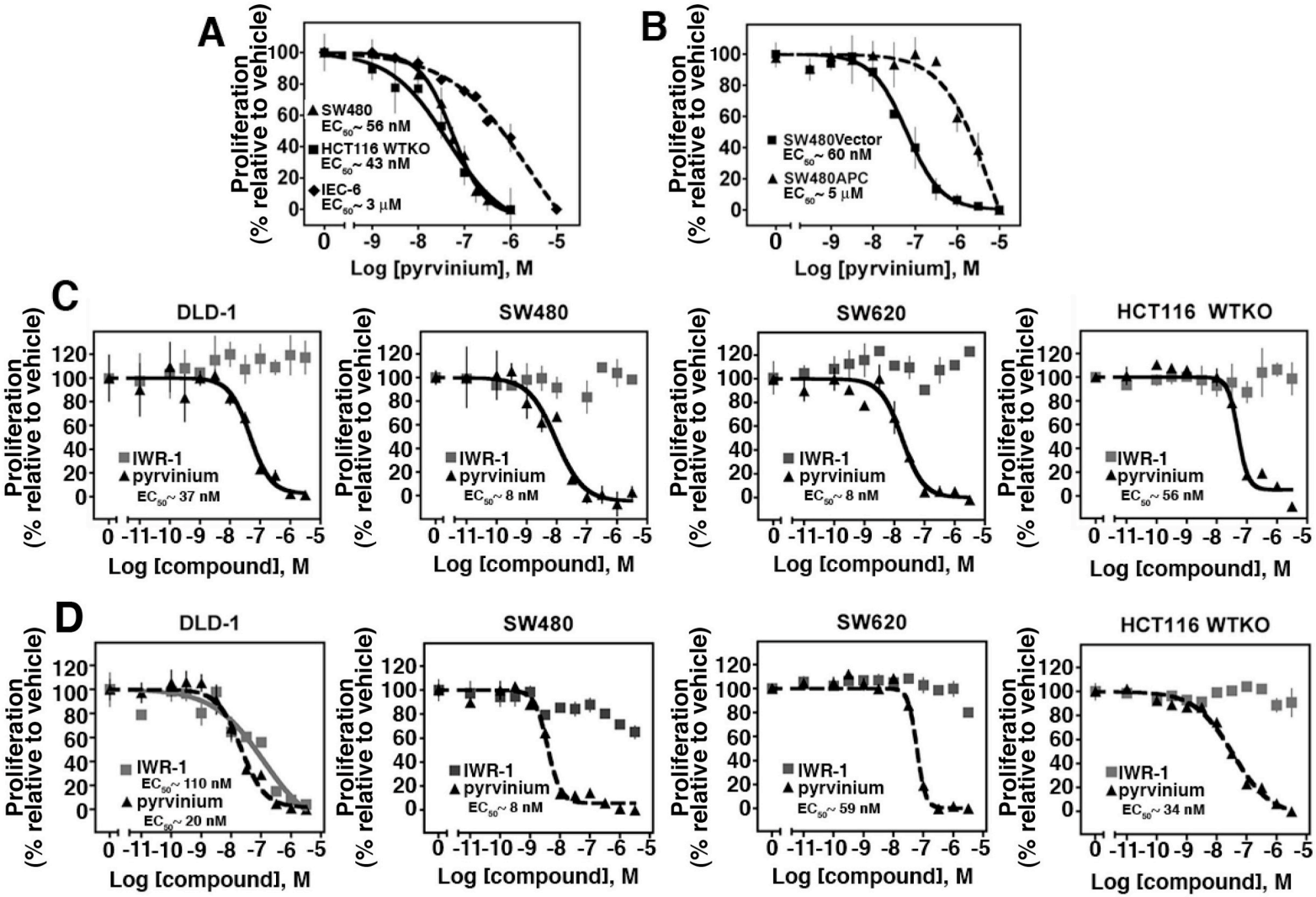
A
Proliferation (% relative to vehicle)
SW480 EC50~ 56 nM
HCT116 WTKO EC50~ 43 nM
IEC-6 EC50~ 3 μM
Log [pyrvinium], M
B
Proliferation (% relative to vehicle)
SW480Vector EC50~ 60 nM
SW480APC EC50~ 5 μM
Log [pyrvinium], M
C
DLD-1
SW480
SW620
HCT116 WTKO
Proliferation (% relative to vehicle)
IWR-1
pyrvinium
EC50~ 37 nM
EC50~ 8 nM
EC50~ 8 nM
EC50~ 56 nM
Log [compound], M
D
DLD-1
SW480
SW620
HCT116 WTKO
Proliferation (% relative to vehicle)
IWR-1
EC50~ 110 nM
pyrvinium
EC50~ 20 nM
EC50~ 8 nM
EC50~ 59 nM
EC50~ 34 nM
Log [compound], M

Figure 3.15. Pyvinium selectively decreases cell viability of colon cancer cells with activating mutations in the Wnt pathway. (A-D) Cell viability assays. Cell viability was determined following treatment with pyrvinium for 72 hours. Mean ± s.e.m is shown (assays performed in quadruplicate). **(A)** Colon cancer cell lines (SW480 and HCT116 WTKO) are more sensitive to pyrvinium than a non-transformed epithelial cell line (IEC-6). **(B)** SW480 cells expressing full-length APC (SW480APC) are more resistant to pyrvinium than SW480 cells transfected with empty vector (SW480Vector). **(C)** Pyrvinium but not IWR-1 decreases viability of colon cancer cells under normal serum conditions. Colon cancer lines (SW480, SW620, HCT116 WTKO, and DLD-1) were treated with the indicated concentrations of pyrvinium or IWR-1 for 72 hours in normal growth media (10% FBS) and cell viability determined. **(D)** Effects of pyrvinium versus IWR-1 on viability of colon cancer cells grown under low serum conditions. Colon cancer lines were treated with the indicated concentrations of pyrvinium or IWR-1 for 72 hours in media with low serum (1% FBS) and cell viability determined.

Because pyrvinium inhibits Wnt signaling in the colon cancer lines SW480 and HCT-116 WTKO, we next tested whether pyrvinium affects the viability of these cells. We observed decreased cell viability at pyrvinium concentrations that cause Wnt pathway inhibition (Figs. 3.2J and 3.15A). Pyrvinium had relatively less effect on viability of IEC-6 cells, a non-transformed epithelial cell line (Fig. 3.15A) (Quaroni, Wands et al. 1979). To further assess whether pyrvinium selectively decreases viability of cells with Wnt pathway mutations, we compared the sensitivity of the SW480 colon cancer line with truncated APC (SW480Vector) to a line in which wild-type, full-length APC has been introduced so as to restore normal Wnt signaling (SW480APC) (Faux, Ross et al. 2004). We found that SW480APC cells are ~80-fold less sensitive to pyrvinium than SW480Vector cells (Figs. 3.15B).

Recently, compounds that inhibit Wnt signaling via Axin stabilization were shown to inhibit viability and proliferation of DLD-1 cells, a colon cancer line mutant for APC(Chen, Dodge et al. 2009; Huang, Mishina et al. 2009). These studies, however, used suboptimal growth conditions (0.5% fetal bovine serum (FBS)) for cultured human cells. Under optimal growth conditions (10% FBS), we found that pyrvinium potently decreased viability of several commonly studied colon cancer lines; in contrast, the Axin stabilizing compound IWR-1 had no effect (Fig. 3.15C). In agreement with previous reports, we detected an effect of IWR-1 on the viability of DLD-1 cells grown under suboptimal growth conditions (0.5% FBS); other colon cancer lines thought to be driven by Wnt signaling, however, were resistant to IWR-1 under these conditions in contrast to pyrvinium (Fig. 3.15D).

Summary

Wnt/β-catenin signaling plays critical roles in metazoan development, stem cell maintenance, and human disease. Using *Xenopus* egg extract to screen for compounds that both stabilize Axin and promote β-catenin turnover, we identified an FDA-approved drug, pyrvinium, as a potent inhibitor of Wnt signaling (EC_{50} ~10 nM). Studies in *Xenopus*, *Drosophila*, and *C. elegans* show pyrvinium inhibits Wnt signaling across phyla, indicating conservation of drug target. We show pyrvinium binds all Casein Kinase 1 (CK1) family members *in vitro* at low nanomolar concentrations and selectively potentiate CK1α kinase activity. CK1α knockdown abrogates the effects of pyrvinium on the Wnt pathway. In addition to its effects on Axin and β-catenin levels, pyrivinium promotes degradation of Pygopus, a Wnt transcriptional component. Pyrvinium treatment of colon cancer cells with mutation of Adenomatous Polyposis Coli or β-catenin inhibits both Wnt signaling and proliferation. Our findings reveal allosteric activation of CK1α as an effective mechanism to inhibit Wnt signaling and highlight a new strategy for targeted therapeutics directed against the Wnt pathway.

CHAPTER IV

POSITIVE FEEDBACK WITHIN THE β-CATENIN DESTRUCTION COMPLEX IMPARTS BISTABLILITY AND MEMORY OF WNT SIGNALING

Introduction

Canonical Wnt signaling is a critical signaling pathway in development and disease and has been the subject of intense study for over 25 years(Clevers 2006). Despite the identification of numerous pathway components, general principles that govern the structure and behavior of the pathway remain to be elucidated. Progress toward this end is made through methodical biochemical/structural analysis combined with theoretical modeling bound by experimentally derived parameters. β-catenin is the key transcription factor required for canonical Wnt signaling. The β-catenin destruction complex is assembled on the scaffold protein Axin and requires other critical factors such as Glycogen Synthase Kinase 3 (GSK3), Casein Kinase 1 (CK1), and Adenomotous Poliposis Coli (APC)(MacDonald, Tamai et al. 2009). This complex acts to phosphorylate β-catenin, thus targeting it for ubiquitination and degradation. How this multicomponent β-catenin destruction module is activated, and upon signaling, becomes inactivated, is a poorly understood process.

The Wnt ligands are morphorgens, eliciting cell proliferation and differentiation responses in embryonic and adult tissue(Ashe and Briscoe 2006). *In vivo*, Wnts often appear to form signal gradients eliciting distinct responses that

correlate with ligand concentration. Despite this observation, the studies are confounded by a plethora of growth factors that crosstalk with each other in time and space within the four dimensional environment of a living animal. Other studies have found sharp borders of responding cells directly adjacent to non-responsive cells (Hayward, Kalmar et al. 2008). These findings raise the queston, is Wnt signal transduction a graded response or binary? Here we uncover a positive feedback loop with the β-catenin destruction complex that instills a binary (bistable) response to a Wnt gradient. Pharmacologic perturbation of the feedback removes bistability and allows for a graded response. These findings suggest the Wnt pathway exists as a binary switch allowing for robust and decisive single cell responses. β-catenin destruction complex feedback also presents a molecular node for signal integration from other pathways that theoretically could modulate the threshold and dynamics of a cell's response to Wnt signaling.

Results

Positive feedback in the β-catenin destruction complex

Previous studies in mammalian cell culture and *in vitro* reconstitution have shown Axin to be a direct target of GSK3(Yamamoto, Kishida et al. 1999). This phosphorylation prevents the degradation of Axin and keeps the β-catenin destruction complex intact(Kimelman and Xu 2006; MacDonald, Tamai et al. 2009). Because *Xenopus* egg extracts are easily amenable to kinetic and biochemical studies and have been shown to faithfully recapitulate signaling dynamics that control β-catenin, we looked at GSK3 regulation of Axin in extracts(Salic, Lee et al. 2000; Lee,

Salic et al. 2003; Cselenyi, Jernigan et al. 2008). Addition of radiolabeled Axin to extracts demonstrated Axin to be a stable protein with slow degradation kinetics (>3 hrs) (Fig. 4.1A,B). Consistent with previous studies, inhibition of GSK3 with LiCl induces the Axin turnover. This degradation event requires both the GSK3 binding site on Axin and the target serines 322 and 326 (Fig. 4.1C)(Yamamoto, Kishida et al. 1999), thus suggesting direct binding is required.

Localized activation of GSK3 by Axin

GSK3 plays a prominent role in many signal transduction pathways(Woodgett 2001). The extremely low concentration of Axin provides a simple means to insulating a pool of GSK3 specifically targeted towards β-catenin. The scaffolding nature of Axin also makes it a candidate to play a role in activating bound GSK3, leading to Axin stability and promoting β-catenin degradation.

We examine GSK3 activity in *Xenopus* egg extracts by phospho-specific antibody that recognizes inhibited GSK3 by phosphorylaton at serine 9 (pS9). Interestingly, addition of recombinant Axin to extracts caused a dramatic reduction in pS9 GSK3 (Fig. 4.2A). A previous study demonstrated a phosphatase requirement for β-catenin degradation(Seeling, Miller et al. 1999). We tested the effect of okadaic acid on the inhibitory phosphorylation on Ser9 of GSK3. As shown in Figure 4.2A, addition of Axin could not overcome the treatement of okadaic acid for pS9 removal, suggesting a requirement for PP2a in the dephosphorylation of GSK3.

We performed deletional analysis of Axin to identify regions that bind necessary factors for serine 9 dephosphorylation on GSK3 (Fig. 4.2B). Axin mutants

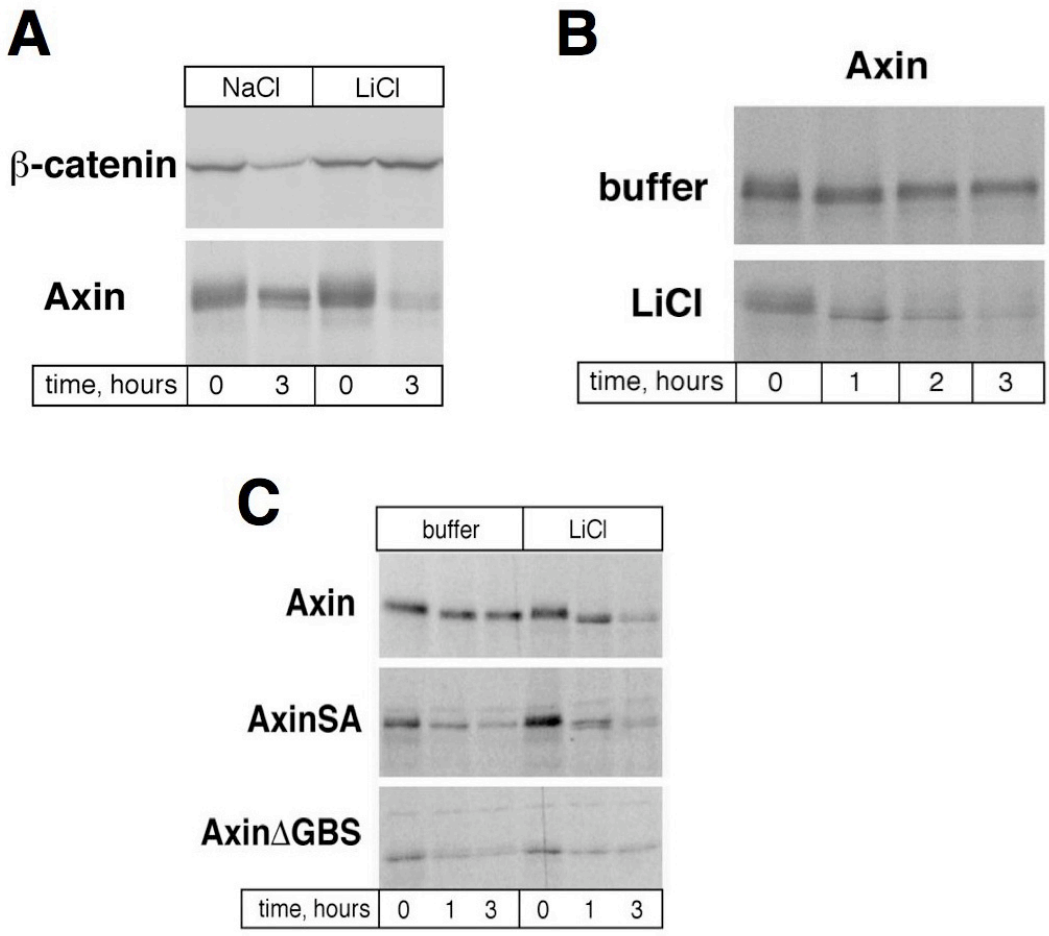

Figure 4.1. Inhibition of GSK3 stimulates Axin turnover. (A-B) Radiolabeled β-catenin and Axin were spiked into *Xenopus* egg extracts. Aliquots were removed at the indicated timepoints and analyzed by autoradiography. LiCl was used at 50 mM. **(C)** Performed as in **(A)** and **(B).** Axin SA contains serine 322 and 326 mutated to alanine. AxindeltaGBS lacks GSK3 binding.

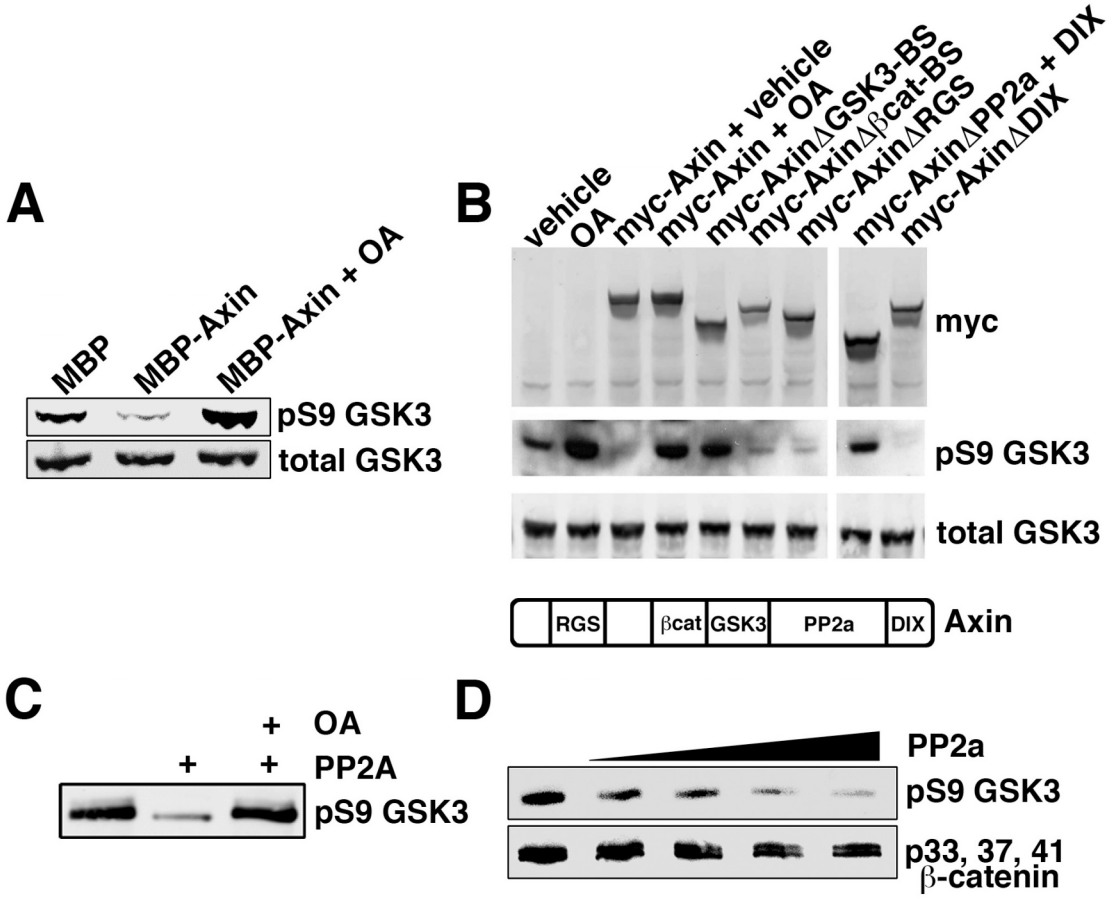

Figure 4.2. Positive feedback in the β-catenin destruction complex. (A) Axin catalyzes pS9 GSK3 removal in extracts. Recombinant MBP-Axin was added to extract and reaction was stopped at 15 mins. **(B)** Axin catalyzes phospho-S9 GSK3 removal in cells. Axin truncation mutants were transfected in HEK 293 cells and lysed 24 hrs later. The lack of pS9 removal demonstrates a requirement for PP2a and GSK3 binding sites. OA was used at 10 nM. **(C)** Serine 9 removal *in vitro* via PP2a. Axin (1 uM) and GSK3 (10 uM) were incubate for 30 mins with ATP to allow for autophosphorylation of GSK3. Then PP2a (1 uM) and OA (10 nM) was added for an additional 30 mins. pS9 was analyzed by western blot. **(D)** PP2a preferentially removes GSK3 serine 9 phosphorylation over sites on b-catenin. Performed as in **(C)** with the addition of recombinant β-catenin (10 uM).

lacking the APC-binding RGS domain (AxinΔRGS) or the β-catenin-binding domain (AxinΔbCBD) were dispensable for serine 9 dephosphorylation, suggesting that neither APC nor β-catenin are required (Fig. 4.2B). The GSK3-binding site Axin mutant (AxinΔGBD), however, had no activity for GSK3 serine 9 dephosphorylation (Fig. 4.2B). Similarly, a fragment without the PP2a and DIX domains did not stimulate serine 9 dephosphorylation (Fig. 4.2B), yet deletion of DIX domain alone maintained dephosphorylation capacity. To test if PP2a could remove serine 9 directly we used purified components *in vitro*. PP2a significantly removed serine 9 and appeared to have specificity for phosphorylated GSK3 over β-catenin (Fig. 4.2C,D). Based on these results, an obvious model for localized activation of GSK3 by Axin emerges; free GSK3 is largely in an inactive state and then, once entering the Axin-PP2a complex, becomes rapidly activated by PP2a leading to an active β-catenin destruction complex.

Theoretical model of the β-catenin destruction complex predicts bistability

To gain insight into how the mutual regulation of GSK3 and Axin could affect the activity of the β-catenin destruction complex as a whole, we developed a mathematical characterization. First, a wiring diagram of all relevant biochemical reactions was schemed (Fig. 4.3). Biochemical reactions based on this present work, previously published data or from logical inference, were mathematically described in a set ordinary differential equations (ODEs). Solutions of this β-catenin destruction complex ODE series predicted bifucation in complex activity (personal communication with J.J. Tyson, Virgina Tech). Increasing signal strength did not

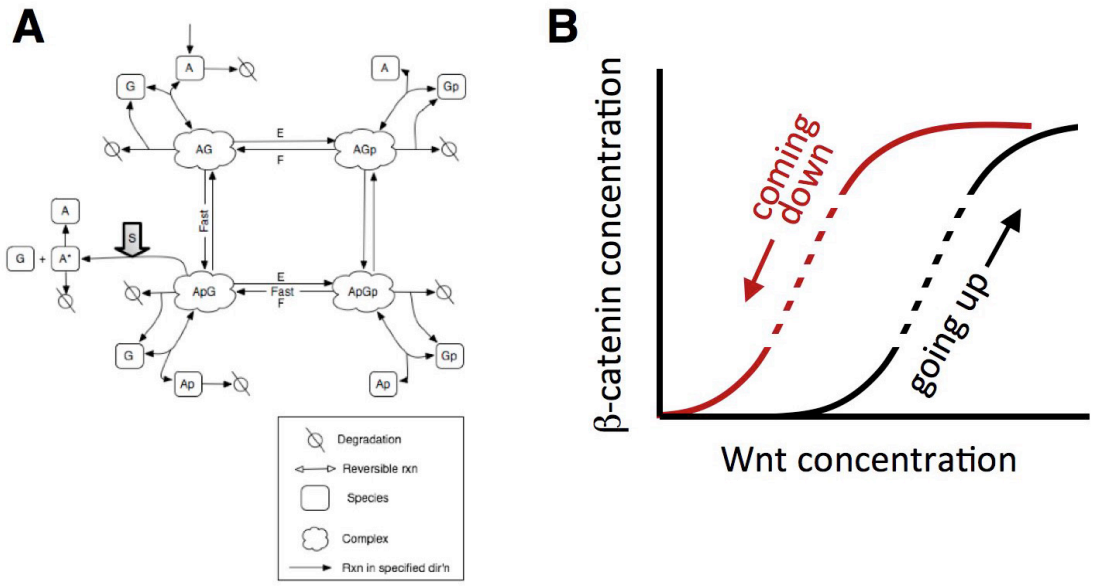

Figure 4.3. Theoretical model of the β-catenin destruction complex predicts bistability. (A) Wiring diagram of all possible molecular species in the β-catenin destruction complex. Abbreviations; A-Axin, G-GSK3, p-phosporylation, E-unknown kinase, F-unknown phosphatase. **(B)** A stylized depiction of bistability and hysteresis. Dotted sections represent meta-stable states that exist only transiently.

lead to a linear decrease in destruction complex activity, rather it had no effect on complex activity until a signal threshold was reached and full complex inhibition occurred. Thus, the system is bistable meaning it can toggle between two stable states, β-catenin destruction complex "on" in the absence of a signal and complex "off" in the presence of signal. For a system to be truly bistable, by definition it should exhibit hysteresis; the signal strength required to flip the complex off is higher than the signal strength needed to maintain the off state(Ferrell 2002; Ferrell, Pomerening et al. 2009). We sought to validate these theoretical predictions experimenatally.

β-Catenin response to stimulus exhibits bistability and hysteresis

Measuring β-catenin response to stimulus by western blot demonstrates a graded response. Thus, β-catenin stabilization could be described as directly proportional to the concentration of Wnt ligand(Fig. 4.4A). Yet, because western blot analysis represents an ensemble average as a result of homogenization of cells by lysis, it is not an accurate characterization of how single cells respond to stimulation(Altschuler and Wu 2010). To test the model predictions of bistability and hysteresis, we needed to observed β-catenin levels in response to increasing stimuli at the single cell level. We chose RKO human intestinal cancer cells for these studies because they contain no mutations in Wnt pathway components and have low membrane bound β-catenin, making the dynamic cytoplasmic pool of β-catenin simpler to quantify. Cells were stimulated for ~12-15 hours, long enough for β-catenin and Axin to reach steady state levels in the active state. (Fig. 4.5, data not

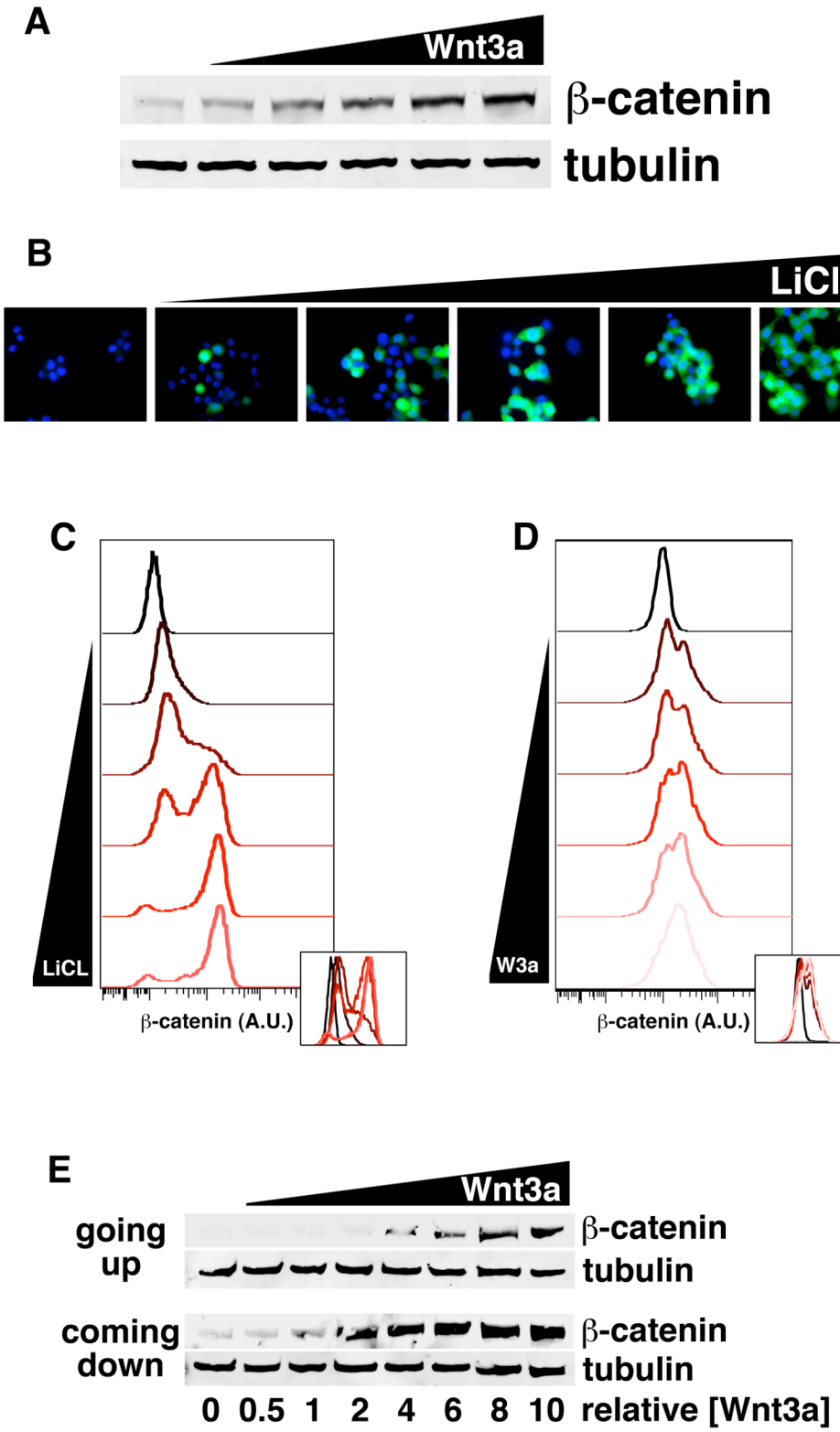
A
Wnt3a
β-catenin
tubulin
B
LiCl
C
LiCL
β-catenin (A.U.)
D
W3a
β-catenin (A.U.)
E
Wnt3a
going up
β-catenin
tubulin
coming down
β-catenin
tubulin
0 0.5 1 2 4 6 8 10 relative [Wnt3a]

Figure 4.4. β-Catenin response to stimulus exhibits bistability and hysteresis. **(A)** Western blot of β-catenin response to increasing concentrations of Wnt3a. **(B)** Immunofluorescent images of β-catenin levels in RKO cells in response to increasing LiCl concentrations (10-80 mM). **(C-D)** Flow cytometry graphs of β-catenin levels in response to increasing LiCl or Wnt3a concentrations. Histograms represent β-catenin levels in a population of 20,000 counted cells. **(E)** Western blot showing changes in activation threshold of cells prestimulated vs. unstimulated cells.

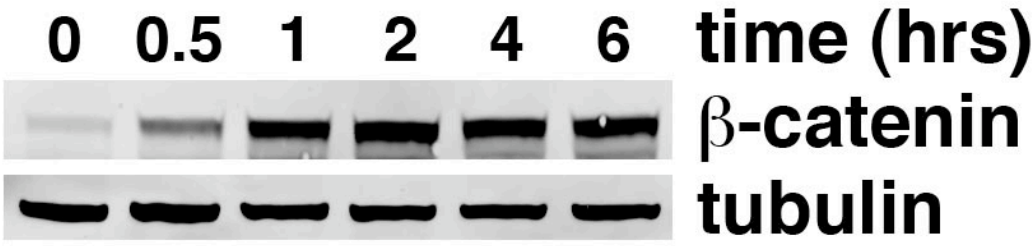

Figure 4.5. Timing of β-catenin stabilization. Western blot for β-catenin in RKO cells treated with a maximal does of Wnt3a.

shown). When these cells are stimulated with LiCl or Wnt3a, immunofluorescent images show an obvious heterogeneity of β-catenin levels at intermediate doses that are reminiscent of switch-like or bistable response (Fig. 4.4B and data not shown). To quantify β-catenin levels in stimulated cells we used flow cytometry (Fig. 4.4C,D). Importantly, we found intermediate doses of LiCl or Wnt3a induced a biphasic β-catenin response; a low or unresponding population as well as a high or fully responding population. This behavior has its mechanistic roots in two possibilities, ultrasensitivity or bistablility(Ferrell and Xiong 2001). Simple coopertivity could explain an ultrasensitive and thus switch-like response. For a response to be bistable it must exhibit hysteresis and demonstrate lowering of activation threshold when cells are starting from a fully stimulated state. To test this we pretreated cells with Wnt3a or control media long enough to fully stabilize β-catenin (6hrs, Fig. 4.5), washed the stimulus away, and applied various doses of Wnt3a. We show that the samples previously stimulated with Wnt3a have a lower activation threshold than control-stimulated cells (Fig. 4.4E). These results demonstrate β-catenin responds to stimulus in a bistable and thus, hysteretic manner.

Feedback produces memory of Wnt stimulation

Wnt signaling induces cell proliferation or differentiation over long developmental time spans(Nusse 2005). Intuitively, tissues receiving a Wnt signal respond decisively even if the Wnt morphogen gradient fluctuates or disappears. This kind of response requires cellular memory(Ajo-Franklin, Drubin et al. 2007; Burrill and Silver 2010). Axin degradation upon signaling represents an irreversible

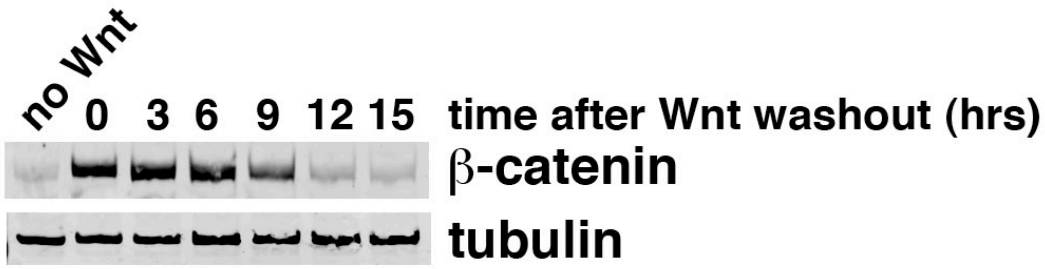

Figure 4.6. Cells display memory of Wnt3a stimulation. RKO cells were stimulated with Wnt3a for 3 hours and then wash with regular media and timepoints analyzed.

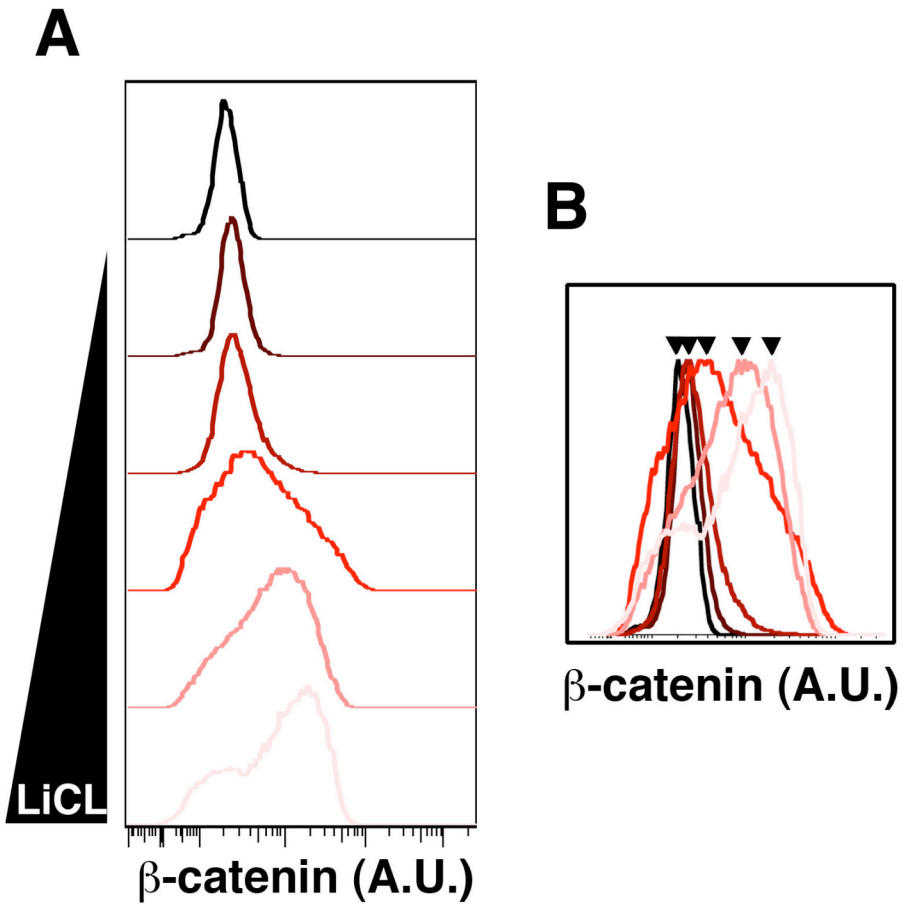

Figure 4.7. Blocking positive feedback removes bistability. (A) RKO cells were treated with IWR-1 (5 uM) 1 hour before Li stimulation (10-80 mM). Cells were then analyzed for β-catenin levels by flow cytometry. **(B)** Overlay of histograms from (A).

leg of destruction complex inhibition feedback. Once cellular Axin concentrations have been depleted, β-catenin destruction complexes cannot form, allowing β-catenin levels to remain high regardless of ligand presence. We stimulate RKO cells for 2 hours with Wnt3a to fully activate receptors and then thoroughly washed away the Wnt3a and monitored β-catenin levels for 24 hours. We found β-catenin stayed elevated for ~9 hours after Wnt3a removal (Fig. 4.6). This is > 7 hours after active receptors (LRP6) have reset to inactive (data not shown, (Bilic, Huang et al. 2007)). This maintenance of β-catenin elevation is consistent with irreversible inhibition of the destruction complex. A decrease in β-catenin after 9 hours suggests time-delayed negative feedback that can reset the β-catenin destruction complex. Interestingly, Axin2 (Axin paralog) is a target gene of the TCF-β-catenin-mediated gene transcription complex and could serve as feedback that senses when Wnt stimulation has achieved terminal transcriptional output(Leung, Kolligs et al. 2002).

Blocking positive feedback removes bistability

Our mathematical model predicts that bistability in β-catenin accumulation comes from positive feedback between Axin and GSK3. When a single feedback loop is removed (GSK3's control of Axin concentrations), the response of β-catenin becomes graded. To test the experimental validity and predictive competency of our model, we chose to block Axin degradation pharmacologically and observe the effect on the switch-like behavior of single cells. To do this we used a recently discovered small molecule, IWR-1, that blocks Axin ubiquitination and degradation(Chen, Dodge et al. 2009). This compound stabilizes Axin but does not

affect the dose-dependent stabilization of β-catenin through GSK3 inhibition (data not shown), thus is ideal for testing system dynamics. We pretreated RKO cells for 1 hour with IWR-1 followed by a LiCl dose-response. We found the bistable response was no longer present and instead was now graded (Fig.4.7 compared with Fig. 4.4C). This demonstrates that Axin degradation upon signaling is required for the switch-like bistable response of β-catenin.

Summary

Wnt/β-catenin signal transduction is a key regulator of metazoan development and its misregulation occurs in many cancers. The multicomponent β-catenin destruction complex maintains low cellular β-catenin in the absence of a signal and becomes inhibited in the presence of certain signals, allowing β-catenin levels to rise. Our biochemical studies have identified positive feedback within the complex between essential components, Axin and GSK3. Mathematical modeling of this positive feedback loop predicts the existence of bistability in the activity of the β-catenin destruction complex as a whole. Using flow cytometry to observe the response of single cells to Wnt signaling, we found cells respond in an "all or none" fashion with no intermediates to Wnt or LiCl. We pharmacologically removed the positive feedback between Axin and GSK3 and converted the all-or-none behavior to a more graded response. These findings help elucidate molecular design features that convert a graded morphogen, such as Wnt, into discrete binary cell fate decisions and provide a mechanism for cellular memory of Wnt stimulation.

CHAPTER V

DISCUSSION AND FUTURE DIRECTIONS

Introduction

The work presented in this thesis represents mostly chemical, biochemical and cell-based expirements to elucidate new levels of Wnt/β-catenin pathway regulation. In the current Chapter, I discuss and provide future directions for the results described in the previous two Chapters. I have broken this section into parts I and II. Part I will specifically discuss the implication of pyrvinium as a Wnt inhibitor, and Part II will discuss the implications of bistability in the Wnt pathway.

Part I

Discussion

Utilizing *Xenopus* egg extracts to recapitulate β-catenin destruction complex activity and receptor-mediated pathway activation, we identified pyrvinium, an FDA-approved drug, as a potent inhibitor of the Wnt pathway. We provide evidence that pyrvinium represents a new class of compounds that inhibit the Wnt pathway by allosteric activation of Casein Kinase 1α. We propose a model in which pyrvinium activates CK1α so as to regulate the stability of β-catenin and Axin in the cytoplasm and Pygopus and TCF/Lef1 in the nucleus. As a result, inhibition of the Wnt pathway at multiple levels occurs (Fig. 3.1).

We showed by coimmunoprecipitation that Pygopus exists in a complex with CK1α. Pygopus is predicted to contain multiple CK1 phosphorylation sites, suggesting that its stability could be directly regulated by CK1α. CK1 has previously been shown to phosphorylate Lef1 *in vitro*(Hammerlein, Weiske et al. 2005). These phosphorylation sites on Lef1 are present in the LEFΔN-VP16 construct, suggesting that the effect of pyrvinium and CK1α on LEFΔN-VP16 activity may also be direct.

Pygopus was originally identified in *Drosophila* as a core transcriptional component of the Wnt pathway(Belenkaya, Han et al. 2002; Kramps, Peter et al. 2002; Parker, Jemison et al. 2002; Thompson, Townsley et al. 2002). In mice, the role of Pygopus in Wnt signaling appears to be more complex in that it is required for a subset of Wnt-mediated developmental processes. This suggests that Pygopus may play a context-dependent role in Wnt signal transduction. Previous studies using colon cancer cell lines with mutations in β-catenin or APC demonstrated that knockdown of Pygopus can inhibit Wnt signaling and decrease cell viability, suggesting that it plays a role in Wnt-driven cancers(Thompson, Townsley et al. 2002; Andrews, Lake et al. 2007). In the Chapter III we demonstrate an additional previously uncharacterized mode of Pygopus regulation; Wnt signaling stabilizes Pygopus levels by slowing its post-translational degradation.

The CK1 family of serine/threonine kinases is constitutively active, ubiquitously expressed, and evolutionarily conserved in eukaryotes(Knippschild, Gocht et al. 2005). CK1 family members have been associated with many cellular processes in addition to Wnt signaling. CK1 isoforms (α, γ, δ, and ε) have a highly conserved catalytic core and differ primarily in their N-terminal and C-terminal

domains. CK1 is regulated by its subcellular localization and inhibitory autophosphorylation of its C-terminal domain. Of the CK1 family members, CK1α is distinct in that it has a minimal C-terminal tail and appears to be the only family member activated by pyrvinium. Although pyrvinium is incapable of stimulating the activity of full-length CK1δ in our *in vitro* assays, it promotes activation of a C-terminally truncated form of CK1δ (CK1δ1-317). Additionally, we demonstrate that in the presence of pyrvinium, CK1α is differentially sensitive to the action of trypsin proteolysis, suggesting pyrvinium-CK1α interaction induces a comformational change.

Why would having a large C-terminal domain block the capacity of CK1 isoforms to be activated by pyrvinium? One possibility is that the C-terminal domain (which has been postulated to act as a pseudosubstrate) binds to the substrate-binding cavity of CK1 and blocks the activating conformational change induced by pyrvinium. Direct proof of this model will require elucidation of the structure of pyrvinium-bound CK1α in future studies.

Assigning specific biological activities to individual CK1 isoforms have been notoriously difficult (even with RNAi knockdowns), possibly due to compensatory effects from the various isoforms. Overexpression studies, on the other hand, may result in phosphorylation of non-physiological substrates. Thus, pyrvinium should prove a useful tool to dissect the biological roles of endogenous CK1α.

Previous studies have implicated pyrvinium in the AKT/mTOR pathway (Esumi, Lu et al. 2004; Rosenbluth, Mays et al. 2008). It is notclear whether these effects are direct because Wnt signaling has also been shown to activate the mTOR

pathway *in vitro* and *in vivo* (Inoki, Ouyang et al. 2006). In previous xenograft studies, oral doses of pyrvinium were given to mice at levels comparable to that given for its original indication (i.e. treatment of humans with pinworms), suggesting bioactivity of pyrvinium at the site of the graft when administered at a safe dose(Esumi, Lu et al. 2004; Yu, Macdonald et al. 2008). In these studies, toxicity of the injected pyrvinium was a limiting factor. It is not clear whether toxicity is due to the compound itself, which has putative alkylating activity, or due to its activation of CK1α, which has other cellular functions. Thus, future studies need to be directed towards testing the bioactivity and toxicity of structurally distinct functional derivatives of pyrvinium.

In a previous study, pyrvinium was shown to significantly potentiate the capacity of doxorubicin, a conventional cytotoxic drug, to inhibit tumor growth(Yu, Macdonald et al. 2008). This observation is consistent with our current study demonstrating that pyrvinium synergizes with 5-FU to induce apoptosis in a highly metastatic colorectal cancer line. Another study identified pyrvinium as an inhibitor of androgen receptor activity, but the authors demonstrated the mechanism of action is not direct, and even speculated it could occur through other pathways including inhibition of the Wnt pathway(Jones, Bolton et al. 2009).

A new functional class of Wnt pathway inhibitors that stabilize Axin by inhibiting tankyrases, a poly(ADP-ribose) polymerase, has recently been identified(Chen, Dodge et al. 2009; Huang, Mishina et al. 2009). Given the roles of CK1α and tankyrases in regulating a range of cellular functions, an obvious future direction for experimentation would be to determine the selectivity for the Wnt

pathway of CK1α activators and tankyrase inhibitors. It is possible that the Wnt pathway is particularly sensitive to the activities of these two enzymes; thus, modest cellular inhibition of tankyrases or activation of CK1α may be sufficient to inhibit Wnt signaling but not to affect other biological processes mediated by these two enzymes. It has been demonstrated that cancer cells in solid tumors are often physiologically dependent ("addicted") on the continued activity of a particular signaling pathway(Weinstein and Joe 2008). Thus if the Wnt pathway is particularly sensitive to CK1α activation and tumors are particularly dependent on the Wnt pathway, its possible a sizable therapeutic window could exist between diseased versus healthy tissue.

Although inhibition of enzymatic activity is a common mode of action for drug discovery, *activation* of an enzyme by small molecules is quite rare(Zorn and Wells 2010). Although small molecule activators of glucokinase have been developed and show great promise for treating type 2 diabetes, the development of small molecule activators of protein kinases for treating human disease has not been, to our knowledge, aggressively pursued(Matschinsky 2009). The pharmocodynamics of kinase activation might be significantly different than kinase inhibiton. It is generally believed that inhibition of tyrosine kinases must be substantial (>90%) and sustained in order to mediate clinically significant responses (e.g. decrease tumor burden). It is unknown if a similar regimen (i.e. substantial and sustained activation) will be required for kinase activators to be clinically efficacious.

In summary, homeostatic regulation of the Wnt pathway must occur for

healthy human development and aging(Angers and Moon 2009). Pathophysiological levels of signaling, through mutation, are implicated in a wide range of cancers, of which a direct connection with colorectal cancer is best understood. Small molecules, such as pyrvinium, that inhibit the Wnt pathway may be useful for treating the large majority of genetic and sporadic cases of colorectal cancer, the second leading cause of cancer-related deaths in the developed world.

Future directions

Structure-activity relationship studies of pyrvinium

Despite pyrvinium's use for more than 50 years in the clinic for the treatment of pinworms in humans, its low bioavailability has limited its usefulness as a cancer therapeutic. Pyrvinium was typically used in the past as a single-dose agent. For pinworms, its limited bioavailability was useful as its activity could be restricted to the intestinal lumen, thereby minimizing systemic effects. It is not clear if chronic oral administration would be effective at reaching intestinal crypts to impact the site of tumor initiation. More importantly, pyrvinium must achieve systematic circulation to enter tumor vasculature and target the entire tumor mass efficiently. Intravenous administration is a possible method of delivery. Yet thorough drug metabolism and pharmocokinetic studies must be conduced to charterize its circulation half-life and tissue toxicities. Pyrvinium's poor bioavailability must be improved.

The fact that pyrvinium is a cation that potentially has alkylating properties (ability to covalently modify organic molecules) also limits its usefulness(Stockert,

Trigoso et al. 1991). It has been shown to bind DNA and have mutagenizing activity in yeast(Dickie, Morgan et al. 1986). These are undesirable properties that add to general toxicity and carcinogenic action of the drug. Ironically, some cancer therapies are aklylating agents.

Thus, going forward it is imperative to perform medicinal chemistry with pyrvinium as the starting scaffold. Generation of pyrvinium analogs tested in kinase assays and cell cuture should allow for strong structure-activity relationship (SAR) analysis. Analogs with greater solubility, bioavailability and lower toxicities should result from this work. Indeed, toward this end, we have collaborated with the Vanderbilt Chemical Synthesis Core to begin SAR studies. Today > 400 compounds have been purchased or synthesized. Testing in embryos, TOPFlash and *in vitro* kinase assays have demonstrated one compound, VU-WS113, is particularly potent.

Biochemical/structural characterization of pyrvinium

In conjunction with medicinal chemistry of pyrvinium, a full biochemical characterization of pyrvinium and promising analogs should be conducted. There are many questions as to its mechanism that remain unanswered. The CK1 family of kinases are considered constituatively active kinases. How do you enhance kinase activity of an active kinase? Does pyrvinium binding lower dissociation constants (K_d) for ATP or substrates, increasing the on/off rates? How is the velocity (V_{max}) of the reaction affected? Complete Michaelis-Menten studies defining pyrviniums effect on CK1α relationship with ATP and multiple substrates are needed. Drawing from our dose responses in our *in vitro* kinase assay, the apparent K_d of pyrvinium

for CK1α appears to be ~ 1 nM. This implies the binding of pyrvinium to CK1α is very tight. The K_d should be more directly defined through fluorescence polarization assays.

Elucidating the direct amino acids on CK1α that interact with pyrvinium is crucial for understanding kinase activation and further compound optimization. There are three approaches useful to answer this question; X-ray crystallography, NMR and molecular modeling. The gold standard would be a high-resolution crystal structure of pyrvinium bound to CK1α. The crystal structure for a truncated form of CK1δ (aa 1-317) has been previously solved(Xu, Carmel et al. 1995; Longenecker, Roach et al. 1996). Importantly, this is the CK1δ truncation that can be activated by pyrvinium and therefore co-crystallization of pyrvinium and CK1 could hypothetically be simplified. Since a structure has been solved, it could serve as a guide for an NMR mapping strategy. NMR has the added advantage of potentially capturing protein dynamics upon drug binding. Also, since the structure is solved, *in silico* molecular modeling might be the lowest hanging fruit, with the downside of it being a strictly theorectical approach and must be validated experimentally.

Mechanisms controlling Pygopus activity and stability

Our small molecule screen in *Xenopus* egg extracts represent a true example of so-called forward chemical genetics(Walling, Peters et al. 2001). The screen was not biased for any singular molecule but instead was restricted to a defined set of molecular events of interest to us (regulation of β-catenin destruction complex) in a milieu of a crude egg extract. Thus, we went into the screen knowing how we

wanted small molecules to affect the destruction complex but did not bias it toward any direct target. As a result, we uncovered a rarely hypothesized mechanism of kinase activation (CK1α) and identified new mechanistic insight into the structure of the pathway (Pygopus regulation). These results raise the question: How is Pygopus regulated by CK1α? The two can co-immunoprecipitate but do they directly interact from individually purified components? Is Pygopus a direct substrate of CK1α and if so, what are the sites of phosphorylation and how do they affect its activity/stability? Pygopus is post-translationally degraded, therefore is this a ubiquitin-mediated process? If so, what is the ubiquitin ligase involved?

Not only does Wnt stabilize Pygopus but LiCl stimulation does as well (data not shown). This suggests GSK3, like its role with β-catenin, can target Pygopus. Interestingly, when Pygopus is stabilized due to LiCl treatment, pyrvinium is still able to decrease Pygopus levels. Thus, unlike β-catenin, CK1α can initiate the destruction of Pygopus regardless of GSK3 activity. The timing and interplay of GSK3 and CK1α regulation of Pygopus should be a productive line of study in the future.

Characterization of CK1 alpha substrates

The identification of CK1α activation as a potent means of inhibiting Wnt/β-catenin signaling, even in the context of activation mutations (APC and β-catenin), bring CK1α's role in the pathways into the limelight again. Interestingly, it has been proposed that phosphorylation of β-catenin on serine 45 by CK1α is constituative and not regulated by Wnt signaling(Gao, Seeling et al. 2002). This would suggest

keeping CK1α active pharmacologically would not enhance β-catenin phosphorylation upon signaling. However, pyrvinium can decrease β-catenin levels upon Wnt signaling. If β-catenin phosphoylation is not enhanced by pyrvinium, the drugs potent effect must be a result of Wnt signaling dynamically regulating CK1α phosphorylation of another pathway member (Axin?) that controls β-catenin stability. Alternatively, unregulated phosphorylation of β-catenin by CK1α could be false. The work supporting this model has not been substantiated by other groups. A more careful inspection of the timing and regulation of CK1α phosphorylation of β-catenin is needed.

This work also points to the possibility of a greatly expanded role for CK1α in the pathway. Axin, Pygopus and TCF all contain CK1 consensus sites and are regulated by pyrvinium, and thus are putative targets of CK1α. A global anaylsis of CK1α would greatly improve our understanding of its role both in Wnt signal transduction and the broader physiology of the cell. Pyrvinium should aid in identifying targets as the kinase can be activated within minutes after drug addition.

Part II

Discussion

Our biochemical studies in *Xenopus* egg extracts and mammalian cell culture have identified a positive feedback loop within the β-catenin destruction complex between Axin and GSK3. Axin potently activates GSK3 by recruiting PP2a to GSK3 and stimulating the removal of an inhibitory phosphorylation event on serine 9. GSK3 then in turn phosphorylates Axin, thus stabilizing it. Our mathematical model

that describes this positive feedback between Axin and GSK3 predicts the existence of bistability in the activity of the β-catenin destruction complex. Bistability is the existence of two stable states within a system, "on" or "off". This is in contrast to how morphogens, such as Wnts, are classically conceived, as graded signals that induce a graded response. We validated the model prediction experimentally by conducting single cell studies to observe the response to Wnt signaling. We found that cells respond in an all-or-none fashion with no intermediates to Wnt or Li ions. Importantly, the model also predicted that removal of one arm of the positive feedback loop would produce a graded response to stimulation. We perturbed the positive feedback between Axin and GSK3 by blocking Axin degradation and converted the all-or-none behavior to a more graded response.

Our description of GSK3-Axin interaction does address a controversy in the Wnt field over the relevance of Axin degradation. Genetic and theoretical studies have suggested Axin is sufficient to control Wnt responsiveness(Lee, Salic et al. 2003; Tolwinski, Wehrli et al. 2003). Other biochemical studies suggest Axin degradation is a secondary event and GSK3 inhibition alone is sufficient for β-catenin stabilization. Our work melds these opposing views and proposes that GSK3 inhibition and Axin degradation are both required for the switch-like behavior of β-catenin stabilization.

How GSK3 is inhibited by Wnt signaling is an active area of current research (reviewed in Introduction). Proposed mechanisms for GSK3 inhibition include phosphorylation at serine 9, dissociation from Axin, and direct inhibition by LRP6(MacDonald, Tamai et al. 2009). Our modeling of serine 9 regulation does not

decifer how GSK3 becomes inhibited upon signaling, but simply dictates that the Axin-bound pool of GSK3 is in a fully active state in the absence of a signal. Importantly, since all of these mechanisms fundamentally describe a block in GSK3 activity toward β-catenin, they are all consistent with our model. Future studies and extension of the model to receptor-mediated events are necessary to fully define the temporal and spatial regulation of GSK3 in response to Wnt signaling.

Wnt signaling has been widely studied in a number of organisms and tissues, yet, to our knowledge, no studies have attempted to quantify β-catenin levels at the single cell level. Often, complexities in tissue structure and fix/staining procedures confound such anaylsis. In the colon epithelial crypts, qualitative anaylsis has lead to opposite conclusions from different laboratories; β-catenin is high at the base of the crypt and decreases moving up, and alternatively is high in only a few cells(Gregorieff and Clevers 2005). In light of our results, we emphasize the need for careful characterization of β-catenin dynamics *in vivo*, through quantification and live cell imaging. Importantly, even though we see switch-like behavior in RKO cells and suggest this might be the dominant behavior of the pathway, our model also provides a mechanism for a graded response. Any event that prevents the turnover of Axin could produce a Wnt response gradient. We suggest the β-catenin destruction complex is a dominant node at which other signaling pathways feed into the Wnt pathway. It is highly possible that within the context of active signaling from other pathways, the dynamics of a Wnt response are modified. Individual cells that make up tissues must integrate multiple signals and could conceivably produce a graded β-catenin response if that served a developmental purpose. Thus, our

model of a β-catenin destruction complex feedback loop provides a molecular node for signal integration with other signaling pathways.

A β-catenin destruction complex feedback loop also provides a mechanism for cellular memory of Wnt stimulation. Axin degradation is an irreversible event that prevents destruction complex formation, even in the absence of a Wnt ligand or active receptors. This mechanism would act to suppress noisy Wnt morphogen presentation. Once a cell recieves a certain threshold of Wnt and responds, that cell becomes insensitive to future fluctuations of ligand concentration. If Axin is not a target gene at a certain space/time, the pathway becomes irreversible indefinitely. Several studies have demonstrated Axin2 (functionally identical to Axin) to be a target gene of the pathway. When and where this gene is expressed in development marks cells responding to Wnt signaling and initiating a termination negative feedback loop. Interestingly, there are known tissues receiving a Wnt signal that do not express Axin2(Yu, Jerchow et al. 2005). Do these represent developmental contexts for prolonged signaling?

We have demonstrated simple and direct cross-regulation of GSK3 and Axin that imparts on/off behavior to the β-catenin destruction complex. This produces robust, sharp and irreversible cell decision making in response to a Wnt signal. The cell-based studies in work provide a broad perspective on the behavior of the complex as a whole. Subsequent studies will undoubtedly identify numerous regulatory factors that layer additional controls on this molecular system.

Future directions

Our characterization of the β-catenin destruction complex leaves the identity and regulation of many molecular players unknown. Before Axin can degrade, the GSK3 phosphorylation sites must be removed. What is the phosphatase? PP2a is in the complex and thus could be a candidate. Protein phosphatase 1 (PP1) has been shown to bind the complex upon signaling and thus could be a strong candidate as well(Luo, Peterson et al. 2007). Initiation of a ubiquitin ligase must also occur. What are the regulatory events here and what is the ligase? ADP-ribosylation has been shown to induce Axin degradation(Huang, Mishina et al. 2009). How does the Wnt signal induce ADP-ribosylation and how does this recruit the ubiquitin ligase?

A number of recent reports have highlighted the role of Axin turnover in tissue homeostasis and disease(Takacs, Baird et al. 2008; Huang, Mishina et al. 2009). Regulation of Axin concentrations has been directly linked to APC concentrations. APC is a core component of the β-catenin destruction complex. Mutations in APC are found in 80% of sporadic colorectal carcinomas(Klaus and Birchmeier 2008). It remains unclear specifically what effects APC mutations have on the complex. Recently it was shown that mutations of APC alone do not drive β-catenin to the nucleus or activate β-catenin mediated transcription; other signals (Ras) are needed for these events(Phelps, Broadbent et al. 2009; Phelps, Chidester et al. 2009). So, precisely what effect does APC loss have on the Wnt pathway? Two studies show that loss of APC prevents Axin degradation. According to our present study, such an event should produce a graded response to stimulus, thus changing a robust, decisive, all-or-none response into a noisy, graded response sensitive to

minute changes in signal strength. This idea should be directly addressed by looking at β-catenin stabilization response in an APC mutant background. This interesting concept is a new layer of complexity to consider as part of drug discovery efforts. Ideal drugs would not simply put a roadblock downstream of oncogenic mutations as this leads to what we currently have with drugs, toxicity and drug resistance. Instead, effective therapies should restore proper cell physiology. This is not trivial and is many years way. If loss of APC does induce a graded signaling response, it will be interesting and imperative to see if small molecule antagonists can be discovered that restore bistability.

The introduction of this thesis describes a number of events that occur to initiate receptor activation and destruction complex inhibition. From a quantitative standpoint, all of the studies remain phenomenological. Biochemical reconstitution and live cell imaging approaches should be used to gain a grasp on the order/timing of these events. The acquisition of measurements such as synthesis/degradation rates, protein-protein binding rates and affinities, and phosphorylation/dephosphorylation rates should be incorporated into computational models of receptor activation and destruction complex inhibition. When our understanding of the molecular players involved in a process reaches a certain threshold, the use of mathematics and computation become necessary to comprehend system dynamics. Many parts of Wnt signal transduction have reached this threshold.

CHAPTER VI

CONCLUDING REMARKS

Through years of research we have come to understand that Wnt/β-catenin signaling plays a critical role in metazoan development, stem cell maintenance, and human disease. The multicomponent β-catenin destruction complex maintains low cellular β-catenin in the absence of a signal and becomes inhibited in the presence of a Wnt ligand, allowing β-catenin levels to rise. We have identified an FDA-approved drug, pyrvinium, as a potent inhibitor of Wnt signaling. We show pyrvinium binds CK1α kinase activity and CK1α knockdown abrogates the effects of pyrvinium on the Wnt pathway. In addition to effects on Axin and β-catenin levels, pyrvinium promotes degradation of Pygopus, a Wnt transcriptional component. Pyrvinium treatment of colon cancer cells with mutation of Adenomatous Polyposis Coli or β-catenin inhibits both Wnt signaling and proliferation. These findings reveal allosteric activation of CK1α as an effective mechanism to inhibit Wnt signaling and highlight a new strategy for targeted therapeutics directed against the Wnt pathway.

Biochemical studies have identified positive feedback within the complex between essential components, Axin and GSK3. Theorectical modeling of this positive feedback loop predicts bistability in the activity of the β-catenin destruction complex and we generated experimental evidence for this through single cell studies. These findings elucidate molecular design features that convert gradients into discrete binary cell fate decisions.

In conclusion, the work presented here ventures into three broad configurations of modern research that overlap significantly with each other: theoretical, experimental and applied biology. Interplay between these realms of biology is essential for the continued discovery of novel biology and the alleviation of human suffering and disease.

BIBLIOGRAPHY

Ajo-Franklin, C. M., D. A. Drubin, et al. (2007). "Rational design of memory in eukaryotic cells." Genes Dev **21**(18): 2271-2276.

Altschuler, S. J. and L. F. Wu (2010). "Cellular heterogeneity: do differences make a difference?" Cell **141**(4): 559-563.

Amit, S., A. Hatzubai, et al. (2002). "Axin-mediated CKI phosphorylation of beta-catenin at Ser 45: a molecular switch for the Wnt pathway." Genes Dev **16**(9): 1066-1076.

Andrews, P. G., B. B. Lake, et al. (2007). "Requirement of Pygopus 2 in breast cancer." Int J Oncol **30**(2): 357-363.

Angers, S. and R. T. Moon (2009). "Proximal events in Wnt signal transduction." Nat Rev Mol Cell Biol **10**(7): 468-477.

Aoki, M., A. Hecht, et al. (1999). "Nuclear endpoint of Wnt signaling: neoplastic transformation induced by transactivating lymphoid-enhancing factor 1." Proc Natl Acad Sci U S A **96**(1): 139-144.

Ashe, H. L. and J. Briscoe (2006). "The interpretation of morphogen gradients." Development **133**(3): 385-394.

Barker, N. and H. Clevers (2006). "Mining the Wnt pathway for cancer therapeutics." Nat Rev Drug Discov **5**(12): 997-1014.

Bejsovec, A. and A. Martinez Arias (1991). "Roles of wingless in patterning the larval epidermis of Drosophila." Development **113**(2): 471-485.

Belenkaya, T. Y., C. Han, et al. (2002). "pygopus Encodes a nuclear protein essential for wingless/Wnt signaling." Development **129**(17): 4089-4101.

Bhanot, P., M. Brink, et al. (1996). "A new member of the frizzled family from Drosophila functions as a Wingless receptor." Nature **382**(6588): 225-230.

Bidere, N., V. N. Ngo, et al. (2009). "Casein kinase 1alpha governs antigen-receptor-induced NF-kappaB activation and human lymphoma cell survival." Nature **458**(7234): 92-96.

Bienz, M. and H. Clevers (2003). "Armadillo/beta-catenin signals in the nucleus--proof beyond a reasonable doubt?" Nat Cell Biol **5**(3): 179-182.

Bilic, J., Y. L. Huang, et al. (2007). "Wnt induces LRP6 signalosomes and promotes dishevelled-dependent LRP6 phosphorylation." Science **316**(5831): 1619-1622.

Blauwkamp, T. A., M. V. Chang, et al. (2008). "Novel TCF-binding sites specify transcriptional repression by Wnt signalling." EMBO J **27**(10): 1436-1446.

Bovolenta, P., P. Esteve, et al. (2008). "Beyond Wnt inhibition: new functions of secreted Frizzled-related proteins in development and disease." J Cell Sci **121**(Pt 6): 737-746.

Boyden, L. M., J. Mao, et al. (2002). "High bone density due to a mutation in LDL-receptor-related protein 5." N Engl J Med **346**(20): 1513-1521.

Bryja, V., G. Schulte, et al. (2007). "Wnt-3a utilizes a novel low dose and rapid pathway that does not require casein kinase 1-mediated phosphorylation of Dvl to activate beta-catenin." Cell Signal **19**(3): 610-616.

Burrill, D. R. and P. A. Silver (2010). "Making cellular memories." Cell **140**(1): 13-18.

Chen, B., M. E. Dodge, et al. (2009). "Small molecule-mediated disruption of Wnt-dependent signaling in tissue regeneration and cancer." Nat Chem Biol **5**(2): 100-107.

Clevers, H. (2004). "Wnt breakers in colon cancer." Cancer Cell **5**(1): 5-6.

Clevers, H. (2006). "Wnt/beta-catenin signaling in development and disease." Cell **127**(3): 469-480.

Cong, F. and H. Varmus (2004). "Nuclear-cytoplasmic shuttling of Axin regulates subcellular localization of beta-catenin." Proc Natl Acad Sci U S A **101**(9): 2882-2887.

Cross, D. A., D. R. Alessi, et al. (1995). "Inhibition of glycogen synthase kinase-3 by insulin mediated by protein kinase B." Nature **378**(6559): 785-789.

Cselenyi, C. S., K. K. Jernigan, et al. (2008). "LRP6 transduces a canonical Wnt signal independently of Axin degradation by inhibiting GSK3's phosphorylation of beta-catenin." Proc Natl Acad Sci U S A **105**(23): 8032-8037.

Dajani, R., E. Fraser, et al. (2003). "Structural basis for recruitment of glycogen synthase kinase 3beta to the axin-APC scaffold complex." EMBO J **22**(3): 494-501.

Davidson, G., W. Wu, et al. (2005). "Casein kinase 1 gamma couples Wnt receptor activation to cytoplasmic signal transduction." Nature **438**(7069): 867-872.

de la Roche, M., J. Worm, et al. (2008). "The function of BCL9 in Wnt/beta-catenin signaling and colorectal cancer cells." BMC Cancer **8**: 199.

De Robertis, E. M. and H. Kuroda (2004). "Dorsal-ventral patterning and neural induction in Xenopus embryos." Annu Rev Cell Dev Biol **20**: 285-308.

Dickie, P., A. R. Morgan, et al. (1986). "The binding of the anthelmintic pyrvinium cation to deoxyribonucleic acid in vitro." Mol Pharmacol **29**(4): 427-435.

Ding, V. W., R. H. Chen, et al. (2000). "Differential regulation of glycogen synthase kinase 3beta by insulin and Wnt signaling." J Biol Chem **275**(42): 32475-32481.

Downey, A. S., C. R. Chong, et al. (2008). "Efficacy of pyrvinium pamoate against Cryptosporidium parvum infection in vitro and in a neonatal mouse model." Antimicrob Agents Chemother **52**(9): 3106-3112.

Emami, K. H., C. Nguyen, et al. (2004). "A small molecule inhibitor of beta-catenin/CREB-binding protein transcription [corrected]." Proc Natl Acad Sci U S A **101**(34): 12682-12687.

Embi, N., D. B. Rylatt, et al. (1980). "Glycogen synthase kinase-3 from rabbit skeletal muscle. Separation from cyclic-AMP-dependent protein kinase and phosphorylase kinase." Eur J Biochem **107**(2): 519-527.

Esumi, H., J. Lu, et al. (2004). "Antitumor activity of pyrvinium pamoate, 6-(dimethylamino)-2-[2-(2,5-dimethyl-1-phenyl-1H-pyrrol-3-yl)ethenyl]-1-me thyl-quinolinium pamoate salt, showing preferential cytotoxicity during glucose starvation." Cancer Sci **95**(8): 685-690.

Farr, G. H., 3rd, D. M. Ferkey, et al. (2000). "Interaction among GSK-3, GBP, axin, and APC in Xenopus axis specification." J Cell Biol **148**(4): 691-702.

Faux, M. C., J. L. Ross, et al. (2004). "Restoration of full-length adenomatous polyposis coli (APC) protein in a colon cancer cell line enhances cell adhesion." J Cell Sci **117**(Pt 3): 427-439.

Ferrell, J. E., Jr. (2002). "Self-perpetuating states in signal transduction: positive feedback, double-negative feedback and bistability." Curr Opin Cell Biol **14**(2): 140-148.

Ferrell, J. E., Jr., J. R. Pomerening, et al. (2009). "Simple, realistic models of complex biological processes: positive feedback and bistability in a cell fate switch and a cell cycle oscillator." FEBS Lett **583**(24): 3999-4005.

Ferrell, J. E. and W. Xiong (2001). "Bistability in cell signaling: How to make continuous processes discontinuous, and reversible processes irreversible." Chaos **11**(1): 227-236.

Fiedler, M., M. J. Sanchez-Barrena, et al. (2008). "Decoding of methylated histone H3 tail by the Pygo-BCL9 Wnt signaling complex." Mol Cell **30**(4): 507-518.

Forde, J. E. and T. C. Dale (2007). "Glycogen synthase kinase 3: a key regulator of cellular fate." Cell Mol Life Sci **64**(15): 1930-1944.

Gao, Z. H., J. M. Seeling, et al. (2002). "Casein kinase I phosphorylates and destabilizes the beta-catenin degradation complex." Proc Natl Acad Sci U S A **99**(3): 1182-1187.

Gerhart, J. (1999). "1998 Warkany lecture: signaling pathways in development." Teratology **60**(4): 226-239.

Gille, H., M. Kortenjann, et al. (1995). "ERK phosphorylation potentiates Elk-1-mediated ternary complex formation and transactivation." Embo J **14**(5): 951-962.

Gleason, J. E., H. C. Korswagen, et al. (2002). "Activation of Wnt signaling bypasses the requirement for RTK/Ras signaling during C. elegans vulval induction." Genes Dev **16**(10): 1281-1290.

Goenka, S. and M. Boothby (2006). "Selective potentiation of Stat-dependent gene expression by collaborator of Stat6 (CoaSt6), a transcriptional cofactor." Proc Natl Acad Sci U S A **103**(11): 4210-4215.

Gomperts, B. D., P. E. R. Tatham, et al. (2009). Signal transduction. Burlington, M.A. ; London, Elsevier/Academic Press.

Gong, Y., R. B. Slee, et al. (2001). "LDL receptor-related protein 5 (LRP5) affects bone accrual and eye development." Cell **107**(4): 513-523.

Grandy, D., J. Shan, et al. (2009). "Discovery and characterization of a small molecule inhibitor of the PDZ domain of dishevelled." J Biol Chem **284**(24): 16256-16263.

Gregorieff, A. and H. Clevers (2005). "Wnt signaling in the intestinal epithelium: from endoderm to cancer." Genes Dev **19**(8): 877-890.

Ha, N. C., T. Tonozuka, et al. (2004). "Mechanism of phosphorylation-dependent binding of APC to beta-catenin and its role in beta-catenin degradation." Mol Cell **15**(4): 511-521.

Hammerlein, A., J. Weiske, et al. (2005). "A second protein kinase CK1-mediated step negatively regulates Wnt signalling by disrupting the lymphocyte enhancer factor-1/beta-catenin complex." Cell Mol Life Sci **62**(5): 606-618.

Harland, R. M. (1991). "In situ hybridization: an improved whole-mount method for Xenopus embryos." Methods Cell Biol **36**: 685-695.

Hatzis, P., L. G. van der Flier, et al. (2008). "Genome-wide pattern of TCF7L2/TCF4 chromatin occupancy in colorectal cancer cells." Mol Cell Biol **28**(8): 2732-2744.

Hayward, P., T. Kalmar, et al. (2008). "Wnt/Notch signalling and information processing during development." Development **135**(3): 411-424.

He, T. C., A. B. Sparks, et al. (1998). "Identification of c-MYC as a target of the APC pathway." Science **281**(5382): 1509-1512.

Hempelmann, E. (2007). "Hemozoin biocrystallization in Plasmodium falciparum and the antimalarial activity of crystallization inhibitors." Parasitol Res **100**(4): 671-676.

Henderson, B. R. and F. Fagotto (2002). "The ins and outs of APC and beta-catenin nuclear transport." EMBO Rep **3**(9): 834-839.

Hendriksen, J., F. Fagotto, et al. (2005). "RanBP3 enhances nuclear export of active (beta)-catenin independently of CRM1." J Cell Biol **171**(5): 785-797.

Hendriksen, J., M. Jansen, et al. (2008). "Plasma membrane recruitment of dephosphorylated beta-catenin upon activation of the Wnt pathway." J Cell Sci **121**(Pt 11): 1793-1802.

Herman, M. (2001). "C. elegans POP-1/TCF functions in a canonical Wnt pathway that controls cell migration and in a noncanonical Wnt pathway that controls cell polarity." Development **128**(4): 581-590.

Hino, S., C. Tanji, et al. (2005). "Phosphorylation of beta-catenin by cyclic AMP-dependent protein kinase stabilizes beta-catenin through inhibition of its ubiquitination." Mol Cell Biol **25**(20): 9063-9072.

Hoppler, S. and C. L. Kavanagh (2007). "Wnt signalling: variety at the core." J Cell Sci **120**(Pt 3): 385-393.

Huang, S. M., Y. M. Mishina, et al. (2009). "Tankyrase inhibition stabilizes axin and antagonizes Wnt signalling." Nature **461**(7264): 614-620.

Ikeda, S., S. Kishida, et al. (1998). "Axin, a negative regulator of the Wnt signaling pathway, forms a complex with GSK-3beta and beta-catenin and promotes

GSK-3beta-dependent phosphorylation of beta-catenin." Embo J **17**(5): 1371-1384.

Inoki, K., H. Ouyang, et al. (2006). "TSC2 integrates Wnt and energy signals via a coordinated phosphorylation by AMPK and GSK3 to regulate cell growth." Cell **126**(5): 955-968.

Inwood, S. (2002). The man who knew too much : the strange and inventive life of Robert Hooke, 1635-1703. London, Macmillan.

Itoh, K., A. Jenny, et al. (2009). "Centrosomal localization of Diversin and its relevance to Wnt signaling." J Cell Sci **122**(Pt 20): 3791-3798.

Itoh, K., V. E. Krupnik, et al. (1998). "Axis determination in Xenopus involves biochemical interactions of axin, glycogen synthase kinase 3 and beta-catenin." Curr Biol **8**(10): 591-594.

Jamora, C., R. DasGupta, et al. (2003). "Links between signal transduction, transcription and adhesion in epithelial bud development." Nature **422**(6929): 317-322.

Jho, E. H., T. Zhang, et al. (2002). "Wnt/beta-catenin/Tcf signaling induces the transcription of Axin2, a negative regulator of the signaling pathway." Mol Cell Biol **22**(4): 1172-1183.

Jones, J. O., E. C. Bolton, et al. (2009). "Non-competitive androgen receptor inhibition in vitro and in vivo." Proc Natl Acad Sci U S A **106**(17): 7233-7238.

Kahler, R. A. and J. J. Westendorf (2003). "Lymphoid enhancer factor-1 and beta-catenin inhibit Runx2-dependent transcriptional activation of the osteocalcin promoter." J Biol Chem **278**(14): 11937-11944.

Kimelman, D. and W. Xu (2006). "beta-catenin destruction complex: insights and questions from a structural perspective." Oncogene **25**(57): 7482-7491.

Kinzler, K. W., M. C. Nilbert, et al. (1991). "Identification of FAP locus genes from chromosome 5q21." Science **253**(5020): 661-665.

Kinzler, K. W. and B. Vogelstein (1996). "Lessons from hereditary colorectal cancer." Cell **87**(2): 159-170.

Klaus, A. and W. Birchmeier (2008). "Wnt signalling and its impact on development and cancer." Nat Rev Cancer **8**(5): 387-398.

Klingensmith, J., R. Nusse, et al. (1994). "The Drosophila segment polarity gene dishevelled encodes a novel protein required for response to the wingless signal." Genes Dev **8**(1): 118-130.

Knight, Z. A. and K. M. Shokat (2005). "Features of selective kinase inhibitors." Chem Biol **12**(6): 621-637.

Knippschild, U., A. Gocht, et al. (2005). "The casein kinase 1 family: participation in multiple cellular processes in eukaryotes." Cell Signal **17**(6): 675-689.

Kofron, M., B. Birsoy, et al. (2007). "Wnt11/beta-catenin signaling in both oocytes and early embryos acts through LRP6-mediated regulation of axin." Development **134**(3): 503-513.

Komekado, H., H. Yamamoto, et al. (2007). "Glycosylation and palmitoylation of Wnt-3a are coupled to produce an active form of Wnt-3a." Genes Cells **12**(4): 521-534.

Korinek, V., N. Barker, et al. (1998). "Two members of the Tcf family implicated in Wnt/beta-catenin signaling during embryogenesis in the mouse." Mol Cell Biol **18**(3): 1248-1256.

Korswagen, H. C., D. Y. Coudreuse, et al. (2002). "The Axin-like protein PRY-1 is a negative regulator of a canonical Wnt pathway in C. elegans." Genes Dev **16**(10): 1291-1302.

Kramps, T., O. Peter, et al. (2002). "Wnt/wingless signaling requires BCL9/legless-mediated recruitment of pygopus to the nuclear beta-catenin-TCF complex." Cell **109**(1): 47-60.

Krieghoff, E., J. Behrens, et al. (2006). "Nucleo-cytoplasmic distribution of beta-catenin is regulated by retention." J Cell Sci **119**(Pt 7): 1453-1463.

Lammi, L., S. Arte, et al. (2004). "Mutations in AXIN2 cause familial tooth agenesis and predispose to colorectal cancer." Am J Hum Genet **74**(5): 1043-1050.

Larabell, C. A., M. Torres, et al. (1997). "Establishment of the dorso-ventral axis in Xenopus embryos is presaged by early asymmetries in beta-catenin that are modulated by the Wnt signaling pathway." J Cell Biol **136**(5): 1123-1136.

Latres, E., D. S. Chiaur, et al. (1999). "The human F box protein beta-Trcp associates with the Cul1/Skp1 complex and regulates the stability of beta-catenin." Oncogene **18**(4): 849-854.

Lee, E., A. Salic, et al. (2003). "The Roles of APC and Axin Derived from Experimental and Theoretical Analysis of the Wnt Pathway." PLoS Biol **1**(1): E10.

Lepourcelet, M., Y. N. Chen, et al. (2004). "Small-molecule antagonists of the oncogenic Tcf/beta-catenin protein complex." Cancer Cell **5**(1): 91-102.

Leung, J. Y., F. T. Kolligs, et al. (2002). "Activation of AXIN2 expression by beta-catenin-T cell factor. A feedback repressor pathway regulating Wnt signaling." J Biol Chem **277**(24): 21657-21665.

Lewis, J. A., C. H. Wu, et al. (1980). "The genetics of levamisole resistance in the nematode Caenorhabditis elegans." Genetics **95**(4): 905-928.

Li, A. and J. J. Blow (2005). "Cdt1 downregulation by proteolysis and geminin inhibition prevents DNA re-replication in Xenopus." Embo J **24**(2): 395-404.

Liu, C., Y. Li, et al. (2002). "Control of beta-catenin phosphorylation/degradation by a dual-kinase mechanism." Cell **108**(6): 837-847.

Liu, X., J. S. Rubin, et al. (2005). "Rapid, Wnt-induced changes in GSK3beta associations that regulate beta-catenin stabilization are mediated by Galpha proteins." Curr Biol **15**(22): 1989-1997.

Logan, C. Y. and R. Nusse (2004). "The Wnt signaling pathway in development and disease." Annu Rev Cell Dev Biol **20**: 781-810.

Longenecker, K. L., P. J. Roach, et al. (1996). "Three-dimensional structure of mammalian casein kinase I: molecular basis for phosphate recognition." J Mol Biol **257**(3): 618-631.

Luo, W., A. Peterson, et al. (2007). "Protein phosphatase 1 regulates assembly and function of the beta-catenin degradation complex." EMBO J **26**(6): 1511-1521.

Lustig, B., B. Jerchow, et al. (2002). "Negative feedback loop of Wnt signaling through upregulation of conductin/axin2 in colorectal and liver tumors." Mol Cell Biol **22**(4): 1184-1193.

MacDonald, B. T., K. Tamai, et al. (2009). "Wnt/beta-catenin signaling: components, mechanisms, and diseases." Dev Cell **17**(1): 9-26.

Major, M. B., N. D. Camp, et al. (2007). "Wilms tumor suppressor WTX negatively regulates WNT/beta-catenin signaling." Science **316**(5827): 1043-1046.

Malo, N., J. A. Hanley, et al. (2006). "Statistical practice in high-throughput screening data analysis." Nat Biotechnol **24**(2): 167-175.

Mao, B., W. Wu, et al. (2002). "Kremen proteins are Dickkopf receptors that regulate Wnt/beta-catenin signalling." Nature **417**(6889): 664-667.

Mao, J., J. Wang, et al. (2001). "Low-density lipoprotein receptor-related protein-5 binds to Axin and regulates the canonical Wnt signaling pathway." Mol Cell **7**(4): 801-809.

Matschinsky, F. M. (2009). "Assessing the potential of glucokinase activators in diabetes therapy." Nat Rev Drug Discov **8**(5): 399-416.

McCrea, P. D., C. W. Turck, et al. (1991). "A homolog of the armadillo protein in Drosophila (plakoglobin) associated with E-cadherin." Science **254**(5036): 1359-1361.

McMahon, A. P. and R. T. Moon (1989). "Ectopic expression of the proto-oncogene int-1 in Xenopus embryos leads to duplication of the embryonic axis." Cell **58**(6): 1075-1084.

McMahon, A. P. and R. T. Moon (1989). "int-1--a proto-oncogene involved in cell signalling." Development **107 Suppl**: 161-167.

McManus, E. J., K. Sakamoto, et al. (2005). "Role that phosphorylation of GSK3 plays in insulin and Wnt signalling defined by knockin analysis." EMBO J **24**(8): 1571-1583.

Mithani, S. K., G. C. Balch, et al. (2004). "Smad3 has a critical role in TGF-beta-mediated growth inhibition and apoptosis in colonic epithelial cells." J Surg Res **117**(2): 296-305.

Miyamoto, D. T., Z. E. Perlman, et al. (2004). "The kinesin Eg5 drives poleward microtubule flux in Xenopus laevis egg extract spindles." J Cell Biol **167**(5): 813-818.

Mosimann, C., G. Hausmann, et al. (2009). "Beta-catenin hits chromatin: regulation of Wnt target gene activation." Nat Rev Mol Cell Biol **10**(4): 276-286.

Murray, A. W. (1991). "Cell cycle extracts." Methods Cell Biol **36**: 581-605.

Nakamura, Y., I. Nishisho, et al. (1991). "Mutations of the adenomatous polyposis coli gene in familial polyposis coli patients and sporadic colorectal tumors." Princess Takamatsu Symp **22**: 285-292.

Niemann, S., C. Zhao, et al. (2004). "Homozygous WNT3 mutation causes tetra-amelia in a large consanguineous family." Am J Hum Genet **74**(3): 558-563.

Nishisho, I., Y. Nakamura, et al. (1991). "Mutations of chromosome 5q21 genes in FAP and colorectal cancer patients." Science **253**(5020): 665-669.

Nusse, R. (2005). "Wnt signaling in disease and in development." Cell Res **15**(1): 28-32.

Nusse, R., A. Brown, et al. (1991). "A new nomenclature for int-1 and related genes: the Wnt gene family." Cell **64**(2): 231.

Nusse, R., A. van Ooyen, et al. (1984). "Mode of proviral activation of a putative mammary oncogene (int-1) on mouse chromosome 15." Nature **307**(5947): 131-136.

Nusslein-Volhard, C. and E. Wieschaus (1980). "Mutations affecting segment number and polarity in Drosophila." Nature **287**(5785): 795-801.

Parker, D. S., J. Jemison, et al. (2002). "Pygopus, a nuclear PHD-finger protein required for Wingless signaling in Drosophila." Development **129**(11): 2565-2576.

Peng, H. B. (1991). "Xenopus laevis: Practical uses in cell and molecular biology. Solutions and protocols." Methods Cell Biol **36**: 657-662.

Perez-Moreno, M. and E. Fuchs (2006). "Catenins: keeping cells from getting their signals crossed." Dev Cell **11**(5): 601-612.

Phelps, R. A., T. J. Broadbent, et al. (2009). "New perspectives on APC control of cell fate and proliferation in colorectal cancer." Cell Cycle **8**(16): 2549-2556.

Phelps, R. A., S. Chidester, et al. (2009). "A two-step model for colon adenoma initiation and progression caused by APC loss." Cell **137**(4): 623-634.

Phillips, B. T. and J. Kimble (2009). "A new look at TCF and beta-catenin through the lens of a divergent C. elegans Wnt pathway." Dev Cell **17**(1): 27-34.

Piao, S., S. H. Lee, et al. (2008). "Direct inhibition of GSK3beta by the phosphorylated cytoplasmic domain of LRP6 in Wnt/beta-catenin signaling." PLoS One **3**(12): e4046.

Piepenburg, O., G. Vorbruggen, et al. (2000). "Drosophila segment borders result from unilateral repression of hedgehog activity by wingless signaling." Mol Cell **6**(1): 203-209.

Pierre, M. and J. Nunez (1983). "Multisite phosphorylation of tau proteins from rat brain." Biochem Biophys Res Commun **115**(1): 212-219.

Polakis, P. (2000). "Wnt signaling and cancer." Genes Dev **14**(15): 1837-1851.

Porter, J. R. (1976). "Antony van Leeuwenhoek: tercentenary of his discovery of bacteria." Bacteriol Rev **40**(2): 260-269.

Price, M. A. (2006). "CKI, there's more than one: casein kinase I family members in Wnt and Hedgehog signaling." Genes Dev **20**(4): 399-410.

Quaroni, A., J. Wands, et al. (1979). "Epithelioid cell cultures from rat small intestine. Characterization by morphologic and immunologic criteria." J Cell Biol **80**(2): 248-265.

Riggleman, B., P. Schedl, et al. (1990). "Spatial expression of the Drosophila segment polarity gene armadillo is posttranscriptionally regulated by wingless." Cell **63**(3): 549-560.

Riggleman, B., E. Wieschaus, et al. (1989). "Molecular analysis of the armadillo locus: uniformly distributed transcripts and a protein with novel internal repeats are associated with a Drosophila segment polarity gene." Genes Dev **3**(1): 96-113.

Rosenbluth, J. M., D. J. Mays, et al. (2008). "A gene signature-based approach identifies mTOR as a regulator of p73." Mol Cell Biol **28**(19): 5951-5964.

Sakanaka, C., J. B. Weiss, et al. (1998). "Bridging of beta-catenin and glycogen synthase kinase-3beta by axin and inhibition of beta-catenin-mediated transcription." Proc Natl Acad Sci U S A **95**(6): 3020-3023.

Salic, A., E. Lee, et al. (2000). "Control of beta-catenin stability: reconstitution of the cytoplasmic steps of the wnt pathway in Xenopus egg extracts." Mol Cell **5**(3): 523-532.

Schmidt-Nielsen, K. (1990). Animal physiology : adaptation and environment. Cambridge, Cambridge University Press.

Schwab, K. R., L. T. Patterson, et al. (2007). "Pygo1 and Pygo2 roles in Wnt signaling in mammalian kidney development." BMC Biol **5**: 15.

Schwarz-Romond, T., C. Asbrand, et al. (2002). "The ankyrin repeat protein Diversin recruits Casein kinase Iepsilon to the beta-catenin degradation complex and acts in both canonical Wnt and Wnt/JNK signaling." Genes Dev **16**(16): 2073-2084.

Schwarz-Romond, T., C. Metcalfe, et al. (2007). "Dynamic recruitment of axin by Dishevelled protein assemblies." J Cell Sci **120**(Pt 14): 2402-2412.

Seeling, J. M., J. R. Miller, et al. (1999). "Regulation of beta-catenin signaling by the B56 subunit of protein phosphatase 2A." Science **283**(5410): 2089-2091.

Semenov, M. V., K. Tamai, et al. (2001). "Head inducer Dickkopf-1 is a ligand for Wnt coreceptor LRP6." Curr Biol **11**(12): 951-961.

Shan, J., D. L. Shi, et al. (2005). "Identification of a specific inhibitor of the dishevelled PDZ domain." Biochemistry **44**(47): 15495-15503.

Shan, J. and J. J. Zheng (2009). "Optimizing Dvl PDZ domain inhibitor by exploring chemical space." J Comput Aided Mol Des **23**(1): 37-47.

Sharma, R. P. and V. L. Chopra (1976). "Effect of the Wingless (wg1) mutation on wing and haltere development in Drosophila melanogaster." Dev Biol **48**(2): 461-465.

Sheth, U. K. (1975). "Mechanisms of anthelmintic action." Prog Drug Res **19**: 147-157.

Siegfried, E., T. B. Chou, et al. (1992). "wingless signaling acts through zeste-white 3, the Drosophila homolog of glycogen synthase kinase-3, to regulate engrailed and establish cell fate." Cell **71**(7): 1167-1179.

Smith, W. C. and R. M. Harland (1991). "Injected Xwnt-8 RNA acts early in Xenopus embryos to promote formation of a vegetal dorsalizing center." Cell **67**(4): 753-765.

Sobrado, P., A. Jedlicki, et al. (2005). "Basic region of residues 228-231 of protein kinase CK1alpha is involved in its interaction with axin: binding to axin does not affect the kinase activity." J Cell Biochem **94**(2): 217-224.

Sokol, S., J. L. Christian, et al. (1991). "Injected Wnt RNA induces a complete body axis in Xenopus embryos." Cell **67**(4): 741-752.

Sparks, A. B., P. J. Morin, et al. (1998). "Mutational analysis of the APC/beta-catenin/Tcf pathway in colorectal cancer." Cancer Res **58**(6): 1130-1134.

Spink, K. E., P. Polakis, et al. (2000). "Structural basis of the Axin-adenomatous polyposis coli interaction." EMBO J **19**(10): 2270-2279.

Stockert, J. C., C. I. Trigoso, et al. (1991). "DNA fluorescence induced by polymethine cation pyrvinium binding." Histochem J **23**(11-12): 548-552.

Sustmann, C., H. Flach, et al. (2008). "Cell-type-specific function of BCL9 involves a transcriptional activation domain that synergizes with beta-catenin." Mol Cell Biol **28**(10): 3526-3537.

Sutherland, C., I. A. Leighton, et al. (1993). "Inactivation of glycogen synthase kinase-3 beta by phosphorylation: new kinase connections in insulin and growth-factor signalling." Biochem J **296 (Pt 1)**: 15-19.

Takacs, C. M., J. R. Baird, et al. (2008). "Dual positive and negative regulation of wingless signaling by adenomatous polyposis coli." Science **319**(5861): 333-336.

Takada, R., Y. Satomi, et al. (2006). "Monounsaturated fatty acid modification of Wnt protein: its role in Wnt secretion." Dev Cell **11**(6): 791-801.

Tamai, K., X. Zeng, et al. (2004). "A mechanism for wnt coreceptor activation." Mol Cell **13**(1): 149-156.

Theisen, H., A. Syed, et al. (2007). "Wingless directly represses DPP morphogen expression via an armadillo/TCF/Brinker complex." PLoS One **2**(1): e142.

Thompson, B., F. Townsley, et al. (2002). "A new nuclear component of the Wnt signalling pathway." Nat Cell Biol **4**(5): 367-373.

Tolwinski, N. S., M. Wehrli, et al. (2003). "Wg/Wnt signal can be transmitted through arrow/LRP5,6 and Axin independently of Zw3/Gsk3beta activity." Dev Cell **4**(3): 407-418.

Toomes, C., H. M. Bottomley, et al. (2004). "Mutations in LRP5 or FZD4 underlie the common familial exudative vitreoretinopathy locus on chromosome 11q." Am J Hum Genet **74**(4): 721-730.

van Amerongen, R., A. Mikels, et al. (2008). "Alternative wnt signaling is initiated by distinct receptors." Sci Signal **1**(35): re9.

van Amerongen, R., M. Nawijn, et al. (2005). "Frat is dispensable for canonical Wnt signaling in mammals." Genes Dev **19**(4): 425-430.

Walling, L. A., N. R. Peters, et al. (2001). "New technologies for chemical genetics." J Cell Biochem Suppl **Suppl 37**: 7-12.

Wehrli, M., S. T. Dougan, et al. (2000). "arrow encodes an LDL-receptor-related protein essential for Wingless signalling." Nature **407**(6803): 527-530.

Weinstein, I. B. and A. Joe (2008). "Oncogene addiction." Cancer Res **68**(9): 3077-3080; discussion 3080.

Whangbo, J. and C. Kenyon (1999). "A Wnt signaling system that specifies two patterns of cell migration in C. elegans." Mol Cell **4**(5): 851-858.

Willert, K., J. D. Brown, et al. (2003). "Wnt proteins are lipid-modified and can act as stem cell growth factors." Nature **423**(6938): 448-452.

Willert, K. and K. A. Jones (2006). "Wnt signaling: is the party in the nucleus?" Genes Dev **20**(11): 1394-1404.

Willert, K., S. Shibamoto, et al. (1999). "Wnt-induced dephosphorylation of axin releases beta-catenin from the axin complex." Genes Dev **13**(14): 1768-1773.

Woodgett, J. R. (2001). "Judging a protein by more than its name: GSK-3." Sci STKE **2001**(100): re12.

Wu, G., H. Huang, et al. (2009). "Inhibition of GSK3 phosphorylation of beta-catenin via phosphorylated PPPSPXS motifs of Wnt coreceptor LRP6." PLoS One **4**(3): e4926.

Wu, X., X. Tu, et al. (2008). "Rac1 activation controls nuclear localization of beta-catenin during canonical Wnt signaling." Cell **133**(2): 340-353.

Xu, Q., Y. Wang, et al. (2004). "Vascular development in the retina and inner ear: control by Norrin and Frizzled-4, a high-affinity ligand-receptor pair." Cell **116**(6): 883-895.

Xu, R. M., G. Carmel, et al. (1995). "Crystal structure of casein kinase-1, a phosphate-directed protein kinase." EMBO J **14**(5): 1015-1023.

Yamamoto, A., T. Nagano, et al. (2005). "Shisa promotes head formation through the inhibition of receptor protein maturation for the caudalizing factors, Wnt and FGF." Cell **120**(2): 223-235.

Yamamoto, H., S. Kishida, et al. (1999). "Phosphorylation of axin, a Wnt signal negative regulator, by glycogen synthase kinase-3beta regulates its stability." J Biol Chem **274**(16): 10681-10684.

Yamamoto, H., H. Komekado, et al. (2006). "Caveolin is necessary for Wnt-3a-dependent internalization of LRP6 and accumulation of beta-catenin." Dev Cell **11**(2): 213-223.

Yokoyama, N., D. Yin, et al. (2007). "Abundance, complexation, and trafficking of Wnt/beta-catenin signaling elements in response to Wnt3a." J Mol Signal **2**: 11.

Yost, C., G. H. Farr, 3rd, et al. (1998). "GBP, an inhibitor of GSK-3, is implicated in Xenopus development and oncogenesis." Cell **93**(6): 1031-1041.

Yu, D. H., J. Macdonald, et al. (2008). "Pyrvinium targets the unfolded protein response to hypoglycemia and its anti-tumor activity is enhanced by combination therapy." PLoS One **3**(12): e3951.

Yu, H. M., B. Jerchow, et al. (2005). "The role of Axin2 in calvarial morphogenesis and craniosynostosis." Development **132**(8): 1995-2005.

Zeng, L., F. Fagotto, et al. (1997). "The mouse Fused locus encodes Axin, an inhibitor of the Wnt signaling pathway that regulates embryonic axis formation." Cell **90**(1): 181-192.

Zeng, X., H. Huang, et al. (2008). "Initiation of Wnt signaling: control of Wnt coreceptor Lrp6 phosphorylation/activation via frizzled, dishevelled and axin functions." Development **135**(2): 367-375.

Zeng, X., K. Tamai, et al. (2005). "A dual-kinase mechanism for Wnt co-receptor phosphorylation and activation." Nature **438**(7069): 873-877.

Zhang, W., J. Yang, et al. (2009). "PR55 alpha, a regulatory subunit of PP2A, specifically regulates PP2A-mediated beta-catenin dephosphorylation." J Biol Chem **284**(34): 22649-22656.

Zorn, J. A. and J. A. Wells (2010). "Turning enzymes ON with small molecules." Nat Chem Biol **6**(3): 179-188.